Deep Drilling at the Dead Sea

Stein, Mordechai; Ben-Avraham, Zvi; Goldstein, Steve; Agnon, Amotz; Ariztegui, Daniel; Brauer, Achim; Haug, Gerald; Ito, Emi; Yasuda, Yoshinori

ISSN: 1816-8957

No. 11, March 2011

Scientific Drilling

Reports on Deep Earth Sampling and Monitoring

Published by the Integrated Ocean Drilling Program with the International Continental Scientific Drilling Program

Editorial Preface

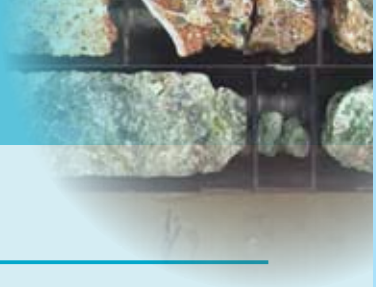

Dear Reader:

The polar regions are very sensitive to environmental change, which makes their ice shields, neighboring lakes and oceans key targets for scientific drilling. In this volume of *Scientific Drilling*, we bring reports about the almost 4-km-deep ice coring in Antarctica (p. 41), which may reveal climate data back to around 1 Ma as well as environmental observations from a lake that has been isolated below the Antarctic ice shield for more than 20 Ma. An extraterrestrial impact in northeast Siberia 3.6 Ma ago created Lake El'gygytgyn, which recorded the onset of Northern Hemisphere glaciations within the lake's oldest sediments, and traced within the younger sediments the ongoing waxing and waning of ice shields that persisted until today's interglacial (p. 29).

Ocean gateways like that of the Bering Sea are key areas in understanding long-term climate change and heat transport to the poles. The Bering Sea—connected to the Arctic Ocean in the north through the narrow Bering Strait and to the Pacific Ocean in the south across the Aleutian Island arc—was sampled by IODP Expedition 323 (p. 4) to address paleo-water mass distribution, terrigenous sediment infill, sea-ice history and other environmental parameters extending back to 5 Ma or more.

Climate changes will impact all humans. However, a large part of Earth's population lives in areas that are affected by the most rapid and unpredictable environmental change: earthquakes. Scientific drilling has taken on the challenge to understand the processes at depths where earthquakes take place, and in line with this, a summary of the San Andreas Fault Zone Observatory at Depth (SAFOD) is presented on page 14. The Dead Sea, lowest point on Earth, is a place where tectonism, climate change and history come together in the most fascinating way. On page 46 we offer a progress report on the attempt to unearth the environmental history of this unique location and how it may have impacted the civilization and the histories of the region.

As part of the preparations for the new International Ocean Discovery Program, planned to start from late 2013, the current IODP is preparing for the most ambitious ever ocean drilling effort—to drill through the entire ocean crust and into the underlying mantle. At a recent workshop funded by the Sloan Foundation (p. 51), the technical feasibility of this challenging endeavor was reviewed, and the science targets were expanded to include the presence of carbon throughout the crust and within the upper mantle. Other workshops addressed plans to drill back in 'deep time' (p. 66) to examine environments and conditions for life at 3,500 Ma, or to examine potential deep fault systems that have been active due to the removal of former ice shields during the recent interglacial (p. 56).

Scientific drilling has clearly taken on the fascinating challenges of understanding Earth systems. Please enjoy from your armchair what this issue has to offer.

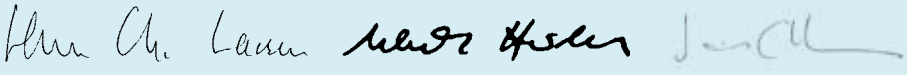

Hans Christian Larsen
Editor-in-Chief

Ulrich Harms
Editor

Jamus Collier
Editor

Front cover: The Deep Lake Drilling System (DLDS) in operation on the Dead Sea in late fall 2010. The ICDP drilling project in Israel, Jordan and Palestine.
Left inset: Two scientists match pieces of basalt collected at Site U1342 in the Bering Sea. (Photo: Carlos Alvarez Zarikian, IODP-TAMU)

Scientific Drilling
ISSN 1816-8957 (printed version)
1816-3459 (electronic version)

Scientific Drilling is a semiannual journal published by the Integrated Ocean Drilling Program (IODP) with the International Continental Scientific Drilling Program (ICDP). The editors welcome contributions on any aspect of scientific drilling, including borehole instruments, observatories, and monitoring experiments. The journal is produced and distributed by the Integrated Ocean Drilling Program Management International (IODP-MI) for the IODP under the sponsorship of the U.S. National Science Foundation, the Ministry of Education, Culture, Sports, Science and Technology of Japan, and other participating countries. The journal's content is partly based upon research supported under Contract OCE-0432224 from the National Science Foundation.

Electronic versions of this publication and information for authors can be found at http://www.iodp.org/scientific-drilling/ and http://www.icdp-online.org/scientific-drilling/. Printed copies can be requested from the publication office.

IODP is an international marine research drilling program dedicated to advancing scientific understanding of the Earth by monitoring and sampling subsea-floor environments. Through multiple drilling platforms, IODP scientists explore the program's principal themes: the deep biosphere, environmental change, and solid Earth cycles.

ICDP is a multi-national program designed to promote and coordinate continental drilling projects with a variety of scientific targets at drilling sites of global significance.

Publication Office
IODP-MI, Tokyo University of Marine Science and Technology,
Office of Liaison and Cooperative Research 3rd Floor,
2-1-6, Etchujima, Koto-ku, Tokyo
135-8533, JAPAN
Tel: +81-3-6701-3180
Fax: +81-3-6701-3189
e-mail: journal@iodp.org
url: www.iodp.org/scientific-drilling/

Contents

Science Reports

Progress Report

Technical Developments

Workshop Reports

Workshop Reports

News and Views

Schedules

IODP Expedition 323—Pliocene and Pleistocene Paleoceanographic Changes in the Bering Sea

by Kozo Takahashi, A. Christina Ravelo, Carlos Alvarez Zarikian, and the IODP Expedition 323 Scientists

doi:10.2204/iodp.sd.11.01.2011

Abstract

High-resolution paleoceanography of the Plio-Pleistocene is important in understanding climate forcing mechanisms and the associated environmental changes. This is particularly true in high-latitude marginal seas such as the Bering Sea, which has been very sensitive to changes in global climate during interglacial and glacial or Milankovitch time scales. This is due to significant changes in water circulation, land-ocean interaction, and sea-ice formation. With the aim to reveal the climate and oceanographic history of the Bering Sea over the past 5 Ma, Integrated Ocean Drilling Program (IODP) Expedition 323 cored a total of 5741 meters of sediment (97.4% recovery) at seven sites covering three different areas: Umnak Plateau, Bowers Ridge, and the Bering slope region. Four deep holes range from 600 m to 745 m spanning in age from 1.9 Ma to 5 Ma. The water depths (819 m to 3173 m) allow characterization of past vertical water mass distribution such as the oxygen minimum zone (OMZ). The results highlight three key points. (1) The first is an understanding of long-term evolution of surface-water mass distribution during the past 5 Ma including past sea-ice distribution and warm and less eutrophic subarctic Pacific water mass entry into the Bering Sea. (2) We characterized relatively stagnant intermediate water mass distribution imprinted as laminated sediment intervals that have been ubiquitously encountered. Today, the OMZ impinges upon the sediments at ~700–1600 m water depths. In the past, the OMZ appears to have occurred mainly during interglacial periods. Changes in low oxygen-tolerant benthic foraminiferal faunas clearly concur with this observation. (3) We also characterized significant changes between glacial episode of terrigenous sedimentary supply and interglacial episode of diatom flux.

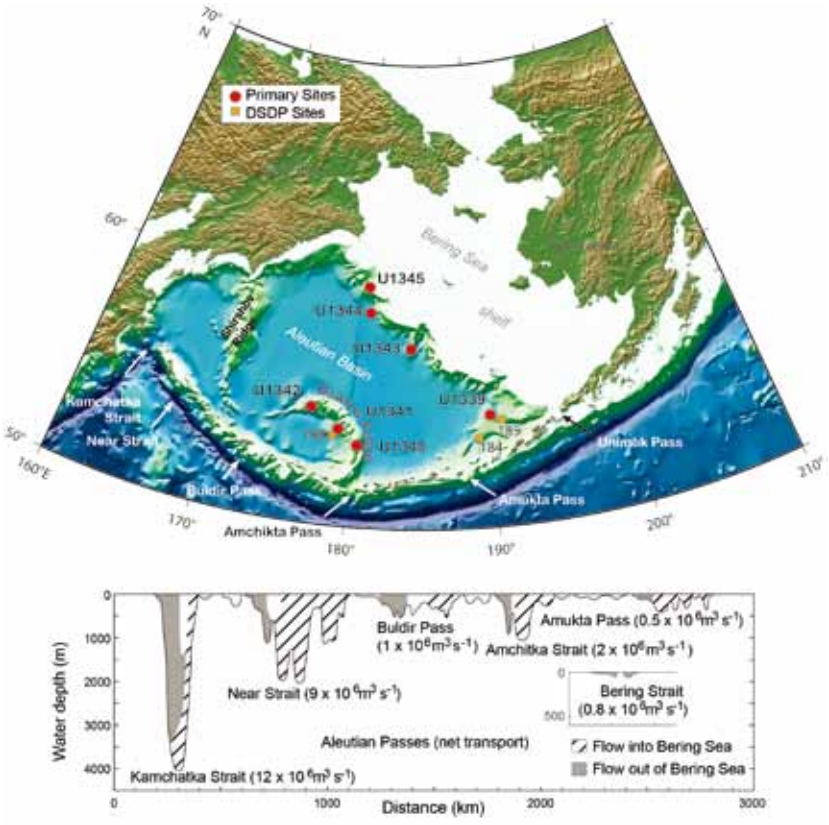

Figure 1. Map illustrating the locations of the seven sites drilled and cored during IODP Exp. 323 in the Bering Sea, along with cross-sections of the passes with volume transport (Sv) in the Aleutian Island arc and the Bering Strait. Note that the horizontal and vertical scales of the Bering Strait are twice that of the Aleutians (from Stabeno et al., 1999; Takahashi, 2005).

Introduction and Goals

The rate and regional expression of recent global warming is difficult to understand and even more difficult to predict because of the complex nature of the climate system, whose components interact nonlinearly with various time lags and on various timescales. Paleoclimatic and paleoceanographic studies provide opportunities to study the dynamics of the climate system by examining how it responds to external forcing (e.g., greenhouse gases and solar radiation changes) and how it generates internal variability due to interacting Earth-system processes. Of note is the amplified recent warming of the high latitudes in the Northern Hemisphere (Solomon et al., 2007), which is presumably related to sea-ice albedo feedback and teleconnections to other regions; both the behavior of sea ice-climate interactions and the role of large-scale atmospheric and oceanic circulation in climate change can be studied with geologic records of past climate changes in the Bering Sea.

Prior to IODP Expedition 323 (Exp 323 hereafter), little was known about the sedimentology and climate history of the Bering Sea outside of a few piston core studies (Cook et al., 2005; Okazaki et al., 2005; Katsuki and Takahashi, 2005; Takahashi et al., 2005) and Sites 188 and 185 (Scholl and Creager, 1973), which were drilled by the Deep Sea Drilling Project (DSDP) in 1971 with old drilling technology and poor recovery. Past studies using piston cores in the Bering Sea indicated that, while current conditions in the Bering Sea promote seasonal sea-ice formation, during the Last Glacial Maximum (LGM) conditions sustained perennial or nearly perennial sea-ice cover (Tanaka and Takahashi, 2005), attesting to the potential utility of sedimentary records in the Bering Sea to examine past sea-ice distributions. In paleoceanographic studies of the North Pacific, the Bering and Okhotsk seas have been implicated as sources of dense oxygenated intermediate water that possibly impacted oceanic and climate conditions throughout the Pacific on glacial-interglacial (Gorbarenko, 1996; Matsumoto et al., 2002) and millennial (Hendy and Kennett, 2003) timescales. In addition, changes in Bering Sea environmental conditions could be related to sea-level and circulation changes, which alter flow patterns through narrow straits that connect the Bering Sea to the Arctic Ocean to the north and the Pacific Ocean to the south. The lack of pertinent Bering Sea material prevented the evaluation of these and other ideas for a long time.

The scientific objectives of Exp 323 are as follows: (1) to elucidate a detailed evolutionary history of climate and surface ocean conditions since the earliest Pliocene in the Bering Sea, where amplified high-resolution changes of climatic signals are recorded; (2) to shed light on temporal changes in the origin and intensity of North Pacific Intermediate Water (NPIW) and possibly deeper water mass formation in the Bering Sea; (3) to characterize the history of continental glaciation, river discharge, and sea ice formation in order to investigate the link between continental and oceanic conditions in the Bering Sea and on adjacent land areas; (4) to investigate linkages through comparison to pelagic records between ocean/climate processes that occur in the more sensitive marginal sea environment and processes that occur in the North Pacific and/or globally (This objective includes evaluating how the ocean/climate history of the Bering Strait gateway region may have affected North Pacific and global conditions.); and (5) to constrain global models of subseafloor biomass and microbial respiration by quantifying subseafloor cell abundance and pore water chemistry in an extremely high productivity region of the ocean. We also aim to determine how subseafloor community composition is influenced by high productivity in the overlying water column.

Seven sites whose terrigenous and biogenic components capture the spatial and temporal evolution of the Bering Sea through the Pliocene and Pleistocene* were successfully drilled with a total core length of 5741 m during Exp 323 (Expedition 323 Scientists, 2010; Takahashi et al., 2011; Fig. 1; Table 1). Additionally, Exp 323 collected a rich archive of information regarding the role of microbes on biogeochemical cycles in ultra-high-productivity environments, the postdepositional processes that impact geochemical, lithologic, and physical properties of the sediment, and past oceanic chemistry preserved in pore waters. This paper presents background on environmental setting and important scientific questions concerning the Bering Sea, followed by pertinent highlights of the scientific findings of Exp 323 mostly obtained onboard *JOIDES Resolution* during the cruise.

***Note**: In this paper we opt to continue using the last major published timescale, in which the base of the Pleistocene is defined by the Global Boundary Stratotype Section and Point (GSSP) of the Calabrian Stage at 1.806 (1.8) Ma (Gradstein et al., 2004).

Geological and Physical Setting

With an area of 2.29×10^6 km^2 and a volume of 3.75×10^6 km^3, the Bering Sea is the third largest marginal sea in the world, surpassed only by the Mediterranean and South China seas (Hood, 1983). Approximately half of the Bering Sea is a shallow (0–200 m), neritic environment, with the majority of the continental shelf spanning the eastern side of the basin off Alaska from Bristol Bay to the Bering Strait (Fig. 1). The northern continental shelf is seasonally ice-covered, but little ice forms over the deep southwest areas. In addition to the shelf regions, two significant topographic highs have better $CaCO_3$ preservation than the deep basins. First is the Shirshov Ridge, which extends south of the Koryak Range in eastern Siberia along 170°E and separates the southwestern part of the Bering Sea into two basins, Komandorski (to the west) and Aleutian (to the east). Second is the Bowers Ridge, which extends 300 km north from the Aleutian Island arc (Fig. 1). The Aleutian Basin is a vast plain 3800–3900 m deep with occasional gradually sloping depres-sions as deep as 4151 m (Hood, 1983).

Table 1. Summary of drilled results for IODP Exp 323 in the Bering Sea.

Area IODP Site Number	Water Depth (mbsl)	Depth DSF (m)	Age (Ma)	Average Sedimentation Rate (cm k.y.$^{-1}$)
Umnak Plateau				
U1339	1868	200	0–0.8	28
Bowers Ridge				
U1340	1295	605	0–5.0	12
U1341	2140	600	0–4.3	12
U1342	819	128	0–1.2*	4.5
Bering Slope				
U1343	1953	745	0–2.4	35
U1344	3173	745	0–1.9	45
U1345	1008	150	0–0.5	29

*Bulk of sediment samples were <1.2 Ma (top 41 mbsf) in age except for the Middle Miocene diatoms located in the samples from directly above the basaltic basement rocks.

Three major rivers flow into the Bering Sea; the Kuskokwim and Yukon rivers drain central Alaska, and the Anadyr River drains eastern Siberia (Fig. 1). The Yukon is the longest of the three rivers and supplies the largest discharge into the Bering Sea. Its discharge peaks in August because of meltwater and is about equal to that of the Mississippi. It has a mean annual flow of 5×10^3 m^3 s^{-1} (Hood, 1983).

Today, a substantial amount of water is transported in and out of the Bering Sea across the Aleutian Island arc and the Bering Strait through passes (Fig. 1). Water mass exchange with the Pacific through the Aleutian Islands, such as through the Kamchatka Strait, is significant, linking Bering Sea conditions to the Pacific climate. The Alaskan Stream, an extension of the Alaskan Current, flows westward along the Aleutian Islands and enters the Bering Sea partially through the Amchitka Strait and to significant extent through the Near Strait west of Attu Island in the eastern Aleutian Islands (Fig. 1). A part of the Subarctic Current also joins the Alaskan Stream, resulting in a combined volume transport of 11 Sv (0.011 km^3 s^{-1}) (Ohtani, 1965).

Bottom and intermediate water in the Bering Sea originates from the North Pacific. After flowing into the Bering Sea it is slightly modified by the mixing of relatively fresh, warm water with very small amounts of bottom water formed within the Bering Sea today (Warner and Roden, 1995). Nutrient concentrations of North Pacific origin are high compared to all other regions in the global oceans; this explains the high productivity in the surface layers and consequent very low oxygen concentrations in intermediate and deep water masses of the Bering Sea today (Fig. 2). The oxygen and nutrient composition of the Bering Sea waters is further modified by denitrification (Lehmann et al., 2005) and respiration of organic matter in the water column (Nedashkovskiy and Sapozhnikov, 1999). Respiration and the development of an OMZ are particularly intense at water depths of ~1000 m (Fig. 2).

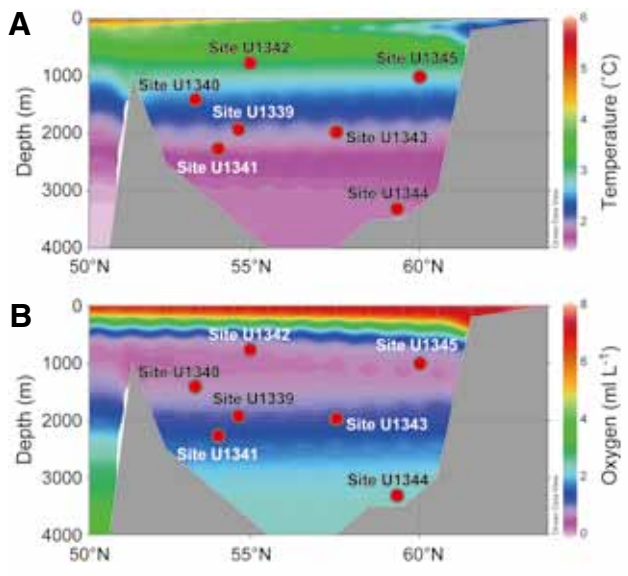

Figure 2. Vertical profiles of [A] temperature and [B] dissolved oxygen along the transect on 180° meridian line in the Bering Sea (data from World Ocean Atlas (2005); figures drawn by Ocean Data View).

Much of the Pacific water entering the Bering Sea is matched by outflow through the Aleutian Islands. The most significant outflow is through the Kamchatka Strait, which has a maximum depth of 4420 m (Stabeno et al., 1999) (Fig. 1). If some component of NPIW or deep water formed in the Bering Sea in past times, particularly when sea level was lower, it would have flowed out through the Kamchatka Strait or a secondary outlet near the Commander-Near Strait at 2000 m (Fig. 1).

The unidirectional northward transport of water masses (0.8 Sv) from the Bering Sea through the Bering Strait to the Arctic Ocean contributes to the salinity and biogeochemical contrast between the Pacific and the Atlantic. The Bering Strait region is one of the most biologically productive regions in the world (Sambrotto et al., 1984). Much of this biologically produced organic matter and the associated nutrients flow into the Arctic Ocean because of the northward current direction. This may profoundly influence the present dominance of carbonate production in the Atlantic versus opal production in the Pacific, as described by models of basin-to-basin fractionation (Berger, 1970) and "carbonate ocean vs. silica ocean" (Honjo, 1990). Flow through the Bering Strait, which is ~50 m deep today (Fig. 1), was certainly different at times of lower sea level or enhanced perennial sea-ice cover. The closing of this gateway and the accompanying changes in ocean and river flow through time could have caused changes in global patterns of circulation or in nutrient and salinity distributions.

Ages and Sedimentation Rates

Among the three drill sites explored in the Bowers Ridge region, both of the deepest holes drilled—Hole U1340A (605 m uncompressed core depth below seafloor (CSF-A), hereafter meters below seafloor (mbsf) and Hole U1341B (600 m mbsf)—represent the time spans from the Holocene to the Pliocene, back to ~5 Ma and 4.3 Ma, respectively (Table 1; Fig. 3). Note that the 4.3 Ma bottom age of Hole U1341B has been revised by an onshore study from the shipboard data (~5 Ma; Expedition 323 Scientists, 2010; Takahashi et al., 2011). The expedition's initial goal of penetrating to ~5 Ma was adequately accomplished at Site U1340, despite the failure of the extended core barrel (XCB) cutting shoe in Hole U1340A, which target depth of penetration was 700 m. In the gateway region sites (at the Bering slope), two deep holes were drilled: Holes U1343E (744 m mbsf) and U1344A (745 m mbsf). Hole U1343E reached ~2.4 Ma, where as Hole U1344A reached ~1.9 Ma (Figs. 3 and 4). Also note that the 2.4 Ma bottom age of Hole U1344A has been revised by an onshore study from the shipboard data (2.1 Ma). At other drill sites, the bottom ages of

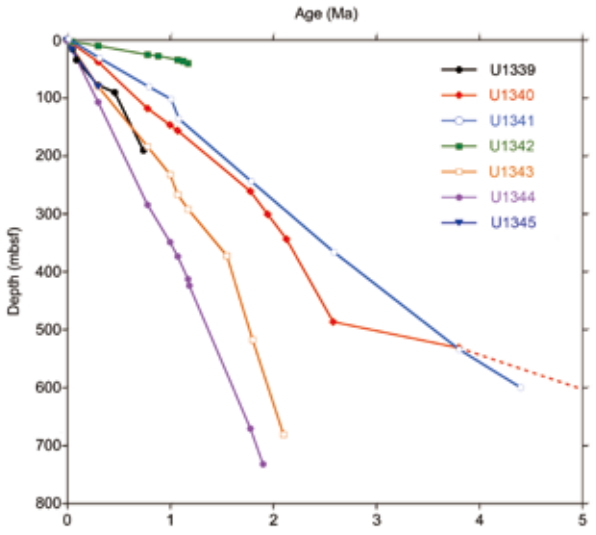

Figure 3. Age vs depth plots showing varying sedimentation rates observed at Sites U1339–U1345. The dashed line at the bottom of Site U1340 indicates the extrapolated bottom age based on the ages found further above.

the sedimentary sequences based on biomagnetostratigraphy are as follows: Site U1339 at Umnak Plateau reached 0.74 Ma, Site U1342 at Bowers Ridge reached 1.2 Ma (with the exception of the middle Miocene sediments just above the basement), and Site U1345 at Bering slope reached 0.5 Ma (Table 1).

The sediments recovered from Bowers Ridge display high mean sedimentation rates (~12 cm k.y.$^{-1}$ at Sites U1340 and U1341) without apparent hiatuses, and are generally appropriate for high-resolution Pliocene–Pleistocene paleoceanographic studies with adequate calcareous benthic foraminiferal preservation in the Pleistocene, but lower preservation in the Pliocene. On the other hand, sediments at these sites are generally barren of planktonic foraminifera and calcareous nannofossils except for the section between ~2.5 Ma and ~3 Ma. The abundance of all siliceous microfossils is generally high, enabling good biostratigraphy and paleoceanographic reconstruction. Furthermore, the upper part of Site U1340 (~20–150 m uncompressed core composite depth, CCSF-A) had obvious soft-sediment deformation due to mass movement possibly caused by local seismic activity. Although such deformation hinders the continuous reconstruction of late Pleistocene high-resolution paleoceanography at this site, information from other drill sites can readily fill the gap.

In the region of the Arctic gateway sites proximal to the Bering slope, the observed sedimentation rates were overwhelmingly high: Hole U1343E had sedimentation rates of 21–58 cm k.y.$^{-1}$ and Hole U1344A had rates of 29–50 cm k.y.$^{-1}$. Sedimentation rates were so high, in fact, that drilling reached ages of only 2.4 Ma and 1.9 Ma, respectively, despite penetration to 745 m mbsf at each site. Such high sedimentation rates stem from the deposition of silt and clay transported by the Yukon and other rivers as well as the terrigenous sediments once deposited on the shelf. In spite of the high percentage of terrigenous material, pertinent biotic proxies including benthic foraminifera and siliceous microfossils are adequately preserved, enabling future paleoceanographic studies. Therefore, the overall coverage of excellent cores to ~5 Ma in the Bowers Ridge region and ~2 Ma in the gateway region allows detailed, continuous high-resolution paleoceanographic studies relevant to global climate change.

Depositional Environments and Lithology

The seven sites drilled during Exp 323 provide a continuous high-resolution record of the evolution of marine sedimentation in the marginal Bering Sea (Fig. 4). Overall, the sediments recovered in the Bering Sea are a mixture of three components: biogenic, siliciclastic, and volcaniclastic. Other accessory lithologies identified include authigenic carbonates (dolomite Fe-rich carbonates and Mg calcite), barite and sulfides. The most prominent sedimentary features observed were decimeter- to meter-scale bedded alternations of sediment color and texture, reflecting alternations in lithology between more siliciclastic and more biosiliceous deposits (Fig. 4). The sediments were generally highly bioturbated. However, fine laminations preserving alternations between millimeter-scale laminae of biogenic and terrigenous material were also present in several of the drilled sites (Fig. 5).

The distributions of the sedimentary components and sedimentary structures, and their variability both within and between the Exp 323 sites account for changes of the biogenic, glaciomarine, terrigenous, and volcanogenic sediment sources and the environmental conditions present during sediment deposition. The scales of these lithologic variations indicate that sedimentation in the Bering Sea has recorded long-term trends that include the critical period of reorganization of Earth's climate from the warm early Pliocene, and the transition into the ice ages. The physiographic settings of the different sites, their water depths, and their locations relative to the sediment source areas account for the marked regional differences in sediment composition, especially between the Pleistocene sections of the Bowers Ridge and the Bering slope sites.

The results of Exp 323 suggest that the history of sedimentation in the Bering Sea is broadly characterized by three main sedimentary phases that occurred between ~5 Ma and ~2.7 Ma, ~2.7 Ma and ~1.74 Ma, and ~1.74 Ma to recent (Fig. 4). The oldest portion of the sedimentary record (~5 Ma to ~2.7 Ma) was retrieved only at Bowers Ridge Sites U1340 and U1341. As illustrated by the age vs depth curves, sedimentation rates during the early middle Pliocene were relatively high (Fig. 3) and characterized by diatom ooze with minor amounts of diatom silt, sponge spicules, and vitric ash. Although the Pliocene sediment is commonly bioturbated, distinct intervals characterized by extensive lamination also occur. The oldest laminated intervals (<3.8 Ma) were observed at Site U1341, although the origin of the lami-

nations, and whether they represent primary or secondary processes is unknown. Notably, especially in the deeper parts of the record, compaction or diagenetic phase transformations might have created secondary sedimentological features, overprinting the primary ones. Isolated ice rafted debris (IRD) pebbles were observed in sediments older than 3.8 Ma only at Site U1340. Limited dropstone occurrence prior to 2.7 Ma was also reported at two sites drilled in the northern Pacific during Leg 145 (ODP Sites 881 and 883) and in the Yakataga Formation in Alaska (Lagoe et al., 1993), which suggests the development of Alpine glaciers prior to the onset of Northern Hemisphere glaciation (NHG) (Krissek, 1995).

The middle section of Sites U1340 and U1341 (~2.7–1.74 Ma) is characterized by beds of diatom ooze with minor amounts of calcareous nannofossils and foraminiferal ooze alternating with diatom silt beds. The latter are composed of subequal proportions of siliciclastic (silt-sized quartz, feldspar, and rock fragments and/or clay) and biogenic components and minor volcaniclastic components. Dropstone occurrence is common—indicating a peak in siliciclastic deposition that has also been observed at Leg 145 sites—and coincides with the beginning of NHG. However, the dramatic drop in paleoproductivity recorded at Site 882 (Haug et al., 1999) is not present at the Bowers Ridge sites where, conversely, the biogenic component is high throughout the late Pliocene and Pleistocene.

All sites drilled during Exp 323 preserve a record of sedimentation ranging from the early Pleistocene through the Holocene (1.74 Ma to recent). Lithologies and sedimentation rates vary between the different sites, as indicated by a basin-wide comparison of the evolution of sedimentation in the Bering Sea during this period (Figs. 3, 4). The lowest sedimentation rates (only 4.5 cm k.y.$^{-1}$) were observed at Site U1342, where laminated foraminifera-rich diatom ooze beds alternate with silty clay beds at timescales ranging in the Milankovitch band (Fig. 5). The same temporal interval corresponds to a much thicker section at Sites U1340 and U1341, where the bedding alternations are less distinct and the abundance of IRD is higher. Although lamination is common at Sites U1342 and U1340, laminae are virtually absent at the deeper Site U1341. At the Bering Sea slope site, sedimentation rates are about three times higher than at the Bowers Ridge sites. At Sites U1339, U1343, and U1344, siliciclastic-rich beds and mixed siliciclastic-biogenic beds alternate cyclically. The sections are pervasively bioturbated, and laminated intervals are rare. Overall, sedimentation on the Bering slope is characterized by higher influence of (1) siliciclastic material delivered by ice sheets and (2) terrigenous sedimentation derived from the continental shelf and slope, which are indented by some of the largest submarine canyons in the world. However, because of their proximity to the continents, it is not clear whether the sediments characterized by high siliciclastic content are recording periods of ice sheet expansion (stadials) or increased runoff (interstadials). IRD is a common feature at all sites during this time period, and it increases significantly in sediments younger than 1 Ma, as is also observed in coeval sediments from the North Pacific based on the results of Leg 145 (Krissek, 1995).

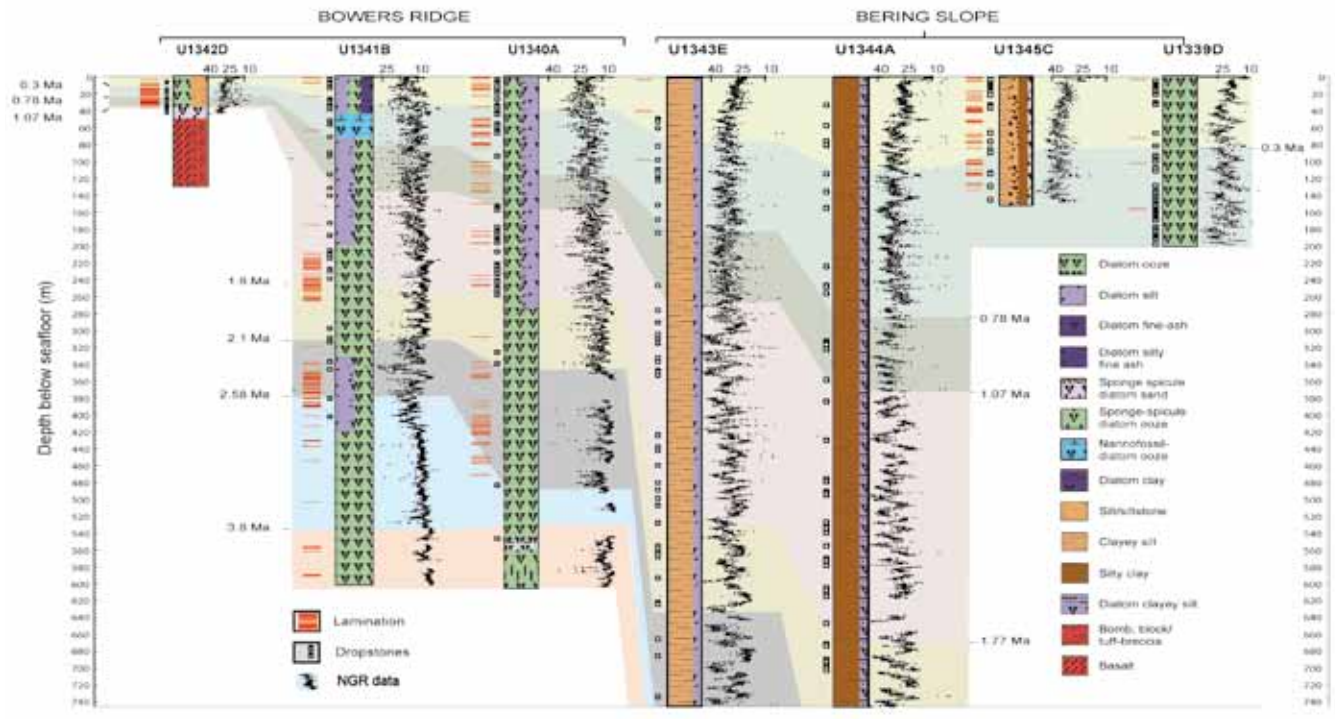

Figure 4. Lithostratigraphic summary of Exp. 323 drill sites. Natural gamma radiation (NGR: counts s^{-1}) data are plotted in black at the right side of the lithology columns (values increase to the left). Laminations are denoted by red horizontal lines. Note that there are many different styles of laminations; future work will determine which laminations are primary features, and which are secondary.

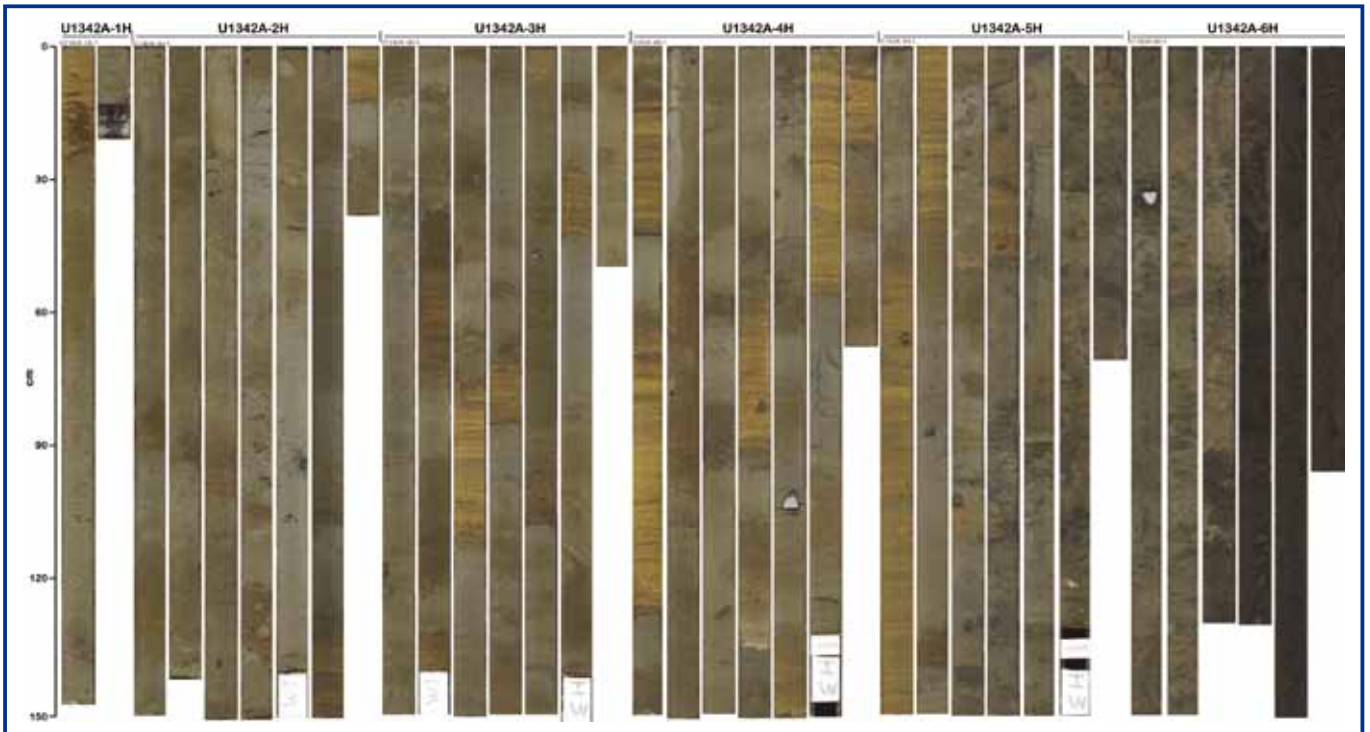

Figure 5. Photographs of Cores 323-U1342A-1H through 6H, bulk of sediments above the underlain volcanic basement rocks, showing ubiquitous occurrences of laminated sediments with horizontally banded features. Site U1342 is located at shallow water depth of 819 m, within today's OMZ (see Fig. 2).

History of Sea-Ice Development

One of the most striking findings of Exp 323 is the general sea-ice distribution history of the Bering Sea for the past 5 Ma. As described earlier, the first sign of sea ice is the presence of pebbles, which are thought to be transported as IRD starting at >3.8 Ma at Site U1340 (Fig. 4), indicating the formation of sea ice or iceberg transportation to the Bowers Ridge region. The bulk of the evolution of sea-ice distribution has been interpreted from shipboard analyses of sea-ice diatoms and sea-ice-related dinoflagellate taxa and to a lesser extent by other diatom taxa and intermediate water-dwelling radiolarians.

The details of sea-ice evolution are derived from changes in the relative abundance of sea-ice diatom taxa, which are represented mainly by *Thalassiosira antarctica* spores (Abelmann, 1992a) and sea-ice dinoflagellates. The first signs of sea ice diatoms and dinoflagellates are subtle increases in their abundances at Bowers Ridge Site U1340, starting at ~3.4 Ma for dinoflagellates and ~2.7 Ma for diatoms, coincident with NHG (Maslin et al., 1996). Later than ~2 Ma the sea-ice assemblage signals become progressively stronger into the present, up to values of ~10%–20% of the total respective assemblages. In contrast to the Bowers Ridge sites, sea-ice cover at the Bering slope sites is markedly severe, indicated by significantly higher sea-ice assemblage percentages. Sea-ice diatom values range from ~10% to 50% during the latest Pliocene and increase from ~30% to 70% during the Pleistocene. Notably, sea-ice diatom and dinoflagellate assemblages clearly show a significant increase in both abundance and amplitudes of variability around the mid-Pleistocene Transition (MPT). Analogous to sea-ice-associated diatom and dinoflagellate taxa, a clear increasing trend in abundance of intermediate water-dwelling radiolarian taxa at the MPT is also observed at Sites U1343 and U1344. This is consistent with the interpretation that the surface water became gradually more affected by the formation of sea ice as climate progressively cooled; in the presence of sea ice, surface-dwelling radiolarians disappeared, and as a consequence, the relative percentages of intermediate water dwellers such as *Cycladophora davisiana* were higher (Abelmann, 1992b; Okazaki et al., 2003).

At Sites U1343 and U1344, which are located closer to the southern boundary of today's seasonal sea-ice maximum extent than the Bowers Ridge sites, a dramatic change in the dominance of dinoflagellate cyst assemblages from autotrophic to heterotrophic taxa is evident at ~1.2–1.5 Ma. This suggests that sea-ice formation occurred well before the time when the abundance of sea-ice taxa significantly increased at ~1 Ma. Along with significant increases of both sea-ice dinoflagellates and diatoms (e.g., *T. antarctica* spores) at ~1 Ma at both sites, there is a rather significant drop in the abundance of the typical pelagic diatom *Neodenticula seminae*. All of these biotic events are within the time interval of the MPT, which spans from ~1.2 Ma to 0.8 Ma and marks the transition from 41 k.y. obliquity ice volume cycles to longer ice age cycles that vary at ~100-k.y. frequencies.

As noted above, the Bowers Ridge and Bering slope regions show distinct differences in the extent of sea-ice cover throughout the last ~2.4 Ma. The extent of sea-ice cover of the latter was substantially greater than that of the

former because of the proximal locations of the three Bering slope sites, which are most prone to perennial sea-ice cover in the Bering Sea. The spatial differences in sea-ice cover today are mainly attributed to the surface water circulation pattern; this spatial difference appears to have persisted for at least 2.4 Ma, implying that the surface water circulation patterns were comparable as well.

Changes in Biological Productivity and Subarctic Pacific Water Mass Entry

Based on the spatial distributions of long-term temporal changes of three diatom taxa (*Coscinodiscus marginatus, Neodenticula*, and *Actinocyclus curvatulus*), it is clear that the influence of subarctic Pacific waters, which are relatively warm and less eutrophic than Bering Sea waters, has typically been strongest at the Bowers Ridge sites, followed by the Umnak site. The weakest influence of this warm water mass has occurred at the Bering slope sites. The same pattern was found by Katsuki and Takahashi's (2005) study of past water mass circulation patterns, which they inferred from sea-ice distributions over the last glacial period. The wide-ranging records from Exp 323 indicate that as climate cooled through the Pleistocene, pelagic water influence at all the sites progressively weakened. Furthermore, the sites closest to straits through which pelagic water flows into the Bering Sea have consistently higher abundances of subarctic diatom species than those downstream of the counterclockwise circulation pattern of the surface water masses.

From the bottom of the holes upward at the Bowers Ridge sites, a marked drop in *C. marginatus* was seen at ~2.8 Ma at Site U1341 and at ~2.6 Ma at Site U1340. This can be interpreted as resulting from a sharp reduction in supply of nutrients due to the development of upper layer stratification. It is apparent that the diatom taxon *C. marginatus* requires a relatively high nutrient supply and tolerates low light intensity. This is substantiated by the fact that (1) today this diatom taxon dwells in the lower euphotic zone off Spain (Nogueira et al., 2000; Nogueira and Figueiras, 2005), and (2) it occurs during early winter (November–January) in the subarctic Pacific and the Bering Sea based on time-series sediment trapping (Takahashi, 1986; Takahashi et al., 1989; Onodera and Takahashi, 2009). This timing of 2.8–2.6 Ma coincides approximately with the so-called end of "opal dump" observed in the subarctic Pacific at ~2.7 Ma, which is coincidental with the onset of NHG (Maslin et al., 1996). Although the reduction in *C. marginatus* around the time of NHG persisted, an overwhelmingly continuous presence of diatom ooze and interbedded diatom ooze and silt sediments accumulated throughout the Pliocene–Pleistocene in the Bering Sea. This clearly suggests that a high amount of opal sedimentation continued after the onset of NHG well into the Pleistocene.

The 5-Ma long-term trend of *Neodenticula* (*N. kamtschatica, N. koizumii, N. seminae,* and *Neodenticula* sp.) in the Bowers Ridge region shows the following patterns. Generally higher percentages of *Neodenticula* in total diatoms are observed from the base of the holes towards younger ages until ~2.8–2.7 Ma. After that, there is a decline in *Neodenticula* with sizable fluctuations, indicating that surface water stratification progressively developed as the climate cooled from the Pliocene into the Pleistocene. As surface waters became increasingly stratified, especially after ~0.9 Ma with Milankovitch-scale 100-k.y. climatic cyclic regimes, *N. seminae* declined with the emerging sea-ice diatoms.

Changes in Bottom and Intermediate Water Conditions

In order to elucidate the history, temporal variability, and intensity of NPIW and deepwater formation in the Bering Sea and its links to surface water processes, the insights provided by the investigation on benthic foraminifera and midwater radiolarians are prerequisites. The Bering Sea sites ranged from 818 m to 3174 m in depth, and they allow for characterization of past vertical water mass distribution and for reconstruction of the history of the OMZ distribution in the region (Fig. 2). Shipboard analyses of sediment samples during Exp 323 show continuous recovery of Pliocene to Holocene deep-sea benthic foraminifera and midwater radiolarians at all sites, although calcareous benthic foraminifera appear to be rare in the Pliocene. The benthic foraminifera composition displays large assemblage changes, likely related to variability in local bottom water oxygen concentration in the bottom waters associated with surface water productivity and/or deepwater ventilation on Milankovitch and shorter timescales. For example, *Bulimina* aff. *exilis*, a common species in Bering Sea samples, is generally regarded as a low oxygen/deep infaunal species and has been found in samples associated with high productivity and low sea ice (Bubenshchikova et al., 2008; Kaiho, 1994).

Previous piston core studies showed a large increase in the intensity of the OMZ during the last deglacial at Umnak Plateau (Okazaki et al., 2005), suggesting a relationship between productivity and terrestrial nutrient supply from melting ice and increased river input. However, there is no information regarding the longer timescale relationship through the Pleistocene. Analysis of fauna from the newly drilled Bering Sea sites will be particularly important in extending this record through the entire Pliocene (at Bowers Ridge) and Pleistocene (at Bowers Ridge and the Bering slope). It will allow us to decipher the onset and evolution of the OMZ and provide further insight into NPIW production in this marginal sea. Furthermore, Site U1344 at ~3200 m (presently located below the OMZ) has the potential to provide records of past deepwater changes.

A striking finding of the expedition was the relatively low oxygen content of intermediate water mass conditions at most sites during the last 5 Ma, as indicated by the presence of episodic laminated sediment intervals throughout the

entire record. The benthic foraminifera *Martinottiella communis* occurred persistently in the Pliocene. The co-occurrence of other low oxygen species (e.g., *Bulimina* aff. *mexicana*), together with the modern distribution of *M. communis* in OMZs, indicates low oxygen conditions persisted throughout the last 5 Ma. However *M. communis* is not recorded in the Bering Sea after ~2 Ma, suggesting changes to deepwater properties after this time. Abundant calcareous benthic species occur after ~2 Ma (e.g., *Bulimina, Globobulimina, Islandiella, Nonionella*, and *Valvulineria*) that are typically indicative of very low oxygen conditions (Bubenshchikova et al., 2008).

High sediment accumulation rate at Sites U1339 and U1345, located within the current OMZ (Figs. 2, 4), reveal high-amplitude variability in the relative abundance of the deep infaunal assemblage for the past 0.8 Ma. This appears to be associated with interglacial-deglacial cyclicity, represented by higher abundance of deep infaunal species (reflecting the lowest bottom water oxygen conditions) during interglacials. This particularly true during the strong interglacial-like Marine Isotope Stages (MIS) 1, 5, and 11. Higher bottom water oxygen concentrations appear to correlate with some glacial periods. Sites U1340, U1343, and U1344 contain well-preserved foraminifera over the last 2 Ma with increasing absolute abundances of benthic and planktonic taxa across the MPT (~0.8–1.1 Ma) in association with an increase in abundance of the polar planktonic foraminifera *Neogloboquadrina pachyderma*. This cooling trend was also observed as an increase in the abundance of sea-ice dinoflagellates and diatoms and coincided with increasing intermediate water-dwelling radiolarians (e.g., *C. davisiana*). Cooling of the surface waters would have enhanced ventilation of the intermediate waters during glacials and would have increased density stratification during interglacials, contributing to a drop in oxygen content in the intermediate and bottom waters at these times. Such a decrease in oxygen content is supported by a possible increase in deep infaunal benthic foraminifera taxa at Sites U1343 and U1344 over the MPT, but higher resolution sampling from existing core material is needed to resolve this.

Microbiology and Geochemistry in High Surface Productivity Environments

The microbiological objectives of Exp 323 were to constrain global models of subseafloor biomass and microbial respiration by quantifying subseafloor cell abundance and pore water chemistry in an extremely high productivity region of the ocean. We also sought to determine how subseafloor community composition is influenced by high productivity in the overlying water column. To meet these objectives, high-resolution sampling for microbiological analyses and pore water chemistry took place at five sites throughout the Bering Sea. Each site was selected based upon its distance from land and its levels of marine productivity determined by annual chlorophyll-a concentrations in the water column.

The geochemical data obtained during the expedition show that the present-day microbial activity along the slope sites (Sites U1339, U1343, U1344, and U1345) is substantially higher and more diverse in terms of respiration pathways than at Bowers Ridge (Sites U1340, U1341, and U1342). At the slope sites, the concentrations of microbial respiration products such as dissolved inorganic carbon (DIC), ammonium, and phosphate are approximately an order of magnitude higher than at Bowers Ridge (Fig. 6). A shallow sulfate-methane transition zone (SMTZ) (~6–11 m mbsf) is also present, indicating that both methanogenesis and sulfate reduction based on methane oxidation occur in these sediments. Pore water data suggest the presence of microbially

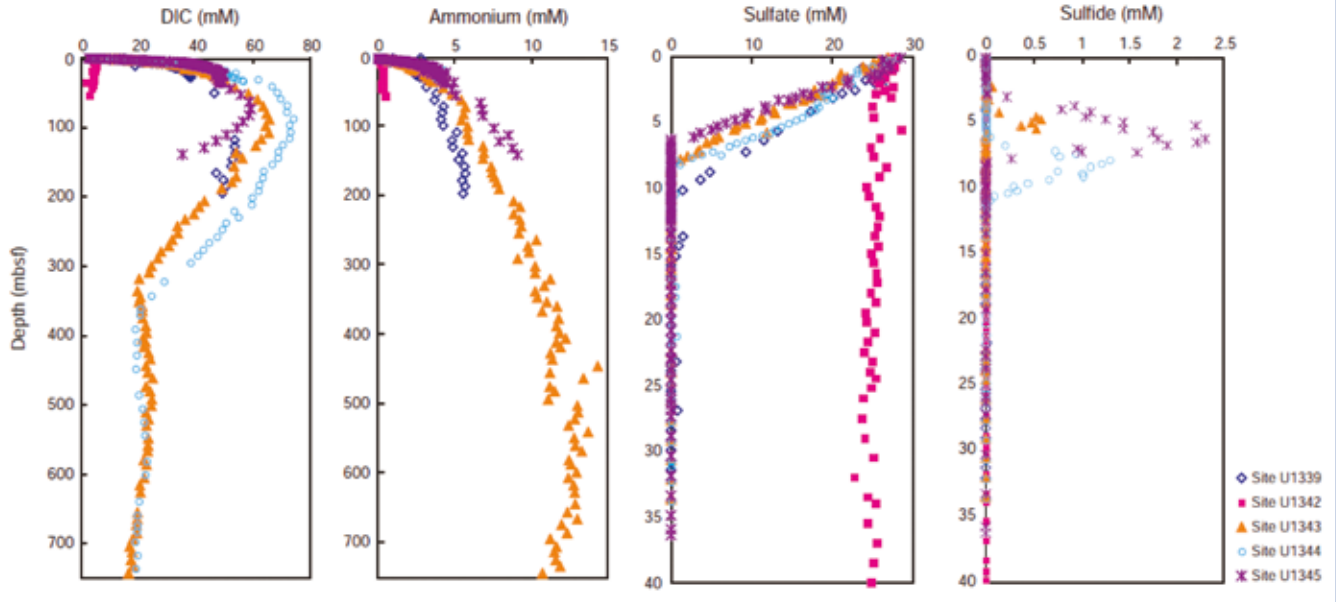

Figure 6. Depth variations in DIC, ammonium, sulfate, and sulfide, illustrating the depth of the SMTZ (~6–11 mbsf) at Sites U1339, U1342, U1343, U1344, and U1345.

mediated Fe and Mn reduction. The geochemical profiles also indicate significant microbial activity as deep as 700 mbsf. In contrast, at Bowers Ridge sulfate penetrates to the basement and is almost unaltered with depth, suggesting only very low rates of microbially mediated sulfate reduction. Methane is mostly below detection limit. The differences in microbial activity at these sites may be caused by differences in water column productivity and sedimentation patterns.

We expect that the differ-ences in the geochemical parameters between the slope and ridge sites will be reflected in microbial abundance and diversity. A larger and more diverse microbial community at the slope sites is likely. Specifically, we expect elevated cell density and an assemblade of bacteria and archaea at the SMTZ. At the slope sites, geochemical profiles suggest that methanogens, iron reducers, manganese reduc-ers, and sulfate reducers exist throughout the sediment column. At Bowers Ridge, geochemical profiles indicate that, at present, diagenetic processes are dominated by nitrate, manganese and iron reducers, while sulfate reducers and methanogens are of minor importance.

Acknowledgements

We thank the captain, operation superintendent, crew, and technicians who assisted us in drilling and sample analyses during Exp 323. Numerous people at IODP-TAMU as the USIO provided their dedicated effort supporting us, including preparation of the expedition and publication of the proceedings. We also thank the crucial members of ODP and IODP Proposal 477, which was initially written and submitted in 1995; without their cooperation this project could have never been materialized. This includes their effort during the site survey cruise on R/V Hakuho-Maru which took place in 1999 as well as the data processing performed afterwards. The curatorial team provided us with their able support during the two time sampling parties at the Kochi Core Center of JAMSTEC. We also thank the following reviewers for their constructive comments on the manuscript: Hans Christian Larsen, Ulrich Harms, Jamus Collier, Mika Saido, Renata Szarek, and Glen Hill.

The IODP Expedition 323 Scientists

K. Takahashi (Co-Chief Scientist), A.C. Ravelo (Co-Chief Scientist), C. Alvarez Zarikian (Staff Scientist), I. Aiello, H. Asahi, G. Bartoli, B. Caissie, M. Chen, E. Colmenero-Hidalgo, M. Cook, K. Dadd, G. Guèrin, Y. Huh, K. Husum, A. Ijiri, M. Ikehara, S. Kender, T. Liu, S. Lund, C. März, A. Mix, M. Ojha, M. Okada, Y. Okazaki, J. Onodera, C. Pierre, T. Radi, N. Risgaard-Petersen, T. Sakamoto, D. Scholl, H. Schrum, Z.N. Stroynowski, E.A. Walsh, and L. Wehrmann.

References

Abelmann, A., 1992a. Diatom assemblages in Arctic sea ice—indicator for ice drift pathways. *Deep-Sea Res., Part A Oceanogr. Res. Papers*, 39(2–1):S525–S538, doi:10.1016/S0198-0149(06)80019-1.

Abelmann, A., 1992b. Radiolarian flux in Antarctic waters (Drake Passage, Powell Basin, Bransfield Strait). *Polar Biol.*, 12(3–4):357–372, doi:10.1007/BF00243107.

Berger, W.H., 1970. Biogenous deep-sea sediments: fractionation by deep-sea circulation. *Geol. Soc. Am. Bull.*, 81(5):1385–1402, doi:10.1130/0016-7606(1970)81[1385:BDS-FBD]2.0.CO;2.

Bubenshchikova, N., Nürnberg, D., Lembke-Jene, L., and Pavlova, G., 2008. Living benthic foraminifera of the Okhotsk Sea: faunal composition, standing stocks and microhabitats. *Mar. Micropaleontol.*, 69(3–4):314–333, doi:10.1016/j.marmicro.2008.09.002.

Cook, M.S., Keigwin, L.D., and Sancetta, C.A., 2005. The deglacial history of surface and intermediate water of the Bering Sea. *Deep-Sea Res., Part II Topical Studies Oceanogr.*, 52(16–18):2163–2173, doi:10.1016/j.dsr2.2005.07.004.

Expedition 323 Scientists, 2010. Bering Sea paleoceanography: Pliocene–Pleistocene paleoceanography and climate history of the Bering Sea. *IODP Prel. Rept.*, 323, doi:10.2204/iodp.pr.323.2010.

Gorbarenko, S.A., 1996. Stable isotope and lithological evidence of late glacial and Holocene oceanography of the northwestern Pacific and its marginal seas. *Quat. Res.*, 46(3):230–250, doi:10.1006/qres.1996.0063.

Gradstein, F.M., Ogg, J.G., and Smith, A.G., 2004. *A Geologic Time Scale 2004*: Cambridge (Cambridge University Press).

Haug, G.H., Sigman, D.M., Tiedemann, R., Pedersen, T.F., and Sarnthein, M., 1999. Onset of permanent stratification in the subarctic Pacific Ocean. *Nature (London, U.K.)*, 401(6755):779–782, doi:10.1038/44550.

Hendy, I.L., and Kennett, J.P., 2003. Tropical forcing of North Pacific intermediate water distribution during late Quaternary rapid climate change? *Quat. Sci. Rev.*, 22(5–7):673–689, doi:10.1016/S0277-3791(02)00186-5.

Honjo, S., 1990. Particle fluxes and modern sedimentation in the polar oceans. *In* Smith, W.O., Jr. (Ed.), *Polar Oceanography (Pt. B): Chemistry, Biology, and Geology*: New York (Academic), 687–739.

Hood, D.W., 1983. The Bering Sea. *In* Ketchum, B.H. (Ed.), *Estuaries and Enclosed Seas*: The Netherlands (Elsevier), 337–373.

Kaiho, K., 1994. Benthic foraminiferal dissolved-oxygen index and dissolved-oxygen levels in the modern ocean. *Geology*, 22(8):719–722, doi:10.1130/ 0091-7613(1994)022<0719:BFDOIA>2.3.CO;2.

Katsuki, K., and Takahashi, K., 2005. Diatoms as paleoenvironmental proxies for seasonal productivity, sea-ice and surface circulation in the Bering Sea during the late Quaternary. *Deep-Sea Res., Part II Topical Studies Oceanogr.*, 52(16–18):2110–2130, doi:10.1016/j.dsr2.2005.07.001.

Krissek, L.A., 1995. Late Cenozoic ice-rafting records from Leg 145 sites in the North Pacific: late Miocene onset, late Pliocene intensification, and Pliocene–Pleistocene events. *In* Rea, D.K., Basov, I.A., Scholl, D.W., and Allan, J.F. (Eds.), *Proc. ODP, Sci. Results*, 145: College Station, TX (Ocean Drilling Program), 179–194. doi:10.2973/odp/proc.sr.145.118.1995.

Lagoe, M.B., Eyles, C.H., Eyles, N., and Hale, C., 1993. Timing of late Cenozoic tidewater glaciation in the far North Pacific. *Geol. Soc. Am. Bull.*, 105(12):1542–1560, doi:10.1130/ 0016-7606 (1993)105<1542:TOLCTG>2.3.CO;2.

Lehmann, M.F., Sigman, D.M., McCorkle, D.C., Brunelle, B.G., Hoffmann, S., Kienast, M., Cane, G., and Clement, J., 2005. Origin of the deep Bering Sea nitrate deficit: constraints from the nitrogen and oxygen isotopic composition of water column nitrate and benthic nitrate fluxes. *Global Biogeochem. Cycles*, 19(4):GB4005, doi:10.1029/2005GB 002508.

Maslin, M.A., Haug, G.H., Sarnthein, M., and Tiedemann, R., 1996. The progressive intensification of Northern Hemisphere glaciation as seen from the North Pacific. *Geol. Rundsch.*, 85(3):452–465, doi:10.1007/BF02369002.

Matsumoto, K., Oba, T., Lynch-Stieglitz, J., and Yamamoto, H., 2002. Interior hydrography and circulation of the glacial Pacific Ocean. *Quat. Sci. Rev.*, 21(14–15):1693–1704, doi:10.1016/ S0277-3791(01)00142-1.

Nedashkovskiy, A.P., and Sapozhnikov, V.V., 1999. Variability in the components of the carbonate system and dynamics of inorganic carbon in the western Bering Sea in summer. *In* Loughlin, T.R., and Ohtani, K. (Eds.), *Dynamics of the Bering Sea. A Summary of Physical, Chemical, and Biological Characteristics, and a Synopsis of Research on the Bering Sea*: Fairbanks (University of Alaska Sea Grant), 311–322.

Nogueira, E., and Figueiras, F.G., 2005. The microplankton succession in the Ria de Vigo revisited: species assemblages and the role of weather-induced, hydrodynamic variability. *J. Mar. Syst.*, 54(1–4):139–155, doi:10.1016/j.jmarsys.2004. 07.009.

Nogueira, E., Ibanez, F., and Figueiras, F.G., 2000. Effect of meteorological and hydrographic disturbances on the microplankton community structure in the Ría de Vigo (NW Spain). *Mar. Ecol. Prog. Ser.*, 203:23–45, doi:10.3354/meps203023.

Ohtani, K., 1965. On the Alaskan Stream in summer. *Bull. Fac. Fish., Hokkaido Univ.*, 15:260–273. (In Japanese).

Okazaki, Y., Takahashi, K., Asahi, H., Katsuki, K., Hori, J., Yasuda, H., Sagawa, Y., and Tokuyama, H., 2005. Productivity changes in the Bering Sea during the late Quaternary. *Deep-Sea Res., Part II Topical Studies Oceanogr.*, 52(16–18):2150–2162, doi:10.1016/j.dsr2.2005.07.003.

Okazaki, Y., Takahashi, K., Yoshitani, H., Nakatsuka, T., Ikehara, M., and Wakatsuchi, M., 2003. Radiolarians under the seasonally sea-ice covered conditions in the Okhotsk Sea: flux and their implications for paleoceanography. *Mar. Micropaleontol.*, 49(3):195–230, doi:10.1016/S0377-8398(03) 00037-9.

Onodera, J., and Takahashi, K. 2009. Long-term diatom fluxes in response to oceanographic conditions at Stations AB and SA in the central subarctic Pacific and the Bering Sea, 1990-1998. *Deep-Sea Research I*, 56(2):189–211. doi:10.1016/j. dsr.2008.08.006.

Sambrotto, R.N., Goering, J.J., and McRoy, C.P., 1984. Large yearly production of phytoplankton in the western Bering Strait. *Science*, 225(4667):1147–1150, doi:10.1126/science.225. 4667.1147.

Scholl, D.W., and Creager, J.S., 1973. Geologic synthesis of Leg 19 (DSDP) results; far North Pacific, and Aleutian Ridge, and Bering Sea. *In* Creager, J.S., Scholl, D.W., et al., *Init. Repts. DSDP*, 19: Washington, DC (U.S. Govt. Printing Office), 897–913, doi:10.2973/dsdp.proc.19.137.1973.

Solomon, S., Qin, D., Manning, M., Marquis, M., Averyt, K., Tignor, M.M.B., Miller, H.L., Jr., and Chen, Z., 2007. *Climate Change 2007: The Physical Science Basis*: Cambridge (Cambridge University Press).

Stabeno, P.J., Schumacher, J.D., and Ohtani, K., 1999. The physical oceanography of the Bering Sea. *In* Loughlin, T.R., and Ohtani, K. (Eds.), *Dynamics of the Bering Sea: A Summary of Physical, Chemical, and Biological Characteristics, and a Synopsis of Research on the Bering Sea*: Fairbanks (University of Alaska Sea Grant), 1–28.

Takahashi, K., 1986. Seasonal fluxes of pelagic diatoms in the subarctic Pacific, 1982–1983. *Deep-Sea Res., Part A Oceanogr. Res. Papers*, 33:1225–1251, doi:10.1016/0198-0149(86)90022-1.

Takahashi, K., 2005. The Bering Sea and paleoceanography. *Deep-Sea Res., Part II Topical Studies Oceanogr.*, 52(16–18):2080–2091, doi:10.1016/j.dsr2.2005.08.003.

Takahashi, K., Honjo, S., and Tabata, S., 1989. Siliceous phytoplankton flux: interannual variability and response to hydrographic changes in the northeastern Pacific. *In* Peterson, D. (Ed.), *Aspects of Climate Variability in the Pacific and Western Americas*. Geophys. Monogr., 151–160.

Takahashi, K., Jordan, R.W., and Boltovskoy, D., 2005. *Deep-Sea Res., Part II Topical Studies Oceanogr.*, 52(16–18):2079–2364, doi:10.1016/j.dsr2.2005.08.002.

Takahashi, K., Ravelo, A.C., Alvarez Zarikian, C.A., and the Expedition 323 Scientists. 2011. *Proc. IODP*, 323: Tokyo Integrated Ocean Drilling Program Management International, Inc.), doi:10.2204/iodp.proc.323.2011.

Tanaka, S., and Takahashi, K., 2005. Late Quaternary paleoceanographic changes in the Bering Sea and the western subarctic Pacific based on radiolarian assemblages. *Deep-Sea Res., Part II Topical Studies Oceanogr.*, 52(16–18):2131–2149, doi:10.1016/j.dsr2.2005.07.002.

Warner, M.J., and Roden, G.I., 1995. Chlorofluorocarbon evidence for recent ventilation of the deep Bering Sea. *Nature (London, U.K.)*, 373(6513):409–412, doi:10.1038/373409a0.

Authors

Kozo Takahashi, Department of Earth & Planetary Sciences, Graduate School of Sciences, Kyushu University, Hakozaki 6-10-1, Higashi-ku, Fukuoka 812-8581, Japan, e-mail: kozo@geo.kyushu-u.ac.jp.

A. Christina Ravelo, Ocean Sciences Department, University of California, 1156 High Street, Santa Cruz, CA 95064, U.S.A.

Carlos Alvarez Zarikian, Integrated Ocean Drilling Program & Department of Oceanography, Texas A&M University, 1000 Discovery Drive, College Station, TX 77845-9547, U.S.A.

and the IODP Expedition 323 Scientists

Related Web Link

http://www.iodp.tamu.edu/scienceops/expeditions/bering_sea.html

Scientific Drilling Into the San Andreas Fault Zone —An Overview of SAFOD's First Five Years

by Mark Zoback, Stephen Hickman, William Ellsworth, and the SAFOD Science Team

doi:10.2204/iodp.sd.11.02.2011

Abstract

The San Andreas Fault Observatory at Depth (SAFOD) was drilled to study the physical and chemical processes controlling faulting and earthquake generation along an active, plate-bounding fault at depth. SAFOD is located near Parkfield, California and penetrates a section of the fault that is moving due to a combination of repeating microearthquakes and fault creep. Geophysical logs define the San Andreas Fault Zone to be relatively broad (~200 m), containing several discrete zones only 2–3 m wide that exhibit very low P- and S-wave velocities and low resistivity. Two of these zones have progressively deformed the cemented casing at measured depths of 3192 m and 3302 m. Cores from both deforming zones contain a pervasively sheared, cohesionless, foliated fault gouge that coincides with casing deformation and explains the observed extremely low seismic velocities and resistivity. These cores are being now extensively tested in laboratories around the world, and their composition, deformation mechanisms, physical properties, and rheological behavior are studied. Downhole measurements show that within 200 m (maximum) of the active fault trace, the direction of maximum horizontal stress remains at a high angle to the San Andreas Fault, consistent with other measurements. The results from the SAFOD Main Hole, together with the stress state determined in the Pilot Hole, are consistent with a strong crust/weak fault model of the San Andreas. Seismic instrumentation has been deployed to study physics of faulting—earthquake nucleation, propagation, and arrest—in order to test how laboratory-derived concepts scale up to earthquakes occurring in nature.

Introduction and Goals

SAFOD (the San Andreas Fault Observatory at Depth) is a scientific drilling project intended to directly study the physical and chemical processes occurring within the San Andreas Fault Zone at seismogenic depth. The principal goals of SAFOD are as follows: (i) study the structure and composition of the San Andreas Fault at depth, (ii) determine its deformation mechanisms and constitutive properties, (iii) measure directly the state of stress and pore pressure in and near the fault zone, (iv) determine the origin of fault-zone pore fluids, and (v) examine the nature and significance of time-dependent chemical and physical fault zone processes (Zoback et al., 2007).

Detailed planning of a research experiment focused on drilling, sampling, and downhole measurements directly within the San Andreas Fault Zone began with an international workshop held in Asilomar, California in December 1992. This workshop highlighted the importance of deploying a permanent geophysical observatory within the fault zone at seismogenic depth for near-field monitoring of earthquake nucleation. Hence, from the outset, the SAFOD project has been designed to achieve two parallel suites of objectives. The first is to carry out a series of experiments in and near the San Andreas Fault that address long-standing questions about the physical and chemical processes that control deformation and earthquake generation within active fault zones. The second is to make near-field observations of earthquake nucleation, propagation, and arrest to test how laboratory-derived concepts about the physics of faulting

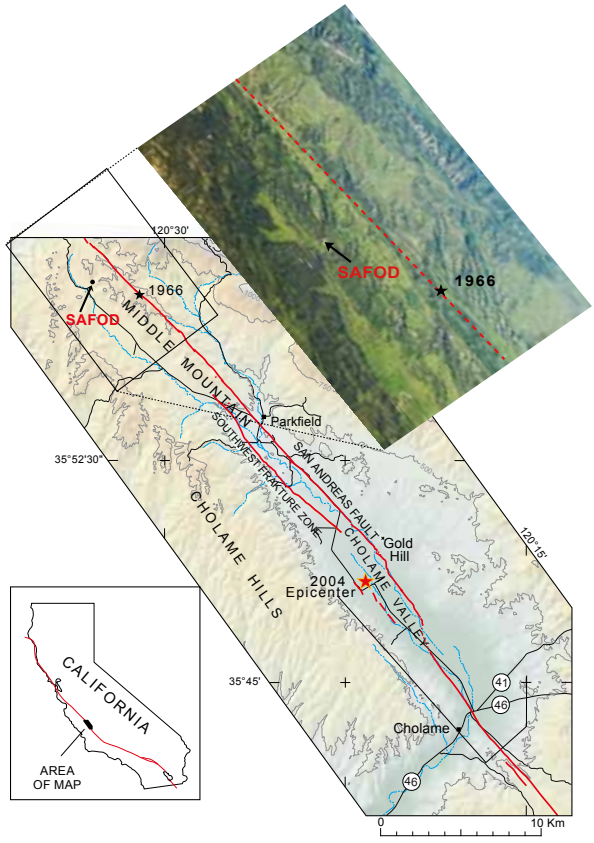

Figure 1. Map of the Parkfield segment of the San Andreas Fault showing the epicenters of the 1966 and 2004 Parkfield earthquakes and the SAFOD drillsite (Rymer et al., 2006). The air photo shows the terrain in the area of the SAFOD drill site and the epicenter of the 1966 Parkfield earthquake.

scale up to earthquakes occurring in nature. In the years following the Asilomar workshop, dozens of planning meetings were held to synthesize the research questions of highest scientific priority that were deemed to be operationally achievable. Numerous other meetings were also held related to site selection and to detailed operational plans for drilling, sampling, downhole measurements, and long-term monitoring.

When planning of the EarthScope initiative got underway at the National Science Foundation (NSF) in the late 1990s, the project was named SAFOD and became one of the three components of EarthScope along with the Plate Boundary Observatory (PBO) and USArray. In 2002, a 2.2-km-deep Pilot Hole was funded by the International Continental Scientific Drilling Program (ICDP) and was drilled at the SAFOD site. The main SAFOD project started when NSF funded the EarthScope proposal in 2003, with substantial cost sharing and operational support for SAFOD provided by the U.S. Geological Survey (USGS), ICDP, and other agencies.

The SAFOD operational plan was designed to address a number of first-order scientific questions related to fault mechanics in a hostile environment where the mechanically and chemically altered rocks in the fault zone are subject to high mean stress, potentially high pore pressure, and elevated temperature. Some of these questions are listed below.

- *What are the mineralogy, deformation mechanisms, and constitutive properties of fault gouge?* Why do some faults creep? What are the strength and frictional properties of recovered fault rocks at *in situ* conditions of stress, fluid pressure, temperature, strain rate, and pore fluid chemistry? What determines the depth of the shallow seismic-to-aseismic transition? What do mineralogical, geochemical, and microstructural analyses reveal about the nature and extent of water-rock interaction?
- *What is the fluid pressure and permeability within and adjacent to fault zones?* Are there super-hydrostatic fluid pressures within some fault zones, and through what mechanisms are these pressures generated and/or maintained? How does fluid pressure vary during deformation and episodic fault slip (creep and earthquakes)? Do fluid pressure seals exist within or adjacent to fault zones, and at what scales?
- *What are the composition and origin of fault-zone fluids and gases?* Are these fluids of meteoric, metamorphic, or mantle origin (or combinations of the three)? Is fluid chemistry relatively homogeneous, indicating pervasive fluid flow and mixing, or heterogeneous, indicating channelized flow and/or fluid compartmentalization?
- *How do stress orientations and magnitudes vary across fault zones?* Are principal stress directions and magnitudes different within the deforming core of weak fault zones compared to the adjacent (stronger) country rock, as predicted by some theoretical models? How does fault strength measured in the near field compare with depth-averaged strengths inferred from heat flow and regional stress directions? What is the nature and origin of stress heterogeneity near active faults?
- *How do earthquakes nucleate?* Does seismic slip begin suddenly, or do earthquakes begin slowly with accelerating fault slip? Do the size and duration of this precursory slip episode, if it occurs, scale with the magnitude of the eventual earthquake? Are there other precursors to an impending earthquake, such as changes in pore pressure, fluid flow, crustal strain, or electromagnetic field?
- *How do earthquake ruptures propagate?* Do they propagate as a uniformly expanding crack, as a slip pulse, or as a sequence of slipping high-strength asperities? What is the effective (dynamic) stress during seismic faulting? How important are processes such as shear heating, transient increases in fluid pressure, and fault-normal opening modes in lowering the dynamic frictional resistance to rupture propagation?
- *How do earthquake source parameters scale with magnitude and depth?* What is the minimum size earthquake that occurs on faults? How is long-term energy release rate partitioned between creep dissipation, seismic radiation, dynamic frictional resistance, and grain size reduction (determined by integrating fault zone monitoring with laboratory observations on core)?
- *What are the physical properties of fault-zone materials and country rock (seismic velocities, electrical resistivity, density, porosity)?* How do physical properties from core samples and downhole measurements compare with properties inferred from surface geophysical observations? What are the dilational, thermoelastic, and fluid-transport properties of fault and country rocks, and how might they interact to promote either slip stabilization or transient over-pressurization during faulting?
- *What processes control the localization of slip and strain?* Are fault surfaces defined by background microearthquakes and creep the same? Would active slip surfaces be recognizable through core analysis and downhole measurements in the absence of seismicity and/or creep?

In addition, a substantial body of evidence indicates that slip along major plate-bounding faults like the San Andreas occurs at much lower levels of shear stress than expected, based upon laboratory friction measurements on standard rock types and assuming hydrostatic pore fluid pressures (i.e., it is a weak fault). Yet, the cause of this weakness has remained elusive (Hickman, 1991). In the context of the San Andreas, two principal lines of evidence indicate that the

fault has low frictional strength: the absence of frictionally-generated heat, and the orientation of the maximum principal stress in the crust adjacent to the fault. A large number of heat flow measurements show no evidence of frictionally generated heat adjacent to the San Andreas Fault (Lachenbruch and Sass, 1980, 1992; Williams et al., 2004), which implies that shear motion along the fault is resisted by shear stresses approximately a factor of five less than fric-tional strength of the adjacent crust. This observation is sometimes referred to as the San Andreas stress/heat flow paradox. Saffer et al. (2003) showed that it is highly unlikely that topographically driven fluid flow has an appreciable effect on these heat flow measurements, indicating that the lack of frictionally-generated heat in the vicinity of the San Andreas Fault is indeed indicative of low aver-age shear stress levels acting on the fault at depth. In addition to the heat flow data, the orientation of principal stresses in the vicinity of the fault also indicates that right-lateral strike slip motion on the fault occurs in response to low levels of shear stress (Zoback et al., 1987; Mount and Suppe, 1987; Oppenheimer et al., 1988).

Why Parkfield? SAFOD is located in central California (Fig. 1) near the town of Parkfield, at the transition between the locked (i.e., seismogenic) portion of the fault to the southeast and the segment of the fault to the northwest where slip dominantly occurs by aseismic creep. The fault is seismically active around SAFOD with numerous sites of repeating microearthquakes, M3 and smaller, occurring on the fault at depths of 2–12 km (Waldhauser et al., 2004). The Parkfield segment of the fault hosts the well-studied seven M6 earthquakes that have ruptured since 1857 (Bakun and McEvilly, 1984). Slip distributions for the last two Parkfield earthquakes—on 28 June 1966 and 28 September 2004—determined using geodetic measurements, indicate that the ruptures terminated a few kilometers southeast of SAFOD (Murray and Langbein, 2006; Harris and Arrowsmith, 2006 and papers therein).

Beginning at the Asilomar meeting, site selection committees winnowed down eighteen potential sites to four, and eventually the northwest end of Parkfield segment was selected. The geology seemed ideal since Salinian granite on the west side of the fault was expected to be juxtaposed against Franciscan melange on the east side, so a major geologic discontinuity was expected when crossing the fault at depth. Also, the San Andreas Fault is quite active in the area, exhibiting a combination of aseismic creep and frequent microearthquakes that would help define the exact location of the active fault trace at depth. In addition, more is known about this section of the San Andreas than any other, due to the intense interest in capturing a M~6 earthquake within a dense network of instrumentation.

After selecting the Parkfield segment of the San Andreas for the SAFOD experiment, the next question of particular importance was where exactly to site the borehole. The site chosen (Fig. 1) was selected near Middle Mountain because repeating microearthquakes could be reached at the shallowest depth possible close to the fault to limit the horizontal reach of the borehole. As shown in the photo inset of Fig. 1, the selected site is a broad, relatively flat area where a 5-acre drill pad could be constructed 1.8 km southwest of the surface trace of the fault. Once this area was identified, a number of detailed geophysical and geologic site studies were carried out to allow results from SAFOD to be placed in the appropriate geological and geophysical context and to assure that the drill site selected would not encounter any large-scale faults or struc-

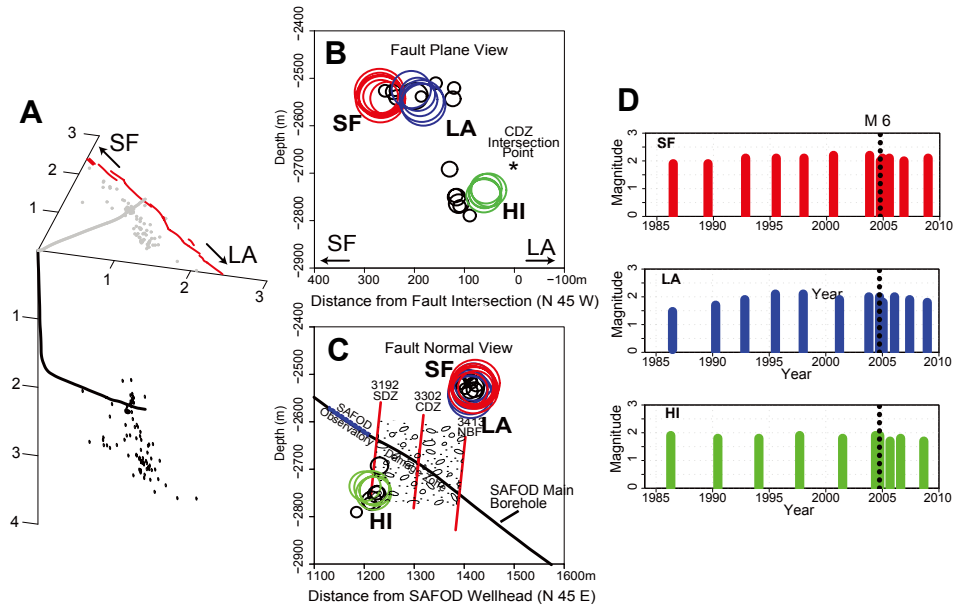

Figure 2. Microearthquakes selected for targeting with SAFOD. [A] 3-D perspective view of the seismicity with respect to the path of the SAFOD borehole, with north pointing up, east to the right, and depth down (all axes in km). [B] View of the plane of the San Andreas Fault at about 2.7-km depth looking to the northeast. The red, blue, and green circles represent seismogenic patches of the San Andreas Fault that produce nearly identical, regularly repeating microearthquakes termed the San Francisco (SF), Los Angeles (LA), and Hawaii (HI) clusters, respectively. The point at which the SAFOD borehole passes through the central deforming zone (CDZ) is shown by the asterisk. [C] Cross-sectional view of these earthquakes looking to the northwest, parallel to the San Andreas Fault, including the trajectory of the SAFOD borehole and the principal faults associated with the damage zone shown in Figs. 3 and 4. Note that the HI events occur about 100 m below the fault intersection at 3192 m (measured depth), indicating that the HI microearthquakes occur on the southwest deforming zone (SDZ). The SF and LA sequences occur on the northwest bounding fault (NBF), as discussed in the text.

tural complexities in the near surface. These studies included an extensive microearthquake survey, high-resolution seismic reflection/refraction profiling, magnetotelluric profiling, ground and closely-spaced aeromagnetic surveys, gravity surveys, and geologic mapping.

The repeating microearthquakes provide targets on the fault plane at depth to guide the drilling trajectory (Fig. 2A) into the microearthquake zone at less than 3 km depth. Another reason for choosing this site is that there are three sets of repeating M~2 earthquakes in the target area. Surrounding these patches, fault slip occurs through aseismic creep. In a view normal to the plane of the San Andreas Fault Zone at 2.65 km depth (Fig. 2B), we see the source zones associated with these three patches (scaled for a ~10-MPa stress drop). The seismograms from each of these source zones are essentially identical (Nadeau et al., 2004), and cross-correlation demonstrates that within ±10 m uncertainty these events are located in exactly the same place on the faults (F. Waldhauser, pers. comm.).

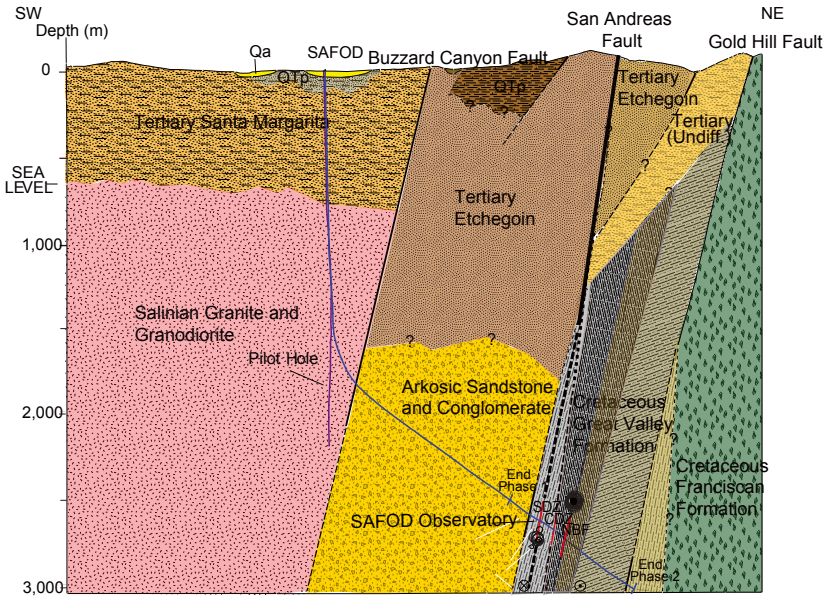

Figure 3. Simplified geologic cross-section parallel to the trajectory of the San Andreas Fault Observatory at Depth (SAFOD) borehole. The geologic units are constrained by surface mapping and the rock units encountered along both the main borehole and the pilot hole. The black circles represent repeating microearthquakes. The three notable fault traces associated with the San Andreas Fault damage zone (SDZ, CDZ, and NBF) are shown in red. The depth at which the SAFOD observatory is deployed is shown.

As shown in Fig. 2B, we refer to the shallower source zone in the direction of San Francisco as the SF events, and the adjacent source zone in the direction of Los Angeles as LA events. Note that the SF and LA patches are adjacent to each other; it is common for LA events to occur immediately after SF events as triggered events. As seen in Fig. 2B, the third cluster of events (in green) occurs on a fault plane to the southwest of that upon which the SF and LA events occur. As this cluster of events is to the southwest of the other two clusters, these are referred to as the Hawaii (HI) events.

The time sequences of the three clusters of repeating earthquakes are shown in Fig. 2C. Note that prior to the M6 Parkfield earthquake of September 2004, each of the three clusters produced an event every ~2.5–3.0 years. Following the Parkfield earthquake, the frequency of the events increased dramatically, apparently due to accelerated creep on this part of the fault resulting from stress transfer from the M~6 main-shock. Following this flurry of events the frequency of the repeaters slowed down and is presently in the process of returning to the background rate exhibited prior to the main shock. Similar behavior has been seen elsewhere along the San Andreas Fault system in California (Schaff et al., 1998).

Note in Fig. 2B that the HI events occur about 100 m below the fault intersection at 3192 m (measured depth), indicating that the HI microearthquakes occur on the southwestern-most of the two actively deforming fault traces identified in the SAFOD crossing. The microearthquake locations shown in Fig. 2 were determined utilizing subsurface recordings of these earthquakes from various geophone deployments in the SAFOD borehole along with surface recordings from the dense Parkfield Area Seismic Observatory (PASO; Thurber et al., 2004). This said, although the accuracy of location of HI is good (being determined by a seismometer deployed in SAFOD directly above the events), the location of SF and LA with respect to HI is relatively uncertain.

SAFOD Pilot Hole

In preparation for SAFOD, a 2.2-km-deep, near-vertical Pilot Hole was drilled and instrumented at the SAFOD site in the summer of 2002. The Pilot Hole was rotary drilled with a 22.2-cm bit, and cased with 17.8-cm outside diameter (OD) steel casing. The Pilot Hole is currently open to a depth of 1.1 km (explained below) and available for instrument testing, cross borehole experiments, and other scientific studies. Hickman et al. (2004) present an overview of the Pilot Hole experiment.

There were a number of important technical, operational, and scientific findings in the Pilot Hole. These include geologic confirmation of the depth at which the Salinian granites and granodiorites would be encountered (Fig. 3), and calibration of geophysical models with direct measurements of seismic velocities (Boness and Zoback, 2004; Thurber et al., 2004), resistivity (Unsworth and Bedrosian, 2004), density, and magnetic susceptibility (McPhee et al., 2004). In

addition, stress measurements in the Pilot Hole were found to be consistent with the strong crust/weak fault model discussed above (Boness and Zoback, 2004; Hickman and Zoback, 2004). In other words, stress differences in the crust 1.8 km from the San Andreas were high and consistent with Byerlee's law, whereas the direction of maximum horizontal stress in the lower part of the hole was nearly orthogonal to the San Andreas Fault. Furthermore, heat flow measured to 2.2 km depth (Williams et al., 2004) was found to be consistent with shallower data in the region, confirming that the shallow measurements are not affected by heat transport and thus indicate no frictional heat being generated by slip on the San Andreas Fault. Hence, the Pilot Hole confirmed that the SAFOD site was indeed an appropriate site for examining possible explanations for the San Andreas stress/heat flow paradox.

After drilling and downhole measurements were completed, the Pilot Hole was used for deployment of a vertical seismic array to record naturally occurring microearthquakes and to image some of the large-scale structures at depth in the vicinity of the San Andreas (Chavarria et al., 2003; Oye and Ellsworth, 2007). This array was also used to record surface explosions as an important part of the effort to constrain seismic velocities in the vicinity of the borehole for achieving the best possible locations of the target earthquakes (Roecker et al., 2004). Use of the Pilot Hole for experiments such as cross-hole monitoring of time-varying shear velocity (Niu et al., 2008) will continue to produce interesting results for years to come. From an engineering perspective, by establishing the depth to basement and the conditions affecting drilling in the upper sedimentary section, the Pilot Hole helped establish key aspects of the engineering design of the upper part of the SAFOD Main Hole.

SAFOD Main Borehole

A great deal of engineering and operational planning went into SAFOD, since drilling, coring, and scientific measurements in the hostile environment of an active, plate-bounding fault zone had never been attempted before. A number of scientific workshops were held on drilling and downhole measurements, fault zone monitoring, and core handling. In addition, a formal advisory structure was established to take advantage of the knowledge and experience of scientists from universities, the USGS and U.S. Department of Energy (DOE) national labs, and the petroleum industry. A Scientific Advisory Board provided high-level scientific guidance for the project. Technical panels on drilling, coring, and safety, downhole measurements, core handling, and downhole monitoring provided invaluable advice on literally hundreds of issues affecting how the project was eventually carried out.

One of the most important aspects of the SAFOD operational plan that came out of this planning process was to carry out the project in three distinct phases. Phase 1, carried out during the summer of 2004, involved rotary drilling vertically to a depth of ~1.5 km, then steering the well at an angle ~60° from vertical toward the repeating microearthquakes described above (Fig. 3). Note that these earthquakes occur to the southwest of the surface trace of the San Andreas, which indicates that at this location the fault dips steeply to the southwest. By design, Phase 1 ended just outside the San Andreas Fault Zone so that relatively large-diameter (24.4 cm) steel casing could be deployed and cemented in place prior to drilling through the active fault zone where substantial drilling problems might be encountered. Results from a number of scientific studies carried out during Phase 1 were needed to establish key engineering parameters (such as the optimal density of the drilling mud) for drilling through the San Andreas Fault during Phase 2 (Paul and Zoback, 2008).

Phase 2 was carried out during the summer of 2005. A relatively large-diameter (21.6 cm) hole was rotary drilled across the San Andreas Fault Zone (Fig. 3). While many of the key scientific objectives of SAFOD require recovery of core samples from the fault zone, we decided to rotary drill through the fault zone for several reasons. First, rotary drilling is far more robust than core drilling. If the borehole turned out to be unstable due to the rock being highly broken up and chemically altered by faulting (which turned out to be the case), and/or high pore pressure was encountered in the fault zone at depth (which was not the case), it would be much easier to deal with such problems and ensure that we would make it all the way across the fault zone with rotary drilling rather than core drilling. Second, rotary drilling produces a larger diameter hole than core drilling. This was needed to carry out a wide range of sophisticated geophysical measurements (especially well logs) in the fault zone with equipment developed for the petroleum industry. When drilling problems are encountered during coring, it is common for the drill rod to get stuck in the hole. When this happens, the sizes of drill bit and coring rods are reduced so that coring can continue through the bottom of the stuck coring rod. Consequently, the diameter of core holes start relatively small and potentially reduces rapidly. As illustrated below, these geophysical measurements proved to be critical for defining the nature of the overall fault zone as well as the active shear zones within it. The final reason for maintaining a relatively large-diameter hole was related to deployment of the observatory instrumentation in the fault zone after drilling. It was important to complete the well with sufficiently large-diameter casing (17.8 cm) to allow a suite of seismometers and accelerometers to be deployed in the borehole.

Phase 3 was carried out during the summer of 2007; it involved drilling multi-lateral holes which start by milling a hole in the side of the steel casing in the Main Hole. By using multilateral drilling to create secondary holes at optimal locations (a technology that is now commonplace in the petroleum industry), we could direct coring efforts within the most important intervals identified during Phase 2. By

design, the samples and physical property measurements of the fault zone obtained during Phase 2 were not the only information available to us to guide Phase 3 coring operations. Due to accelerated fault creep following the 2004 earthquake, the casing deployed across the fault zone following Phase 2 was deformed at specific places which directly indicated the active strands of the San Andreas at depth.

Phase 1 and 2 Operational Overview. As mentioned above, Phases 1 and 2 were rotary drilled. In order to obtain as much scientific information as possible during drilling, a comprehensive real-time sampling of drill cuttings, drilling fluid, and formation gases in the drilling mud was carried out. Following each phase, a suite of geophysical measurements was obtained, and a limited amount of coring was done at each depth where casing was set.

As can be seen in Fig. 3, the Main Hole starts vertically and at approximately 1.5 km depth; directional drilling techniques were employed to slowly deviate the borehole (eventually at an angle ~60° from vertical) in order to intersect the San Andreas Fault in the vicinity of the repeating target earthquakes. A wide range of information is available online including that related to real-time operations (Table 1). One source of information that provides a convenient overview of Phases 1 and 2 are the Commercial Mud Logs, which deliver also lithologic descriptions of the drill cuttings. Numerous faults were observed in all of the rock units drilled through (Boness and Zoback, 2006). Bradbury et al. (2007) described the mineralogy of drill cuttings in terms of fault zone composition and geologic models.

The first geologic surprise that occurred during Phase 1 was that soon after deviating the borehole toward the San Andreas Fault, we drilled through a major fault zone at a vertical depth of 1.8 km (interpreted to be the Buzzard Canyon Fault, see Fig. 3) as we passed out of the Salinian granitic basement rocks and into previously unknown arkosic sandstones and conglomerates, with some interbedded shales (Boness and Zoback, 2006; Solum et al., 2006). In general, these are strongly cemented rocks that are likely derived from weathering of Salinian granites and granodiorites. Draper Springer et al. (2009) described this section in some detail and pointed to at least a dozen significant faults within it. While they argued for this being a depositional unit formed proximal to the Salinian granite, they suggested that it may have been translated along strike by as much as ~300 km. One reason this unit had not been identified by geophysical surveys through the site area is that these rocks are so strongly cemented that their seismic velocities and resistivity do not vary significantly from the fractured Salinian granites and granodiorites (Boness and Zoback, 2006).

At a measured depth along the borehole of 1460 m (while still drilling in the granite/granodiorite), a planned pause in drilling took place to run steel casing into the hole before further drilling. Prior to casing the hole, a suite of geophysical logs was run. After running the casing into the hole and cementing it in place, 7.9 meters of fractured and faulted hornblende-biotite granodiorite core were obtained. In addition, fluid samples were taken at this depth, and a small-scale hydraulic fracturing experiment was done to constrain the magnitude of the least principal stress.

After drilling resumed, Phase 1 continued to a total vertical depth of 2507 m. As shown in Fig. 3, Phase 1 drilling ended in the arkosic sandstone/conglomerate section. At the end of Phase 1 drilling a second suite of geophysical logs was run. Boness and Zoback (2006) presented a summary of the Phase 1 lithologies and geophysical logs. After cementing steel casing into the wellbore, an 11.6-m core—composed of fractured and faulted arkosic sandstone and conglomerate—was obtained, and fluid sampling was then performed.

One mishap that occurred during Phase 1 was a collision between the Main Hole and the Pilot Hole at 1.1 km depth. Because of the respective layouts of the drilling equipment used for the Pilot and Main Holes, the wellheads of the two boreholes were located only 6.75 m apart. In an attempt to avoid collision of the two holes at depth, repeated gyroscopic surveys of both holes and directional drilling were used. This is commonplace in the oil industry where dozens of wells are often drilled from the same platform or drill site. After the incident, we learned that the collision was caused by poor calibration of one set of the gyroscopic survey instruments. The lasting impact of the hole collision is loss of access to the lower part of the Pilot Hole, as the casing is severely damaged at 1.1 km depth. The Pilot Hole seismic

Table 1. Accessing SAFOD Data Online.

Description	URL
EarthScope Data Portal – Information about and access to all SAFOD EarthScope data and samples	http://www.earthscope.org
IRIS DMC – SAFOD seismological data archive including assembled data sets	http://www.iris.edu/hq
Northern California Earthquake Data Center – Earthquake catalogs and seismograms for all local networks including SAFOD, High-Resolution Seismic Network (HRSN) and NCSN	http://www.ncedc.org/safod/
ICDP Web site – Direct access to all data obtained as drilling, logging and coring operations were underway. Bibliography of SAFOD papers.	http://safod.icdp-online.org
Online Core Viewer – Photographs of all cores and samples taken for scientific study	http://www.earthscope.org/data/safod_core_viewer
Phase 3 Core Atlas – High-resolution images of Phase 3 cores as well as preliminary lithologic and microstructural descriptions	http://www.icdp-online.org/upload/projects/safod/phase3/Core_Photo_Atlas_v4.pdf
General information about the Parkfield Experiment	http://earthquake.usgs.gov/research/parkfield/index.php

array was also lost as a consequence of the accident; the lowermost twenty-five levels were severed during the intersection, and the remaining seven levels were decommissioned in the spring of 2005 when an unsuccessful attempt was made to regain access to the Pilot Hole below the intersection.

During the nine-month hiatus (September 2004 to June 2005) between the end of Phase 1 and the beginning of Phase 2, a number of seismometers were deployed in the SAFOD Main Hole as part of an instrument testing program for eventual deployment of the SAFOD observatory. A number of shots were set off while the seismometers were in the borehole to better constrain the velocity model and reduce uncertainty in the location of the target earthquakes. In addition, an eighty-level, 240-component seismic array was made available by Paulsson Geophysical Services, Inc. (PGSI) and recorded by Geometrics at no cost to the project. This array was deployed in the borehole for a period of five weeks in order to test its suitability for recording microearthquakes and to record additional shots for structural imaging (Chavarria and Goerrtz, 2007). In addition to recording microearthquakes and shots during this period, a tectonic (i.e., non-volcanic) tremor was recorded on this array. The tremor occurred in the lower crust directly below the surface trace of the San Andreas Fault for at least 70 km to the northwest and 80 km to the southeast of SAFOD (Shelly and Hardebeck, 2010). The likely source of the tremor recorded by the PGSI array was in the vicinity of the energetic tremor source near Cholame (Nadeau and Dolenc, 2005) near the base of the crust (~25 km; Shelly and Hardebeck, 2010).

As shown in Fig. 3, Phase 2 drilling passed from the arkosic sandstones and conglomerates into mudstones and shales at a depth of 2600 m, and at a position ~500 m southwest of the surface trace of the San Andreas Fault. Microfossil evidence from core obtained at the bottom of the Phase 2 hole indicates that these formations are part of the Cretaceous Great Valley sequence, which was deposited on the North American plate in a forearc environment at a time when subduction was occurring along the western margin of California (K. McDugall, pers. comm., 2005). In the long-term geologic sense, the contact between the Salinian-derived arkosic sandstones and conglomerates and the Great Valley formation is the boundary between the Pacific and North American plates. As shown by progressive deformation of the casing discussed below (Fig. 4), the south-westernmost of the active traces of the San Andreas Fault Zone at depth is located several tens of meters to the northeast of this geologic boundary.

No evidence was found that we had encountered the Franciscan Formation in the borehole, even though it is exposed at the surface about 600 m east of the San Andreas Fault (Fig. 3), and was predicted by several of the geophysical surveys conducted in advance of drilling. However, there is evidence of serpentinite directly within the fault zone associated with either the Coast Range ophiolite or Franciscan formation. Hence, there is likely serpentinite in contact with the San Andreas along strike and/or at greater depth. A reasonable conceptual model is that slivers of Great Valley and the Franciscan are intermixed at depth along the fault, just as they are found in surface exposures at several locations in central California.

Rotary drilling through the San Andreas Fault during Phase 2 was accomplished with no small amount of difficulty—some caused by the fault zone, some caused by unrelated operational problems (for example, the top drive, an extremely important component of the drill rig, broke and was inoperable for two weeks). We also noted a considerable degree of time-dependent wellbore failure (Paul and Zoback, 2008), especially after passing through the active traces of the San Andreas Fault Zone. An appreciable amount of time was required to clean the hole through wash and ream operations. In fact, the combined result of time-dependent wellbore instabilities and a mistake by the drilling crew resulted in the drillstring being stuck in the hole for four days at a vertical depth of 2800 m. Despite these problems, drilling across the entire fault zone was successfully achieved. Comprehensive cuttings and gases were sampled over the entire Phase 2 interval (Table 2), and a number of geophysical measurements were made in real-time as drilling across the fault zone was underway (Run 4, Table 3). After the hole was drilled, a comprehensive suite of geophysical logs was obtained, and fifty-two 19-mm-diameter side-wall cores were obtained in the open hole (Run 4, Table 3). After the hole was cased and cemented, 3.9 meters of core (mudstones of the Great Valley formation, mentioned above) were obtained from the very bottom of the hole.

Phase 1 and 2 Real-time Sampling. Drill cuttings and formation gases were collected in real time as drilling was taking place. Drill cuttings were collected every 3 m and preserved in both washed and unwashed states, and larger volumes of cuttings were collected at less frequent intervals, as were samples of the drilling mud. Table 2 summarizes the cuttings samples, side-wall cores, and the three cores obtained after casing was cemented into place at various depths. Photographs, detailed descriptions, and other information about the extensive collection of cuttings are available online (Table 1). A summary of the lithologies encountered during Phases 1 and 2 is provided by Solum et al. (2006) and Bradbury et al. (2007), principally based on X-ray diffraction (XRD) analyses and optical analyses of mineralogy and texture of the cuttings, augmented by the spot and sidewall cores.

The near-continuous collection of cuttings revealed a number of lithologic changes along the trajectory of the hole that correlated very well with geophysical logs and other information. In addition, analysis of these cuttings revealed trace amounts of serpentine and a high level of clay minerals in the localized intervals that proved to be the active San

Table 2. Summary of Physical Samples Obtained from SAFOD.

Types of samples	Phase 1	Phase 2	Phase 3
Washed cuttings, small sample bags	3 sets, every 3 m	3 sets, every 3 m	intermittent depths
Washed cuttings, large (15 cm x 25 cm) sample bags	every 30 m	every 30 m	
Washed cuttings, large (25 cm x 43 cm) sampole bags	every 91 m	every 91 m	
Unwashed cuttings	every 3m	every 3 m	
Drilling mud	every 30 m	every 30 m	
Core	8.5 m at 1.5 km MD, 10 cm diameter	3.7 of 6.6 cm diameter core at 4 km MD	Core 1.1 run, 11.08 m 3141.1–3153.6 m MD 10 cm diameter
	11 m at 3.0 km MD, 10 cm diameter		Core 2 runs 1–3, 12.03 m, 3186.7–3200.4 m MD 10 cm diameter Core 3 runs 4–5, 16.15 m, 3294.9–3313.5 m MD 10 cm diameter
Sidewall cores		52 small (2 cm dia. x 2.5 cm) side wall cores between 3.1 and 4.0 km MD	
Miscellaneous rock samples	3 samples	40 samples	

Andreas Fault Zone (Solum et al., 2006). Moore and Rymer (2007) demonstrated that some of the serpentinite in the fault zone has been altered to talc, an unusual mineral in that it has exceptionally low frictional strength and is thermodynamically stable over the range of depths and pressures characteristic of the upper crust in this region. They speculated that if talc is widespread in the fault zone, it could explain both the strength of the fault and its creeping behavior.

Gases coming into the well as the borehole was being drilled yielded a great deal of useful data. This technology, in which gas is separated from the drilling mud as it comes to the surface, was also used in the Pilot Hole where gas anomalies correlated with shear zones in the granite/granodiorite (Erzinger et al., 2004). During Phases 1 and 2, implementation of this technology showed a number of important correlations with major faults and geologic boundaries. One finding of particular interest reported by Wiersberg and Erzinger (2007) is that there is a marked difference in the concentration of $^{3}He/^{4}He$ across the San Andreas Fault. On the southwest side of the fault this ratio is ~0.4, whereas on the northeast side of the fault it is ~0.9. This data and differences in the relative concentrations of hydrogen, carbon dioxide, and methane on the two sides of the fault indicate that the San Andreas Fault has very low permeability and hydrologically separates the Pacific and North American plates (Wiersberg and Erzinger, 2008).

Downhole Measurements. A wide range of downhole measurements was carried out as part of SAFOD Phases 1 and 2 (Table 3). As the structure and properties of the San Andreas Fault Zone are of most importance, we show in Fig. 4A a summary of the geophysical logs from Phase 2 along with some of the main lithologic units encountered.

An approximately 200-m-wide damage zone of anomalously low P- and S-wave velocities and low resistivity (Fig. 4A) is interpreted to be the result of both physical damage and chemical alteration of the rocks due to faulting as well as the unusual, fault-related minerals (discussed above) that were noted during drilling. There are also a number of localized zones where the physical properties are even more anomalous. Repeated measurements of the shape of the steel casing deployed in the borehole revealed that the steel casing was being deformed by fault movement in at least two places. Figure 4C shows the casing radius (as measured using a 40-finger caliper) as a function of position around the hole. While the amount of deformation associated with the 3302-m shear zone is more pronounced than the

Table 3. SAFOD Geophysical Logging Data.

Run	Depth Range (Measured Depth)	Logging Technique	Parameters Measured
Run 1	602.5–1443.5 m	Open Hole, Wireline	Density, porosity, gamma, caliper, resistivity, cross-dipole sonic velocity, FMI
Run 2a	1368–2030 m	Open Hole, Wireline	Density, porosity, gamma, caliper, resistivity, sonic velocity, FMI, UBI, ECS
Run 2b	1890–3043 m	Open Hole, Pipe Conveyed	Density, porosity, gamma, caliper, resistivity, sonic velocity, FMI
Run 3	1356–3033 m	Cased Hole, Wireline	Sonic velociy, elemental chemistry, cement bond
Run 4	3045–3712 m	Open Hole, Logging While Drilling	Density, porosity, gamma, caliper, resistivity, FMI
Run 5	3045–3965 m	Open Hole, Pipe Conveyed	Density, porosity, gamma, caliper, resistivity, sonic velocity, FMI
Runs 6–11*	2953–3815 m	Cased Hole, Wireline	Caliper, direction, temperature

* Runs 6–11 include caliper logs run 6 different times between September 2005 and June 2007

3192-m shear zone, both of these zones represent portions of the overall San Andreas Fault Zone in which active creep deformation is occurring. We refer to the actively deforming zones at 3192 m as the Southwest Deforming Zone (SDZ) and 3302 m as the Central Deforming Zone (CDZ). Note the remarkable similarity of the anomalously low compressional (Vp) and shear (Vs) wave velocities and resistivity within these two deformation zones (Fig. 4B). These two shear zones were primary targets for coring during Phase 3.

The HI earthquake cluster occurs on the SDZ about 100 m below the point where the borehole passed through this fault (Fig. 1). Recent relocations of the SAFOD target earthquakes indicate that the SF/LA cluster correlates with the fault at 3413 m, as shown in Fig. 2D (Thurber et al., 2010). This fault defines the northeastern edge of the damage zone and has geophysical characteristics very similar to the SDZ and CDZ (Fig. 2A); hence, it has been designated as the Northeast Boundary Fault (NBF). However, unlike the SDZ and CDZ, no casing deformation was detected on the NBF in any of the caliper logs run in 2005 through 2007 (Runs 6–11, Table 3).

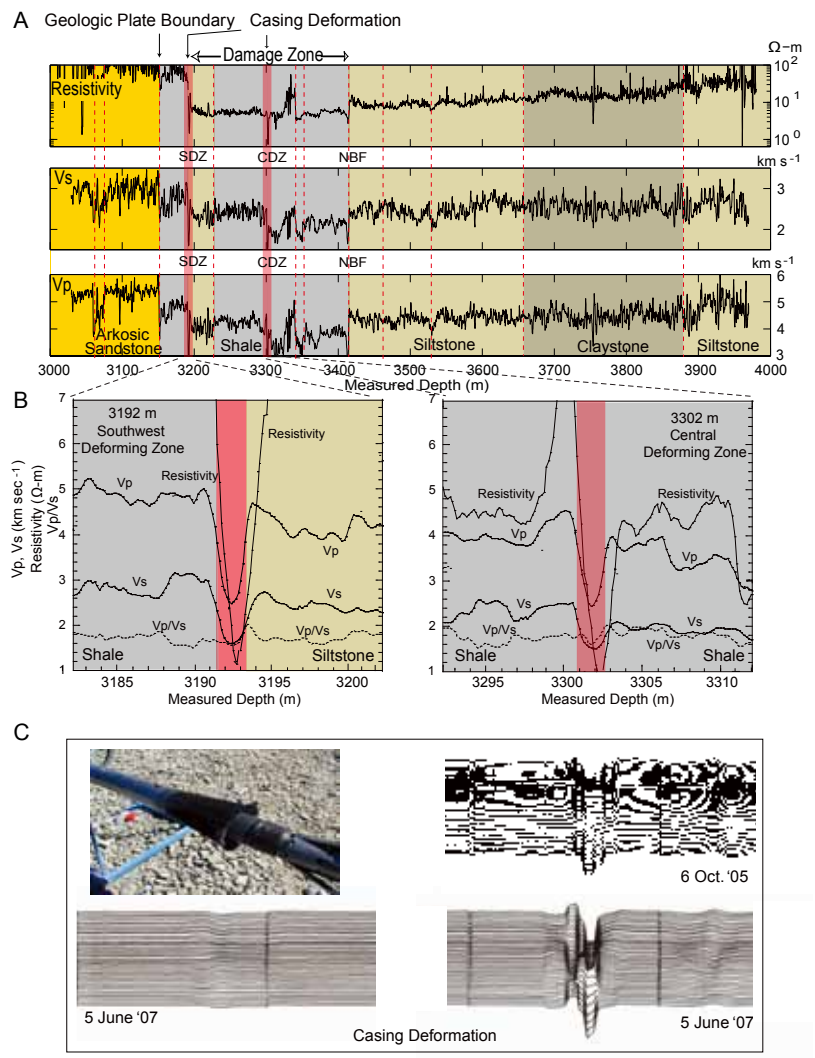

Figure 4. [A] Selected geophysical logs and generalized geology as a function of measured depth along the Phase 2 SAFOD borehole. The dashed red lines indicate some of the many faults encountered. The thick red lines indicate where fault creep deformed the Phase 2 cased borehole at the SDZ and CDZ. Depth in this figure represents the measured depth along the length of the wellbore. [B] The SDZ and CDZ correlate with localized zones (shown in red) where the geophysical log properties from Phase 2 are even more anomalous than in the surrounding damage zone. The same is true of the fault at the northeast boundary of the damage zone, the NBF. [C] After the borehole was cased and cemented, a 40-finger caliper (see photo) was used to measure the casing radius at various times (the depth scales are the same as in [B]). The caliper data obtained on 6 October 2005 showed significant casing deformation within the CDZ. When the casing was resurveyed on 5 June 2007, more deformation was observed at the depth of the CDZ, and slight deformation was observed at the SDZ. Although the NBF is geophysically quite similar to the SDZ and CDZ (see [A]) and is associated with the SF and LA earthquake sequences (Figs. 2 and 3), no casing deformation was identified at that depth.

A number of other important downhole measurements were made during Phases 1 and 2. Boness and Zoback (2006) reported that to within 200 m of the active trace of the fault, the direction of maximum horizontal stress remains at a high angle to the San Andreas Fault, consistent with measurements made in SAFOD at greater distances and with regional data that imply that fault slip occurs in response to low resolved shear stress. Zoback and Hickman (2007) reported that stress magnitudes are consistent with the prediction of high mean stress within the fault zone (Rice, 1992; Chery et al., 2004) and a classical Anderson/Coulomb reverse/strike-slip stress state outside it. Together with the stress state determined in the Pilot Hole (Hickman and Zoback, 2004), the results from the SAFOD Main Hole are consistent with a strong crust/weak fault model of the San Andreas. Almeida et al. (2005) carried out a paleostress analysis using slip directions on the faults encountered in the core obtained at the end of Phase 1 and also found a direction of maximum horizontal compression at a very high angle to the San Andreas Fault.

Further support for the low frictional strength of the San Andreas comes from temperature measurements in the SAFOD Main Hole. Heat flow data from the Pilot Hole were consistent with measurements made at relatively shallow depth and imply no frictionally generated heat by the San Andreas Fault (Williams et al., 2004). Heat flow measurements made in the Main Hole indicate no systematic change in temperature as a function of distance from fault. Hence, these data are also consistent with an absence of frictionally generated heat (Williams et al., 2005).

The possibility of extremely high pore pressure within the San Andreas Fault

Zone (near or above the weight of the overburden) has been one of the leading hypotheses to explain its low frictional strength (Rice, 1992). Two lines of evidence indicate an absence of severely elevated pore pressure (near-lithostatic, or greater) within the fault zone required to explain the low frictional strength of the San Andreas. Highly elevated fluid pressures were not observed during drilling in the fault zone. Such pressures would have resulted in influxes of formation fluid into the wellbore if the pore pressure was appreciably greater than the drilling mud pressure. While the density of the drilling mud was about 40% greater than hydrostatic pore to stabilize the borehole, in the strike slip/reverse faulting stress state that characterizes the SAFOD area (Hickman and Zoback, 2004), pore pressures within the deforming fault zone would have to exceed the overburden stress in Rice's model (1992) for a weak fault in an otherwise strong crust. In addition, analysis of the rates of formation gas inflow during periods of no drilling (Wiersberg and Erzinger, submitted) shows no evidence of elevated pore pressure within the fault zone relative to the country rock, and the Vp/Vs ratio is relatively uniform (~1.7) across the ~200-m-wide damage zone and the localized shear zones within it (Fig. 4B). As Vp decreases severely at very elevated pore pressure (i.e., at very low effective stress), Vs would not be affected as much, and the Vp/Vs ratio would be expected to decrease (Mavko et al., 1998). Altogether, none of these observations indicate the presence of anomalously high pore pressure in the fault zone.

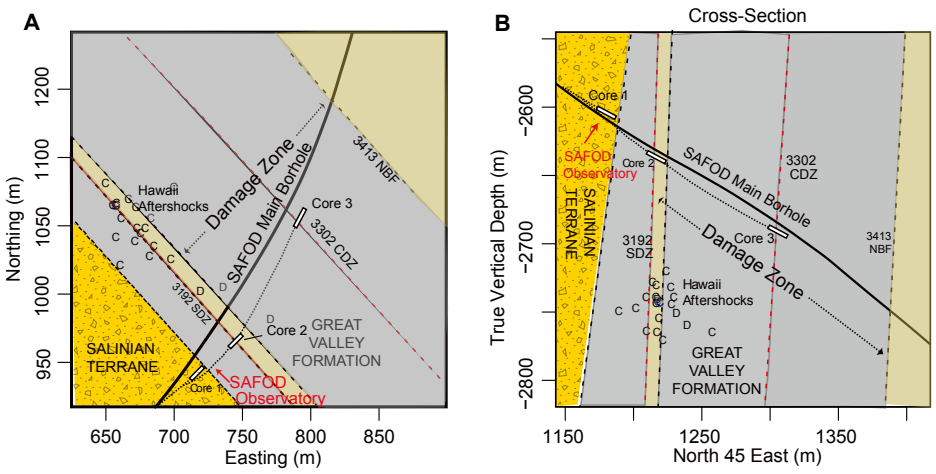

Figure 5. [A] Map view and [B] cross-section of the trajectory of the rotary-drilled SAFOD main borehole as it passed through the San Andreas Fault Zone at a depth of ~2700 m, as well as the trajectories of the sidetrack boreholes used to obtain core samples along the actively deforming traces of the fault during Phase 3. Note the positions of the SDZ, CDZ, and NBF and the extent of the damage zone as defined in Figs. 2, 3, and 4. Also shown are single-station locations of the aftershocks of the 11 August 2006 Hawaii target earthquake recurrence; these were made using a seismometer in the main hole at a true vertical depth of 2660 m. The "C" and "D" symbols refer to the polarity of the P-wave from each aftershock. Because the borehole seismometer is offset to the northeast from the fault trace, the transition from "C" to "D" occurs where expected for right lateral slip on the fault.

Phase 3 – Coring the San Andreas Fault Zone

During Phase 3 the SAFOD engineering and science teams successfully exhumed 39.9 meters of 10-cm-diameter continuous core, including cores from the two actively deforming traces of San Andreas Fault Zone (the SDZ and CDZ; Zoback et al., 2010). Figure 5 shows the sidetracks drilled laterally off the SAFOD main borehole in map and cross-sectional views. Note the position of the cores with respect to the various contacts and shear zones described above. As shown, Core 1 was obtained close to the contact between the arkosic sandstones and conglomerates of the Salinian Terrane and the shales, mudstones and siltstones associated with the Great Valley Formation. The first sidetrack was abandoned and cemented off after retrieving Core 1 due to a drilling mishap. A second sidetrack was undertaken that enabled us to obtain Cores 2 and 3 (Table 2) across the SDZ and CDZ. After obtaining the cores across the active shear zones, the hole was slightly enlarged to allow for installation of 18-cm-diameter casing and eventual deployment of the SAFOD observatory. The casing was installed and cemented to a measured depth of 3214 m (as measured in the Phase 3 hole), which is ~17 m beyond the center of the SDZ as extrapolated from the Phase 2 to the Phase 3 holes. The casing could not be installed to greater depth in the Phase 3 hole due to progressive borehole instability and bridging.

When the cores reached the surface, they were carefully cleaned, labeled, and photographed, and they have been stored at 4°C to prevent desiccation and microbial activity. The core is currently stored at the IODP Gulf Coast Repository (GCR) at Texas A&M University. High-resolution photographs and descriptions of all Phase 3 cores (as well as supplemental information including thin-section analysis, results from preliminary XRD analysis and core-log depth integration) are presented in a comprehensive Core Atlas (Table 1). One page of the core atlas is presented in Fig. 6, which shows a section of the core that crosses the SDZ. The foliated gouge matrix is highly altered, both chemically (e.g., there is much less silica and different clay mineralogy than observed in the rocks outside the fault zone) and mechanically (e.g., there is pervasive shearing observed on planes of varied orientation within the core). Clasts of various types of rock are seen in the gouge matrix, most notably clasts of serpentinite including a large piece of sheared serpentinite with calcite veins.

To date, over 350 samples from the Phase 3 core have been distributed to investigators from around the world for laboratory analyses and testing; the latest results from these studies were discussed at two SAFOD special sessions of the 2010 annual meeting of the American Geophysical Union. These include studies of the mineralogy and chemical evolution of the fault zone, the physical properties of fault zone materials, the frictional strength of fault and country rock under a wide variety of loading conditions, and the evolution of deformation mechanisms and fluid-rock interaction within the fault zone over time. Procedures for requesting samples or gaining access to the SAFOD thin-section collection are available online (Table 1). The GCR staff is responsible for maintaining records of core, cuttings and fluid sample requests filled; names of people to whom these samples were provided; and the final disposition of samples (date samples returned and condition of samples). The GCR staff is also responsible for entering data and results from SAFOD sample investigations into the EarthScope Data Portal, which is currently under construction (Table 1).

SAFOD Observatory

In preparation for the establishment of a geophysical observatory deep within the fault, a series of nineteen temporary deployments of seismometers, accelerometers, and tiltmeters in the Main Hole and an additional eight deployments in the Pilot Hole were conducted between 2002 and 2008, leading up to the deployment of the SAFOD observatory in September 2008 (data available online, Table 1).

Seismic data collected during the temporary deployments are yielding important new findings on the structure of the San Andreas Fault and properties of the earthquakes that it produces. By combining surface and borehole observations of surface explosions and local earthquakes with double-difference tomography, Zhang et al. (2009) determined a detailed Vp, Vs, and Vp/Vs model for the SAFOD crustal volume. Their results refined earlier tomographic models for SAFOD to clearly image a deep low-velocity zone along the San Andreas Fault. This low-velocity zone supports the propagation of both P- and S-type fault zone guided waves. Observation of these waves on seismometers placed inside the fault zone places strong constraints on its geometry and continuity. Ellsworth and Malin (in press) determined that the low-velocity zone in which these waves propagate coin-cides with the zone of extensive rock damage seen in the downhole measurements (Fig. 4). The waveguide extends to the northwest and southeast of SAFOD for at least 8 km. Wu et al. (2010) used the dispersion properties of the S-type guided waves recorded in the Main Hole to show that the low-velocity wave-guide extends downward to near the base of the seismogenic zone at 10–12 km depth.

The short hypocentral distances and high-Q environment of the SAFOD boreholes make it possible to study source parameters to smaller magnitude than with data from instruments in shallow boreholes or on the surface. Only a small fraction (<1%) of the San Andreas Fault surface near SAFOD produces earthquakes, with the remainder of the fault moving through aseismic creep. The earthquakes that do occur are predominately located within clusters of repeating events. Static stress drops range from as low as 0.1 MPa to 100 MPa (Imanishi and Ellsworth, 2006). The upper limit is comparable to the laboratory-derived frictional strength of the country rock from outside of the damage zone (Lockner et al., in press). McGarr and Fletcher (2010) determined the yield stress for a repeat of the SF target earthquake of 64 MPa. These results suggest that the target events and other repeating earthquakes occur where the fault juxtaposes normal crustal rocks patches embedded within an otherwise weak, creeping fault. As a consequence, there is no contradiction between such high stress drop events and an intrin-sically weak, creeping San Andreas Fault in a strong crust, as indicated by the *in situ* stress and heat-flow measurements in the SAFOD Pilot Hole and Main Hole.

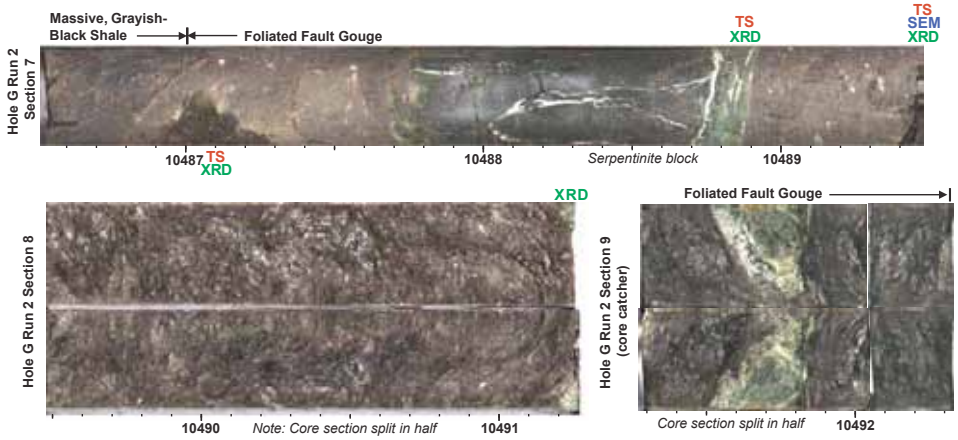

Figure 6. Photographs of the section of core 2 that crosses the SDZ (see Figs. 4 and 5) as they appear in the Photographic Atlas of the SAFOD Phase 3 (Table 1). The colored lettering indicates where samples were used for TS, XRD, and SEM presented in the Phase 3 Core Atlas. Note that the center and bottom photos are of the core sections split in half. Measured depths (in the sidetrack) are shown in feet (1 ft=30.48 cm).

The twenty-seven experimental deployments also guided the selection of sensors for the observatory and revealed mechanical and environmental issues that dictated the design of the observatory. The ambient temperature of up to 120°C at the planned depth of the observatory controlled the choice of downhole electronics and sensors. More seriously, the borehole fluid contains gases that penetrate past conventional O-rings and wireline insulation. Consequently, a design was

selected that isolated all electrical and optical control lines and all sensors from contact with the wellbore fluid. The system was designed to be positively coupled to the casing and fully retrievable for maintenance when required.

The installation of the SAFOD observatory was completed on 28 September 2008. The observatory instruments were deployed approximately 100 m above the Hawaii target earthquake zone (Figs. 2, 5). As shown schematically in Fig. 7, the observatory instrumentation consisted of five pods containing different types of sensors. Pods 1 and 3 each contained a 3-component seismometer and a 3-component accelerometer, Pods 2 and 4 each contained a 2-axis tiltmeter, and Pod 5 contained a 3-component seismometer and accelerometer as well as a passive electromagnetic (EM) coil. The goal of the EM ex-periment was to determine if electromagnetic waves are radiated by the earthquake source. All of the instruments were housed in sealed steel pods that isolate them from contact with the wellbore fluids. The pods were attached to the outside of steel pipe (6-cm 'EUE' tubing) and coupled to the casing by decentralizing bow springs. The seismic and tilt systems were completely independent of each other, with separate power and data telemetry lines encapsulated in 6.4-mm-diameter stainless steel tubing with pressure-tight connections in and out of the pods.

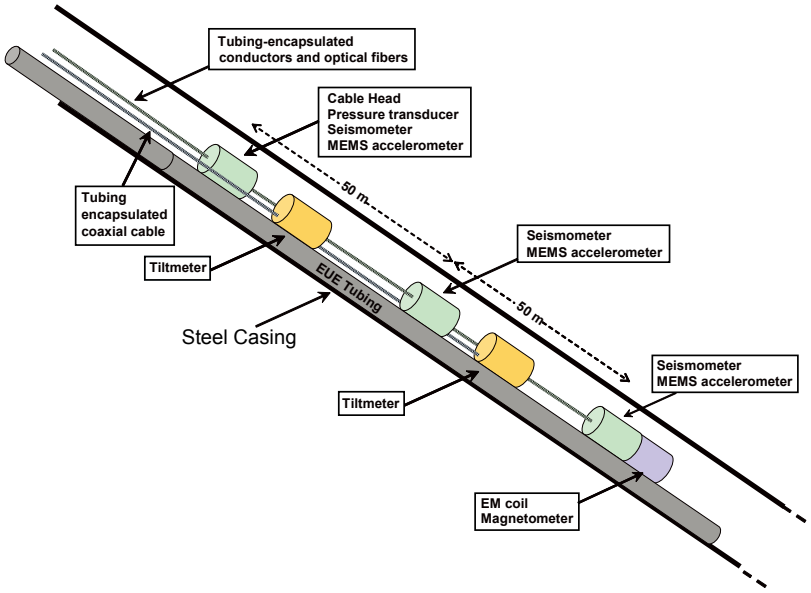

Figure 7. Schematic diagram of the instrumentation deployed in the SAFOD observatory above the location of the HI repeating earthquake sequence (see Fig. 5).

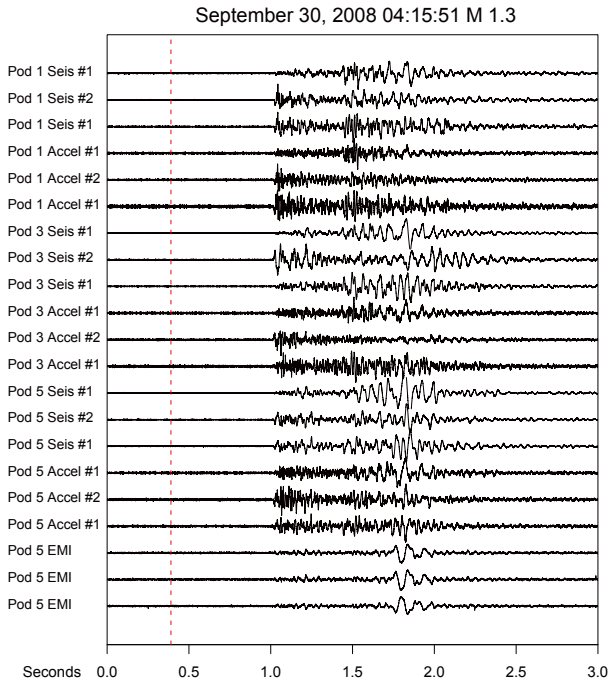

Figure 8. Seismograms from an M 1.3 microearthquake on 30 September 2008 recorded on the SAFOD observatory. The origin time of the microearthquake is shown by the dashed red line. The lower three traces are the output of the passive electromagnetic coil.

The seismic system was based on the Oyo Geospace DS150 digital borehole seismometer with a set of 3-component, 15-Hz Omni-2400 geophones in each sonde. MEMS accelerometers replaced the geophones in additional DS150 units. The passive EM coil in Pod 5 was also digitized by a DS150. Fiber-optic telemetry was used to transmit the 4000-sample-per-second data from all seven DS150 units to the surface, where they were recorded on a USGS Earthworm computer system. The Earthworm system archived the data locally on LT3 tapes, downsampled selected channels to 250 samples per second and transmitted them to the Northern California Seismic Network (NCSN) where they were integrated into the real-time data system and archived at the Northern California Earthquake Data Center (NCEDC). Continuous full-sample-rate data are archived at the NCEDC and at the IRIS Data Management Center. The two borehole tiltmeters were manufactured by Pinnacle Technologies. Each tiltmeter produced two channels of tilt data—recorded at one sample per 3 seconds—which were transmitted to the NCEDC for processing and archiving.

An example of the data produced by the SAFOD observatory instruments is shown (Fig. 8) for an earthquake located ~2.5 km from the array. The EM trace appears three times because the EM signal was recorded at three different gains. Note that the EM signal appears at the same time as the seismic waves. Hence, the EM signal is the result of shaking of the coil within the Earth's magnetic field by the seismic waves as they pass the instrument.

Unfortunately, the SAFOD observatory instruments began to develop electronic problems soon after installation, and attempts to keep the instruments running were ultimately unsuccessful. An expert panel convened by NSF is currently in the process of examining the failed instrumentation. Leakage of water into pods was the probable cause of failure, although the actual failure point will not be known until the NSF panel report is completed. Fortunately, the SAFOD observatory was designed to permit ongoing access to the deepest part of the Main Hole through the inside of the EUE tubing (Fig. 7) to which the instrument pods were attached. A seismometer with three 15-Hz Omni-2400 geophones was deployed on wireline inside the EUE tubing in early December 2008, and this continues to operate as of March 2011. Data are digitized at the surface at 1000 samples per second and transmitted directly into the NCSN and are archived at the NCEDC (Table 1). While not a substitute for the observatory's full suite of digital seismometers and accelerometers, this interim instrument has allowed continuous observation of the target earthquakes to continue, and has produced important data including recordings of the SF and LA target earthquakes repeat in December 2008 (Fig. 9). The temporary geophone is planned to remain in operation until NSF develops a plan for installation of a new observatory.

In addition to the SAFOD observatory, an optical-fiber interferometric strainmeter was permanently installed at the conclusion of Phase 1 drilling in 2004 (Blum et al., 2010). Two optical-fiber loops were placed in the annulus formed by the 311-mm inside diameter (ID) initial casing and the 245-mm OD casing. The fiber sensors were attached to the outside of the inner casing as it was lowered into the well and then cemented in place. Each loop was anchored at the upper end at 9 m depth. One loop was anchored at the lower end at 864 m, and the other at 782 m, making strainmeters of 855 m and 773 m length, respectively. Although the longer loop failed in September 2007, vertical strain data continues to be produced from the shorter loop. Coseismic strain steps for local events have been reported by Blum et al. (2010) that are in general agreement with elastic dislocation theory.

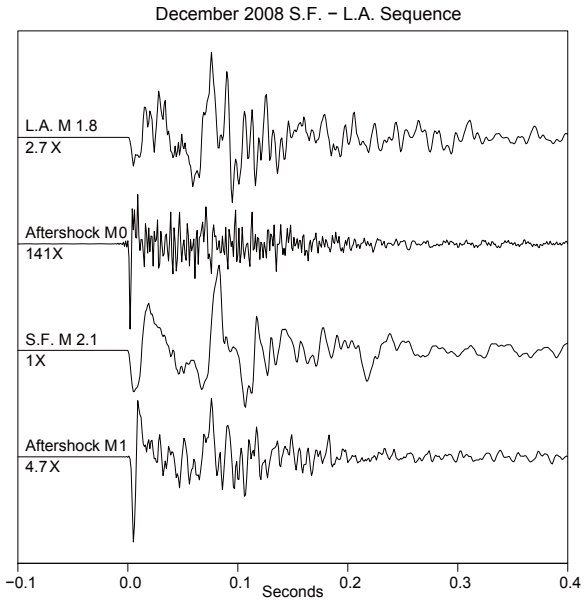

Figure 9. Seismograms from an SF and LA repeating earthquake sequence that occurred in December 2008. This earthquake was recorded on a 3-component seismometer deployed within the EUE tubing at a position just above the SAFOD observatory.

Summary

We have already learned much about (i) the structure and physical properties of the fault zone at depth, (ii) the composition of fault zone rocks, (iii) the stress, temperature, and fluid pressure conditions under which earthquakes occur, and (iv) the absence of deep-seated fluids in fault zone processes. With the distribution of the Phase 3 core to researchers around the world now underway, we can expect new insights into the physical and chemical mechanisms controlling faulting and fault zone evolution within this major plate boundary fault. In addition, the observatory, even in its currently reduced state, is providing high-quality near-field seismograms that may lead to novel observations of rupture nucle-ation and other insights into the nature of the earthquake source and structure of the fault at seismogenic depth.

Acknowledgements

Scores of scientists, graduate students, engineers and technicians too numerous to name contributed immeasurably to the success of SAFOD. We would particularly like to thank Louis Capuano and Jim Hanson of ThermaSource, Inc., the prime drilling contractor, and the many individuals who served on the SAFOD Advisory Board and Technical Panels. We would especially like to thank Roy Hyndman of the Pacific Geoscience Center who served as Chair of the SAFOD Advisory Board. Funding for the project was provided by the NSF's EarthScope Program, with additional support from the USGS, the ICDP, Stanford University, and NASA. Any use of trade, product, or firm names is for descriptive purposes only and does not imply endorsement by the U.S. government.

References

Almeida, R., Chester, J., Chester, F., Kirschner, D., Waller, T., and Moore, D., 2005. Mesoscale structure and lithology of the SAFOD Phase I and II core samples. *Eos Trans. AGU*, 86 (52), Fall Meeting Suppl., Abstract T21A-0451.

Bakun, W., and McEvilly, T., 1984. Recurrence models and Parkfield, California, earthquakes. *J. Geophys. Res.*, 89(B5): 3051–3058.

Blum, J., Igel, H., and Zumberge, M., 2010. Observation of Rayleigh-wave phase velocity and coseismic deformation using an optical fiber, interferometric vertical strainmeter at the SAFOD Borehole, California. *Bull. Seismol. Soc. Am.*, 100(5A):1879–1891, doi:10.1785/0120090333.

Boness, N., and Zoback, M.D., 2004. Stress-induced seismic velocity anisotropy and physical properties in the SAFOD Pilot Hole in Parkfield, CA. *Geophys. Res. Lett.*, 31:L15S17, doi:10.1029/2003GL019020.

Boness, N., and Zoback, M.D., 2006. A multi-scale study of the mechanisms controlling shear velocity anisotropy in the San Andreas Fault Observatory at Depth. *Geophysics*, 7(5):F131–F146, doi:10.1190/1.2231107.

Bradbury, K.K., Barton, D.C., Solum, J.G., Draper, S.D., and Evans, J.P., 2007. Mineralogic and textural analyses of drill cuttings from the San Andreas Fault Observatory at Depth (SAFOD) boreholes: initial interpretations of fault zone composition and constraints on geologic models. *Geosphere*, 3(5):299–318, doi:10.1130/GES00076.1.

Chavarria, J., and Goerrtz, A., 2007. The use of VSP techniques for fault zone characterization: an example from the San Andreas Fault. *The Leading Edge*, 26(6):770–776, doi:10.1190/1.2748495.

Chavarria, J., Malin, P., Catchings, R., and Shalev, E., 2003. A look inside the San Andreas fault at Parkfield through vertical seismic profiling. *Science*, 302(5651):1746, doi:10.1126/science.1090711.

Chery, J., Zoback, M.D., and Hickman, S., 2004. A mechanical model of the San Andreas fault and SAFOD pilot hole stress measurements. *Geophys. Res. Lett.*, 31(15):L15S13, doi:10.1029/2004GL019521.

Draper Springer, S.D., Evans, J.P., Garver, J.I., Kirschner, D., and Janecke, S.U., 2009. Arkosic rocks from the San Andreas Fault Observatory at Depth (SAFOD) Borehole, Central California: implications for the structure and tectonics of the San Andreas fault zone. *Lithosphere*, 1:206–226, doi:10.1130/L13.1.

Ellsworth, W.L., and Malin, P., in press. Deep rock damage in the San Andreas Fault revealed by P- and S-type fault zone guided waves. *In* Fagereng, A., Toy, V.G., and Rowland, J. (Eds), *Geology of the Earthquake Source: A Volume in Honor of Rick Sibson:* London (Geological Society of London).

Erzinger, J., Wiersberg, T., and Dahms, E., 2004. Real-time mud gas logging during drilling of the SAFOD pilot hole in Parkfield, CA. *Geophys. Res. Lett.*, 31(15): L15S18, doi:10.1029/2003GL019395.

Harris, R.A., and Arrowsmith, J.R., 2006. Introduction to the special issue on the 2004 Parkfield earthquake and the Parkfield earthquake prediction experiment. *Bull. Seismol. Soc. Am.*, 96(4B):S1–S10, doi:10.1785/0120050831.

Hickman, S., 1991. Stress in the lithosphere and the strength of active faults. *In* Shea, M.A. (Ed.), *U.S. National Report International Union Geodesy and Geophysics, 1987–1990: Contributions in Tectonophysics:* Washington, DC (American Geophysical Union), 759–775.

Hickman, S., and Zoback, M.D., 2004. Stress measurements in the SAFOD pilot hole: implications for the frictional strength of the San Andreas fault. *Geophys. Res. Lett.*, 31:L15S12.

Hickman, S., Zoback, M.D., and Ellsworth, W., 2004. Introduction to special issue: preparing for the San Andreas fault observatory at depth. *Geophys. Res. Lett.*, 31:L12S01, doi:10.1029/2004GL020688.

Imanishi, K., and Ellsworth, W.L., 2006. Source scaling relationships of microearthquakes at Parkfield, CA, determined using the SAFOD Pilot Hole seismic array. *In* Abercrombie, R., McGarr, A., Di Toro, G., and Kanamori, H. (Eds.), *Earthquakes: Radiated Energy and the Physics of Faulting, Geophysical Monograph Series 170:* Washington, DC (American Geophysical Union), 81–90.

Lachenbruch, A.H., and Sass, J.H., 1980. Heat Flow and Energetics of the San Andreas Fault Zone. *J. Geophys. Res.*, 85(11):6185–6223.

Lachenbruch, A.H., and J.H. Sass, 1992. Heat flow From Cajon Pass, fault strength and tectonic implications. *J. Geophys. Res.*, 97(B4):4995–5015, doi:10.1029/91JB01506.

Lockner, D.A., Morrow, C., Moore, D.E., and Hickman, S., in press. Low strength of deep San Andreas Fault gouge from SAFOD core. *Nature*.

Mavko, G., Mukerjii, T., and Dvorkin, J., 1998. *Rock Physics Handbook:* Cambridge, U.K. (Cambridge University Press).

McGarr, A., and Fletcher, J.B., 2010. Laboratory-based maximum slip rates in earthquake rupture zones and radiated energy. *Bull. Seismol. Soc. Am.*, 100(6):3250–3260, doi:10.1785/0120100043.

McPhee, D.K., Jachens, R.C., and Wentworth, C.M., 2004. Crustal structure across the San Andreas Fault at the SAFOD site from potential field and geologic studies. *Geophys. Res. Lett.*, 31(12):L12S03, doi:10.1029/2003GL019363.

Moore, D.E., and Rymer, M.J., 2007. Talc-bearing serpentinite and the creeping section of the San Andreas fault. *Nature*, 448(16):795–797, doi:10.1038/nature06064.

Mount, V.S., and Suppe, J., 1987. State of stress near the San Andreas fault: implications for wrench tectonics. *Geology*, 15:1143–1146, doi:10.1130/0091-7613(1987)15<1143:SOSNTS>2.0.CO;2.

Murray, J., and Langbein, J., 2006. Slip on the San Andreas fault at Parkfield, California, over two earthquake cycles, and the implications for seismic hazard. *Bull. Seismol. Soc. Am.*, 96:S283–S303, doi:10.1785/0120050820.

Nadeau, R., and Dolenc, D., 2005. Nonvolcanic tremors deep beneath the San Andreas fault. *Science*, 307(5708):389, doi:10.1126/science.1107142.

Nadeau, R.M., McEvilly, T.V., Michelini, A., Uhrhammer, R.A., and Dolenc, D., 2004. Detailed kinematics, structure and recurrence of micro-seismicity in the SAFOD target region. *Geophys. Res. Lett.*, 31:L12S08.

Niu, F., Silver, P.G., Daley, T.M., Cheng, X., and Majer, E., 2008. Preseismic velocity changes observed from active source monitoring the Parkfield SAFOD drill site. *Nature*, 454:204–208, doi:10.1038/nature07111.

Oppenheimer, D.H., Reasenberg, P.A., and Simpson, R.W., 1988. Fault-plane solutions for the 1984 Morgan Hill California earthquake sequence: evidence for the state of stress on the Calaveras fault. *J. Geophys. Res.*, 93:9007–9026, doi:10.1029/JB093iB08p09007.

Oye, V., and Ellsworth, W.L., 2007. Small-scale structures derived from microearthquake locations using SAFOD and HRSN data., *Eos, Trans. AGU*, 88(52), Fall Meet. Suppl., Abstract T53C-03.

Paul, P., and Zoback, M.D., 2008. Wellbore-stability study for the SAFOD borehole through the San Andreas Fault, SPE-102781-PA, *SPE Drilling and Completion*, 23(4):394–408, doi: 10.2118/102781-PA.

Rice, J.R., 1992. Fault stress states, pore pressure distributions, and the weakness of the San Andreas fault. *In* Evans, B., and

Wong, T.F. (Eds.), *Fault Mechanics and Transport Properties of Rocks:* San Diego, CA (Academic Press), 475–503, doi:10.1016/S0074-6142(08)62835-1.

Roecker, S., Thurber, C., and McPhee, D., 2004. Joint inversion of gravity and arrival time data from Parkfield: new constraints on structure and hypocenter locations near the SAFOD drill site. *Geophys. Res. Lett.*, 31:1–4, doi:10.1029/2003GL019396.

Rymer, M.J., Tinsley, J.C., Treiman, J.A., Arrowsmith, J.R., Clahan, K.B., Rosinski, A.M., Bryant, W.A., Snyder, H.A., Fuis, G.S., Toke, N.A., and Bawden, G.W., 2006. Surface fault slip associated with the 2004 Parkfield, California, earthquake. *Bull. Seismol. Soc. Am.*, 96(B4):S11–S27, doi:10.1785/0120050830.

Saffer, D.M., Bekins, B.A., and Hickman, S., 2003. Topographically driven groundwater flow and the San Andreas heat flow paradox revisited. *J. Geophys. Res.*, 108(B5):2274.

Schaff, D., Beroza, G., and Shaw B., 1998. Postseismic response of repeating aftershocks. *Geophys. Res. Lett.*, 25(24):4549–4552, doi:10.1029/1998GL900192.

Shelly, D.R., and Hardebeck, J.L., 2010. Precise tremor source locations and amplitude variations along the lower-crustal central San Andreas Fault. *Geophys. Res. Lett.,* 37:L14301, doi:10.1029/2010GL043672.

Solum, J.G., Hickman, S.H., Lockner, D.A., Moore, D.E., van der Pluijm, B.A., Schleicher, A.M., and Evans, J.P., 2006. Mineralogic characterization of protolith and fault rocks from the SAFOD main hole. *Geophys. Res. Lett.*, 33:L21314, doi:10.1029.2006GL027285.

Thurber, C., Roecker, S., Zhang, H., Baher, S., and Ellsworth, W.L., 2004. Fine-scale structure of the San Andreas fault zone and location of the SAFOD target earthquakes. *Geophys. Res. Lett.*, 31:L12S02, doi:10.1029/2003GL019398.

Thurber, C., Roecker, S., Zhang, H., Bennington, N., and Peterson, D., 2010. Crustal structure and seismicity around SAFOD: a ten-year perspective. *Eos, Trans. AGU*, 91, Fall Meeting Suppl., Abstract T52B-01.

Unsworth, M., and Bedrosian, P.A., 2004. Electrical resistivity structure at the SAFOD site from magnetotelluric exploration. *Geophys. Res. Lett.*, 31(12):L12S05, doi:10.1029/2003GL019405.

Waldhauser, F., Ellsworth, W.L., Schaff, D.P., and Cole A., 2004. Streaks, multiplets, and holes: High-resolution spatio-temporal behavior of Parkfield seismicity. *Geophys. Res. Lett.*, 31:L18608, doi:10.1029/2004GL020649.

Wiersberg, T., and Erzinger, J., 2007. A helium isotope cross-section study through the San Andreas Fault at seismogenic depths. *Geochem. Geophys. Geosyst.*, 8(1):Q01002, doi:10.1029/2006GC001388.

Wiersberg, T., and Erzinger, J., 2008. On the origin and spatial distribution of gas at seismogenic depths of the San Andreas Fault from drill mud gas analysis. *Appl. Geochem.*, 23:1675–1690, doi:10.1016/j.apgeochem.2008.01.012.

Wiersberg, T., and Erzinger, J., 2011. Chemical and isotope compositions of drilling mud gas from the San Andreas Fault Observatory at Depth (SAFOD) boreholes: Implications on gas migration and the permeability structure of the San Andreas Fault, *Chem. Geol.*, doi:10.1016/j.chemgeo.2011.02.016

Williams, C.F., Grubb, F.V., and Galanis, S.P., 2004. Heat flow in the SAFOD pilot hole and implications for the strength of the San Andreas fault. *Geophys. Res. Lett.*, 31:L15S14.

Williams, C.F., D'Alessio, M.A., Grubb, F.V., and Galanis, S.P., 2005. Heat flow studies in the SAFOD main hole. *Eos, Trans. AGU*, 86(52), Fall Meeting Suppl., Abstract T23E-07.

Wu, J., Hole, J.A., and Snoke, J.A., 2010. Fault zone structure at depth from differential dispersion of seismic guided waves: evidence for a deep waveguide on the San Andreas Fault. *Geophys. J. Int.*, 182:343–354.

Zhang, H., Thurber, C., and Bedrosian, P.A., 2009. Joint inversion for Vp, Vs, and Vp/Vs at SAFOD, Parkfield, California. *Geochem. Geophys. Geosyst.*, 10(11):Q11002, doi:10.1029/2009GC002709.

Zoback, M.D., and Hickman, S.H., 2007. Preliminary results from SAFOD Phase 3: implications for the state of stress and shear localization in and near the San Andreas Fault at depth in central California. *Eos, Trans. AGU*, 88(52), Fall Meeting Suppl., Abstract T13G-03.

Zoback, M.D., Hickman, S., and Ellsworth, W., 2007. The role of fault zone drilling. *In* Kanamori, H., and Schubert, G. (Eds.), *Earthquake Seismology—Treatise on Geophysics Vol. 4*: Amsterdam (Elsevier), 649–674.

Zoback, M.D., Hickman, S., and Ellsworth, W.L., 2010. Scientific drilling into the San Andreas Fault. *Eos, Trans. AGU*, 91(22):197–204, doi:10.1029/2010EO220001.

Zoback, M.D., Zoback, M.L., Mount, V.S., Suppe, J., Eaton, J.P., Healy, J.H., Oppenheimer, D., Reasenberg, P., Jones, L., Raleigh, C.B., Wong, I.G., Scotti O., and Wentworth, C., 1987. New evidence for the state of stress on the San Andreas fault system. *Science*, 238:1105–1111, doi:10.1126/science.238.4830.1105.

Authors

Mark Zoback, Department of Geophysics, Stanford University, Stanford, CA 94305-2215, U.S.A., e-mail: zoback@stanford.edu.

Stephen Hickman and William Ellsworth, U.S. Geological Survery, 345 Middlefield Road MS 977, Menlo Park, CA 94025-3591, U.S.A.

and the SAFOD Science Team

Figure Credits

Fig. 1: air photo courtesy of M. Rymer

The Lake El'gygytgyn Scientific Drilling Project – Conquering Arctic Challenges through Continental Drilling

by Martin Melles, Julie Brigham-Grette, Pavel Minyuk, Christian Koeberl, Andrei Andreev, Timothy Cook, Grigory Fedorov, Catalina Gebhardt, Eeva Haltia-Hovi, Maaret Kukkonen, Norbert Nowaczyk, Georg Schwamborn, Volker Wennrich, and the El´gygytgyn Scientific Party

doi:10.2204/iodp.sd.11.03.2011

Abstract

Between October 2008 and May 2009, the International Continental Scientific Drilling Program (ICDP) co-sponsored a campaign at Lake El´gygytgyn, located in a 3.6-Ma-old meteorite impact crater in northeastern Siberia. Drilling targets included three holes in the center of the 170-m-deep lake, utilizing the lake ice cover as a drilling platform, plus one hole close to the shore in the western lake catchment. At the lake's center. the entire 315-m-thick lake sediment succession was penetrated. The sediments lack any hiatuses (i.e., no evidence of basin glaciation or desiccation), and their composition reflects the regional climatic and environmental history with great sensitivity. Hence, the record provides the first comprehensive and widely time-continuous insights into the evolution of the terrestrial Arctic since mid-Pliocene times. This is particularly true for the lowermost 40 meters and uppermost 150 meters of the sequence, which were drilled with almost 100% recovery and likely reflect the initial lake stage during the Pliocene and the last ~2.9 Ma, respectively. Nearly 200 meters of underlying rock were also recovered; these cores consist of an almost complete section of the various types of impact breccias including broken and fractured volcanic basement rocks and associated melt clasts. The investigation of this core sequence promises new information concerning the El´gygytgyn impact event, including the composition and nature of the meteorite, the energy released, and the shock behavior of the volcanic basement rocks. Complementary information on the regional environmental history, including the permafrost history and lake-level fluctuations, is being developed from a 142-m-long drill core recovered from the permafrost deposits in the lake catchment. This core consists of gravelly and sandy alluvial fan deposits in ice-rich permafrost, presumably comprising a discontinuous record of both Quaternary and Pliocene deposits.

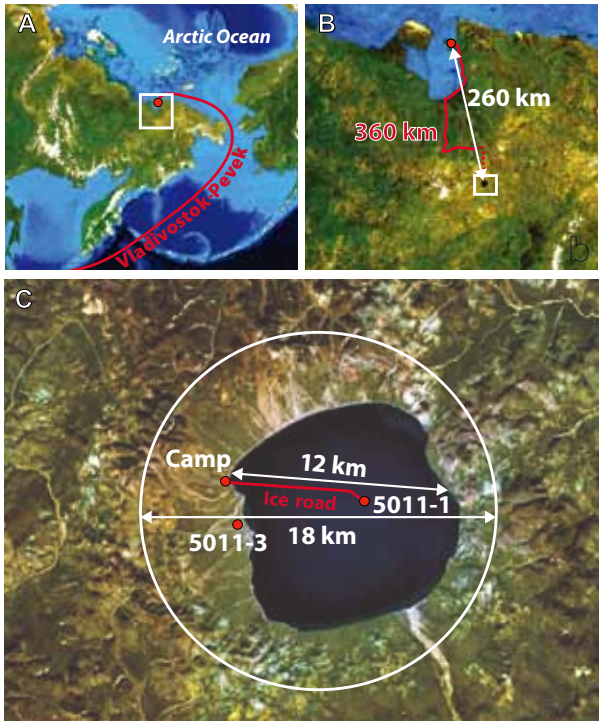

Figure 1. Location and setting of Lake El´gygytgyn. [A] The lake is located in central Chukotka, NE Russia, about 850 km west of the Bering Strait. The drill rig and all equipment arrived at the lake first by barge from Vladivostok along the route in red. [B] All logistics were based out of the town of Pevek, a gold mining center located on the coast of the East Siberian Sea. Helicopters were used to transport scientists, food and delicate equipment out to the drill site, whereas the 17 shipping containers with the drilling system were transported by truck. [C] Satellite image of Lake El´gygytgyn Crater showing dimensions, regional relief, the locations of ICDP Sites 5011-1 and 5011-3, and the location of crater rim (white circle).

Introduction

Lake El´gygytgyn is located 100 km to the north of the Arctic Circle in remote Chukotka, northeastern Russia (67°30' N, 172°05' E; Fig. 1). The lake lies within a meteorite impact crater measuring 18 km in diameter (Gurov et al., 1978, 2007) that was created 3.6 million years ago in volcanic target rocks (Layer, 2000). Today, the lake is 170-m-deep and has a roughly circular shape with a diameter of 12 km. Higher sediment supply from the western and northern reaches of the crater over time has caused the displacement of the lake toward the southeastern part of the basin. The sediments in the surrounding lake catchment are derived from slope processes and fluvial activity. Regionally these sediments are thought to contain permafrost to a depth of 500 m (Yershov, 1998). A seismic survey on the lake floor detected more than 300 meters of lacustrine sediments above an impact breccia and brecciated volcanic bedrock (Gebhardt et al., 2006), confirming the assumption that the basin had escaped continental-scale glaciations since the time of the impact (Glushkova, 2001).

Because of its unusual origin and high-latitude setting in western Beringia, scientific drilling at Lake El´gygytgyn

offered unique opportunities across three geoscientific disciplines. These include (i) paleoclimate research, allowing the time-continuous reconstruction of the climatic and environmental history of the terrestrial Arctic back into the mid-Pliocene for the first time; (ii) permafrost research, promising a better understanding of the history and present behavior of the Arctic's frozen surficial materials; and (iii) impact science, providing new insights into planetary cratering processes and the response of volcanic target rocks. This report summarizes aspects of the pre-site surveys which provided the impetus for drilling, highlights the challenging, sometimes gut-wrenching drilling logistics, and outlines some results and first interpretations from the limited on-site and ongoing off-site analyses of the lake sediments, impact rocks, and permafrost deposits.

Pre-site Surveys

A first international expedition was carried out on Lake El'gygytgyn early in spring 1998. Using the lake ice as a platform, six participants from Germany, Russia, and the U.S.A. conducted initial shallow coring in the deepest part of the lake. Succeeding expeditions in summer 2000 and spring and summer 2003 included eleven and sixteen participants, respectively (Melles et al., 2005). These projects provided a more comprehensive understanding of the modern setting and processes operating in the crater, the Late Quaternary climatic and environmental history of the region, and the structure of the impact crater and the thickness and architecture of its lacustrine sediment infill (Brigham-Grette et al., 2007, and references therein).

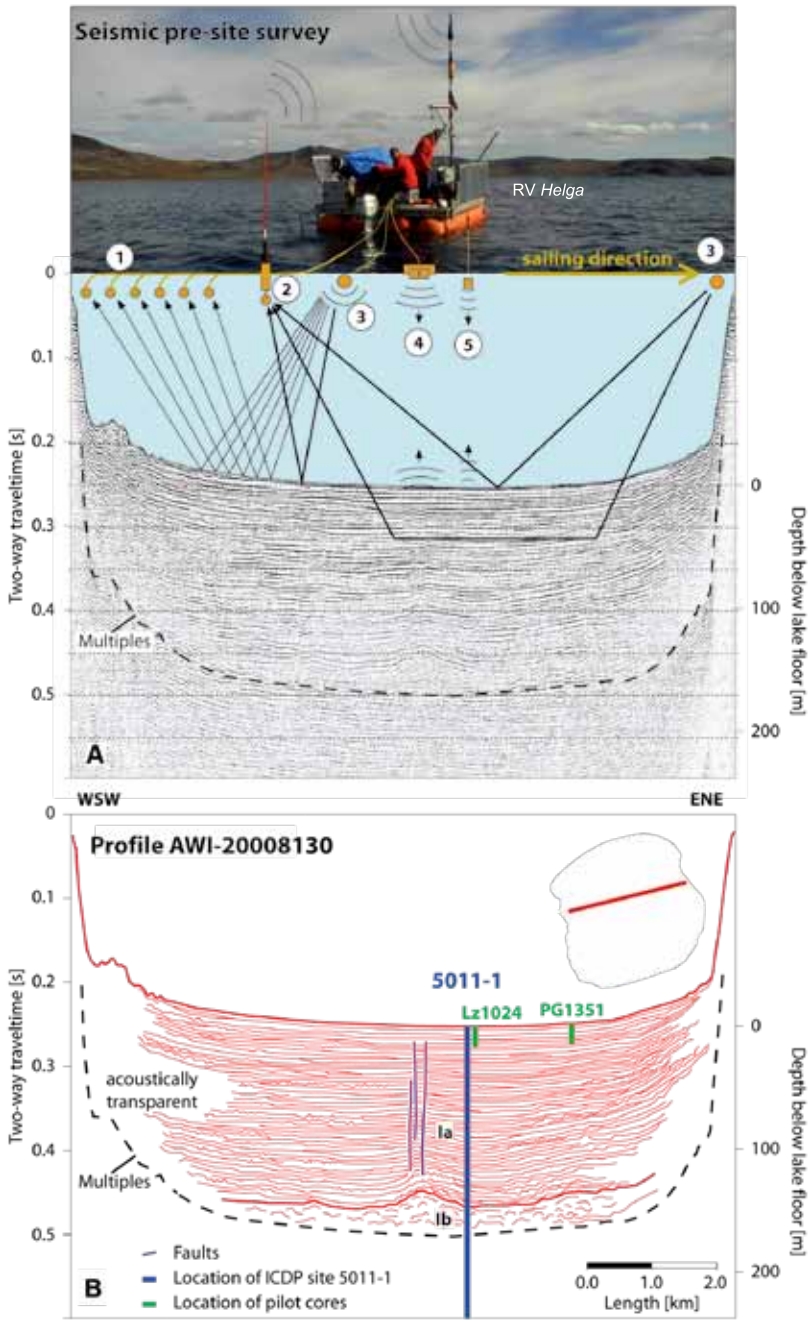

Figure 2. Seismic stratigraphy of Lake El'gygytgyn sediments. Multi-channel reflection profile AWI-20008130 is given as seismic image [A] and interpreted line drawing [B], with the trackline of the seismic profile shown in the inset. Seismic equipment used during the pre-site surveys in 2000 and 2003 is shown in the diagram: (1) streamer (multi-channel: 14 channels, 260 m total length; single-channel: 20 elements single hydrophone), (2) sonobuoy (stationary hydrophone; seismic refraction and wide angle data), (3) airgun (expedition 2000: Bolt 600B, 5 inch^3; expedition 2003: Mini-GI gun, 26 inch^3), (4) sediment echosounder (3.5 kHz, penetration of ~40 m), and (5) bathymetric echosounder (water depth measurements along track lines). Note that the upper part of the sediments (Unit Ia) is seismically well-layered and interfingered by acoustically transparent mass movement deposits mainly in the proximal parts, while the lower part (Unit Ib) is acoustically more massive and chaotic.

The climate at Lake El'gygytgyn is cold, dry, and windy. In 2002, the mean annual air temperature was -10.3°C, with extremes ranging from -40°C in winter to +26°C in summer (Nolan and Brigham-Grette, 2007). The annual precipitation amounted to ~200 mm water equivalent. Dominant wind directions were either from the north or from the south. The mean hourly wind speed was 5.6 m s^{-1}, with strong winds above 13.4 m s^{-1} occurring every month but more frequently in winter. The modern vegetation in the catchment of Lake El'gygytgyn is herb-dominated tundra with rare local patches of low shrubs, particularly willow (*Salix*) and dwarf birch (*Betula nana*) (Lozhkin et al., 2007a). Ice formation on Lake El'gygytgyn usually starts in October (Nolan et al., 2003). The blanketing snow cover melts in May/June, whereas the lake ice, which reaches a maximum thickness of 1.5–2.0 m, starts disintegration with the formation of moats at the shore in June/July and culminates in open water by mid-July/August. Biogenic primary production in this ultra-

oligotrophic lake is concentrated in the short ice-free period in summer, but considerable phytoplankton growth also takes place beneath the ice cover (Cremer and Wagner, 2003; Cremer et al., 2005). Lake El′gygytgyn today is a cold-monomictic system with slightly acidic pH. The water column down to 170 m is stratified in winter but completely mixed in summer, though never exceeding 4°C (Nolan and Brigham-Grette, 2007). About fifty streams enter the lake at 492 m above sea level (a.s.l.) from the catchment that extends to the crater rim up to 935 m a.s.l.; however, fluvial sediment supply to the lake is very low, because the watershed of 293 km^2 is less than three times the lake's surface area of 110 km^2. In addition, much of the sediment today is captured and deposited at the mouth of the inflows in shallow lagoons that are dammed by gravel bars formed by wave and lake ice action. The restricted fluvial input together with the low primary production produces remarkably clear surface waters, giving a Secchi transparency depth of 19 m in summer.

The first 13- and 16-m-long sediment cores from central Lake El′gygytgyn yielded basal ages of ~250 kyr and 340 kyr before present (BP), respectively, confirming that very low and relatively constant sedimentation rates are characteristic of both interglacial and glacial times (Forman et al., 2007; Juschus et al., 2007; Nowaczyk et al., 2007). The highly variable characteristics of the sediment underscore the sensitivity of this lacustrine system to regional climatic and environmental change (Asikainen et al., 2007; Brigham-Grette et al., 2007; Cherepanova et al., 2007; Lozhkin et al., 2007a, 2007b; Melles et al., 2007; Minyuk et al., 2007). Shallow cores were also taken of sub-recent mass movement deposits first identified in seismic profiles as originating from the steep (up to 30°) lake slopes (Niessen et al., 2007). This case study demonstrated that debris and density flows can be associated with significant erosion on the lake slopes, but these processes usually do not reach the lake center, where suspension clouds produced by these events in most cases accumulate as non-erosive turbidites (Juschus et al., 2009). Complementary information concerning Late Quaternary lake-level fluctuations, cryogenic weathering, and landscape development was obtained by ground-penetrating radar surveys and investigations of sediment stratigraphic sections exposed in the catchment of Lake El′gygytgyn (Schwamborn et al., 2006, 2008a, 2008b; Glushkova and Smirnov, 2007; Glushkova et al., 2009).

During summer seismic surveys conducted in 2000 and 2003, a 3.5-kHz echosounder with high spatial resolution (up to 40 m penetration) was combined with single-channel and multi-channel airgun seismic systems to provide the clearest information possible of the deeper lacustrine sediments and the structure of the impact crater underneath (Gebhardt et al., 2006; Niessen et al., 2007). Both systems were run simultaneously for efficiency from a small open platform resting on four inflatable pontoons (Fig. 2). Sonobuoy refraction data from the lake center formed the basis of a five-layer velocity-depth model. The results show that the El′gygytgyn Crater has an uplifted central ring structure with its top in about 330 m depth below lake floor (mblf); the structure was built by impact breccia and buried by alluvial deposits in the northwestern part of the basin. Above this structure, two lake sediment units were identified based on seismic characteristics. According to the air gun reflection data, the upper unit down to 170 mblf appeared to be well stratified, while the lower unit appeared to be more massive (Fig. 2). Draping of the uplift structure is visible and inferred in the lower part of the upper unit. Both units were shown to be intercalated with thick mass movement deposits largely confined to marginal areas. Because these units also lack seismic discontinuities suggestive of glacial overriding or lake desiccation, a nearly time-continuous sediment record following the impact event was expected from parts of the central lake.

Drilling Operation

Drilling in remote northeastern Russia was a massive logistical undertaking. In summer 2008, the majority of the technical equipment and field supplies were transported in fifteen shipping containers from Salt Lake City, U.S.A. to Pevek, Russia by way of Vladivostok and the Bering Strait (Fig. 1). Additional freight from Germany (two containers) joined the cargo in Vladivostok via the Trans-Siberian Railway. In Pevek, the combined cargo was loaded onto trucks driven with bulldozer assistance more than 350 km

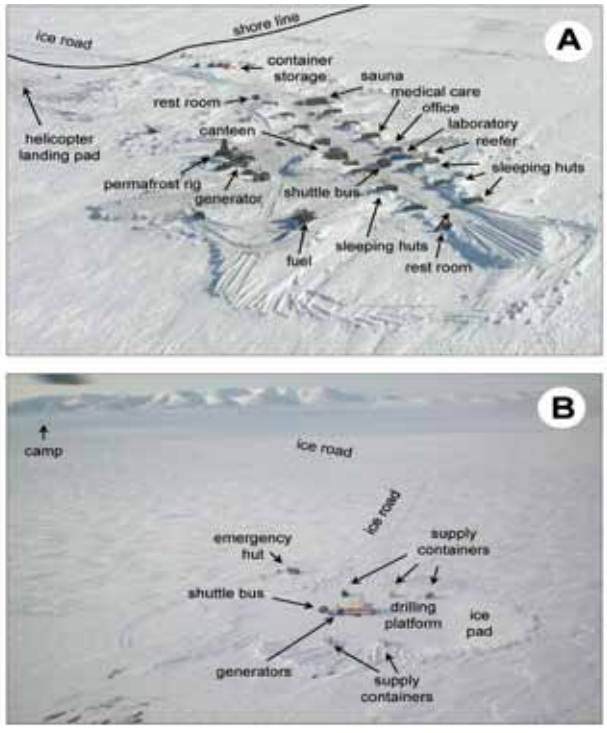

Figure 3. Aerial views of [A] the field camp on the western shore of Lake El′gygytgyn and [B] the drilling platform on the ice pad at ICDP Site 5011-1. The camp was designed for up to 36 people with facilities for maintaining two 12-hour shifts. The ice pad was first cleared of snow and then artificially flooded with lake water to thicken and strengthen the ice to roughly 2 meters. A gas-powered electrical generator fueled all operations. Crew changes along the 7-km ice road to the camp were accomplished by shuttle bus and Russian all-terrain vehicles.

Table 1. Penetration, drilling and core recovery at ICDP Sites 5011-1 and 5011-3 in the El´gygytgyn Crater (all data given in field depth).

Site	Hole	Type of Material	Penetrated (mblf)	Drilled (m)	Recovered (m)	Recovery (%)
5011-1	1A	lake sediment	146.6	143.7	132.0	92
	1B	lake sediment	111.9	108.4	106.6	98
	1C	total	517.3	431.5	273.8	63
		lake sediment		225.3	116.1	52
		impact rocks		207.5	157.4	76
5011-3		permafrost deposits	141.5	141.5	129.9	91

over winter roads and cross-country to Lake El´gygytgyn. There, the operation was supported by a temporary winter camp that was designed for up to thirty-six people and set up on the western lake shore (Fig. 3A). In the camp, a laboratory container for whole-core measurements of magnetic susceptibility stood next to a reefer in which the sediment cores were kept from freezing.

The project completed one borehole into permafrost deposits in the western lake catchment (ICDP Site 5011-3) and three holes at 170 m water depth in the center of the lake (Site 5011-1; Figs. 1, 4; Table 1). Permafrost drilling at Site 5011-3 was conducted from 23 November until 12 December 2008. Using a mining rig (SIF-650M) employed by a local drilling company (Chaun Mining Corp., Pevek), the crew reached a depth of 141.5 m with 91% recovery. After drilling, the borehole was permanently instrumented with a thermistor chain for future ground temperature monitoring as part of the "Global Terrestrial Network for Permafrost" (GTN-P) of the International Permafrost Association (IPA), thus contributing to our understanding of future permafrost behavior in light of contemporary rapid change.

In January/February 2009 an ice road between the camp and Site 5011-1 on Lake El´gygytgyn was established (Figs. 1, 3B). Subsequently, an ice pad of 100 m diameter at the drill site was artificially thickened to 2.3 m to allow for lake drilling operations from the 100-ton drilling platform. The Russian GLAD 800 was developed for extreme cold and operated by the U.S. consortium DOSECC. It consisted of a modified Christensen CS-14 diamond coring rig positioned on a mobile platform that was weather-protected by insulated walls and a tent on top of the 20-m-high derrick. The system was permanently imported into Russia, where it is now available for scientific drilling projects at no cost until 2014.

Drilling at Site 5011-1 was conducted from 16 February to 26 April 2009. The drill plan included the use of casing anchored into the sediment to allow drilling to start at a field depth of 2.9 mblf. Holes 1A and 1B had to be abandoned after twist-offs at 147 mblf and 112 mblf, respectively. In Hole 1A the Hydraulic Piston Corer (HPC) system was used down to 110 mblf, followed by the Extended Nose Corer (EXC) below. The recovery achieved with these tools was 92%. Similarly, drilling with HPC down to 100 mblf and with EXC below provided 98% recovery in Hole 1B. Hole 1C was first drilled by HPC between 42 mblf and 51 mblf, in order to recover gaps still existing in the core composite from Holes 1A and 1B, and was then continued from 100 mblf. Due to the loss of tools during the twist-offs, further drilling had to be performed with the Alien Bit Corer (ALN). The employment of this tool may at least partly explain a much lower recovery of the lake sediments in Hole 1C (total 52%), although this could also be due to the higher concentration of gravel and sand in these deeper lake sediments. The recovery jumped up to almost 100% again at a depth of 265 m, when the tool was changed to a Hard rock Bit Corer (HBC), which has a smaller

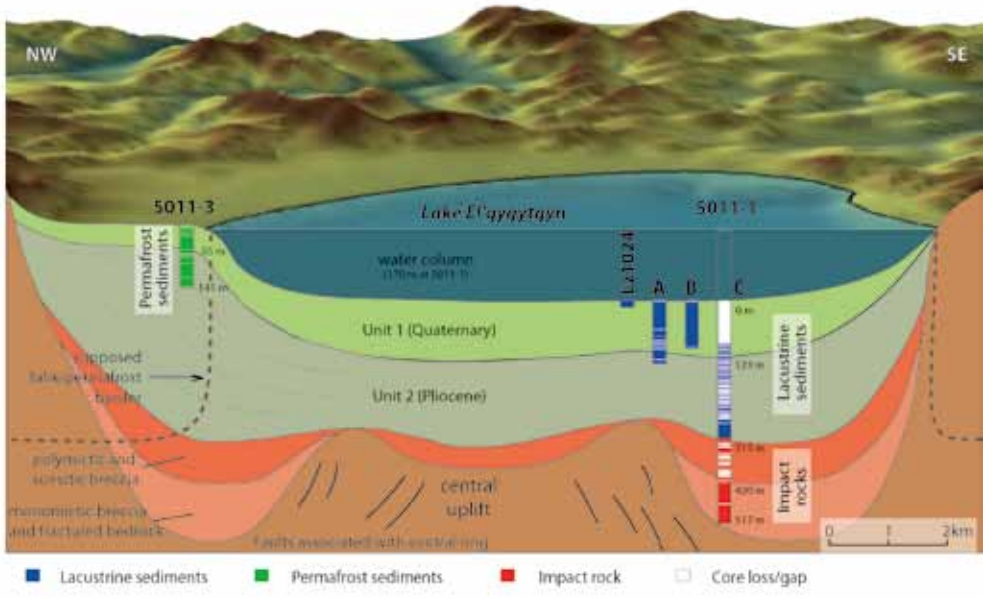

Figure 4. Schematic cross-section of the El´gygytgyn basin stratigraphy showing the locations of ICDP Sites 5011-1 and 5011-3. At Site 5011-1, three holes (1A, 1B, and 1C) were drilled to replicate the Quaternary sections. Hole 1C further penetrated the remaining lacustrine sequence and then 200 m into the impact rock sequence. Lz1024 is a 16-m-long pilot core taken in 2003 that overlaps between the lake sediment surface and the beginning of the drill cores 1A and 1B at Site 5011-1.

diameter than the tools employed before. The boundary between lake sediments and impact rocks was encountered at 315 mblf. Further drilling into the impact breccia and brecciated bedrock down to 517 mblf by HBC took place with 76% recovery.

On-site processing of the cores recovered at Site 5011-1 involved magnetic susceptibility measurements with a multisensor core logger (MSCL, Geotek Ltd.) down to a depth of 380 mblf. Initial core descriptions were conducted based on macroscopic and microscopic investigations of the material contained in core catchers and cuttings (lake sediments) and on the cleaned core segments not cored with liners (impact rocks). Additionally, downhole logging was carried out in the upper 394 m of Hole 1C by the ICDP Operational Support Group (OSG), employing a variety of slim hole wireline logging sondes. Despite disturbance of the electrical and magnetic measurements in the upper part of the hole, due to the presence of metal after the twist-offs at Holes 1A and 1B and to some technical problems, these data provide important information on the *in situ* conditions in the hole (e.g., temperature, natural gamma ray, U, K, and Th contents) and permit depth correction of the individual core segments.

Lake Sediments

Based on the whole-core magnetic susceptibility measurements on the drill cores from ICDP Site 5011-1, the field team was able to confirm that the core composite from Holes 1A to 1C provided nearly complete coverage of the uppermost 150 m of the sediment record in central Lake El´gygytgyn (Fig. 5), and that the gap between the top of the drill cores and the sediment surface was properly recovered by the upper part of a 16-m-long sediment core (Lz1024) taken during the 2003 site survey (Fig. 6). The construction of a final composite core record was completed during core processing and subsampling, which began in September 2009 at the University of Cologne, Germany, with the involvement of scientists from Russia and the U.S. The cores were first split lengthwise, and both core halves were macroscopically described and documented by high-resolution line scan images (MSCL CIS Logger, Geotek Ltd.). One core half was then used for measurements of color spectra and magnetic susceptibility in 1-mm increments (SCL2.3 Logger, GFZ Potsdam). This same core was then scanned using X-ray fluorescence (XRF) analyses of light and heavy elements and X-radiography in steps of 2.0 mm and 0.2 mm, respectively (ITRAX Core scanner, Cox Analytical Systems). Measurements of P-wave velocity and gamma-ray density (MSCL Logger, Geotek Ltd.) were then conducted in steps of 2 mm at the Alfred Wegener Institute in Bremerhaven, Germany, before the cores were continuously subsampled back in Cologne with u-channels for paleomagnetic and rock magnetic measurements. Subsequently, 2-cm-thick slices were continuously sampled from the core composite, excluding deposits from mass movement events, and split into eight aliquots of different sizes for additional biological and geochemical analyses. These aliquots, along with some irregular samples from replicate cores (e.g., for luminescence dating or tephra analyses), were subsequently sent to the science team members responsible for their analyses. In addition, thin sections were

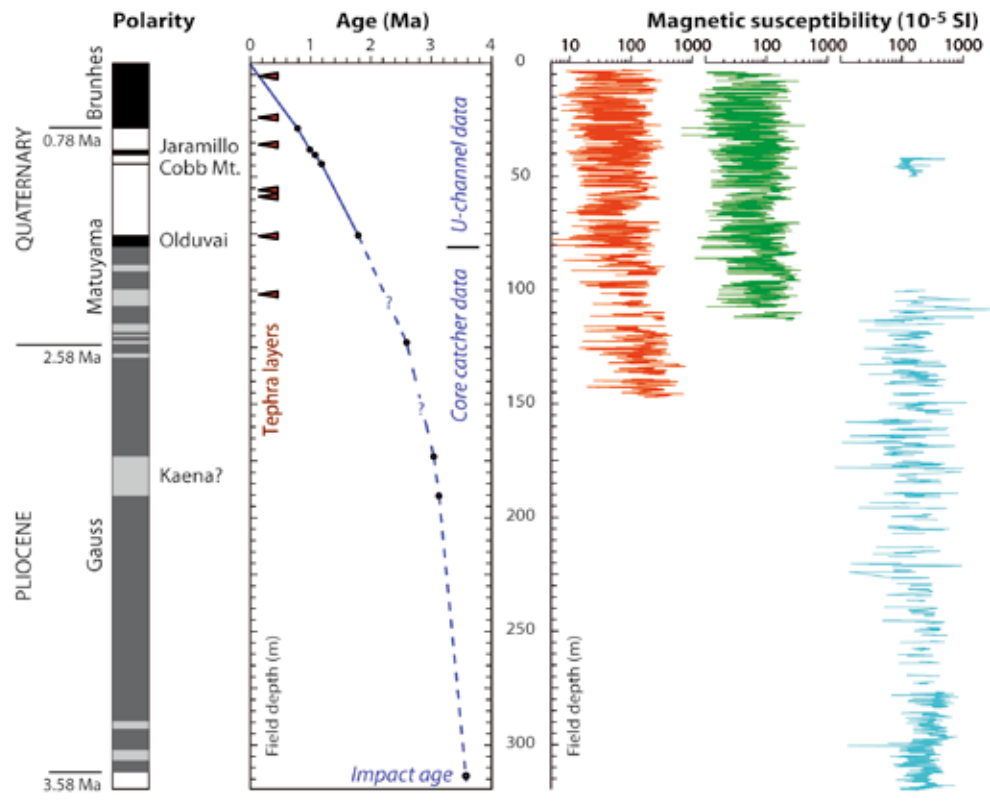

Figure 5. Preliminary paleomagnetic geochronology (left column) of the 315-m-thick lake sediment record from ICDP Site 5011-1 in the central part of Lake El´gygytgyn (for location see Figs. 1 and 4). Black and dark gray refer to normal polarity, white and light gray to reversed polarity, with gray shades representing uncertain interpretations. The age model presented still needs to be confirmed by ongoing paleomagnetic measurements on u-channels and dating of volcanic ash (tephra) layers. The data available so far indicate significantly decreasing sedimentation rates from the Pliocene into the Quaternary. The magnetic susceptibility (MS) data measured in the field (right columns) illustrate the high variability throughout the sediment succession, and that a core composite from Holes 1A, 1B, and 1C provides an almost complete record down to about 150 mblf, representing the uppermost Pliocene and the entire Quaternary.

prepared from representative sections of the cores to facilitate microanalysis of the various lithologies identified during visual core descriptions. In 2011, the remaining untouched core halves will be shipped to the U.S. National Lacustrine Core Repository (LacCore) at the University of Minnesota for long-term archiving.

The current chronological information from the lake sediments relies predominantly on paleomagnetic measurements, which were continuously carried out on the u-channel samples at the GFZ, Potsdam, Germany. In the uppermost 78 m of the core composite, as yet based on uncorrected field depths, magnetozones with normal/reversed polarity can clearly be related to established polarity chrons and subchrons (Ogg and Smith, 2004), including the boundary between the Brunhes and Matuyama chrons (0.781 Ma; ~28.5 mblf), the Jaramillo subchron (1.072–0.988 Ma; ~40.5–38.0 mblf), the termination of the Cobb Mountain subchron (1.173 Ma; ~44.2 mblf; its onset is masked by sediment disturbances at this level), and the termination of the Olduvai subchron (1.778 Ma; 75.5 mblf; Fig. 5). Below 78 mblf, paleomagnetic information is currently (December, 2010) restricted to initial measurements on semi-oriented discrete samples, which were taken roughly every ~3 m from the core catcher samples in Holes 1A, 1B, and 1C. While these results need to be confirmed by the ongoing u-channel measurements, they suggest that the boundary between the Gauss and Matuyama chrons (2.581 Ma) is located at ~123 mblf, where initial palynological data is consistent with an age close to the Pliocene/Pleistocene boundary. The sediment section with reversed polarity found in the upper part of the normal polarity Gauss chron is tentatively interpreted as the Kaena subchron (3.116–3.032 Ma; ~190–173 mblf). Based on these results, and the assumption that Lake El′gygytgyn was formed shortly after the impact event at 3.58 ± 0.04 Ma (Layer, 2000), long-term sediment accumulation rates are found to be at a maximum in the early part of the record and to decrease in more recent deposits. Specifically, sedimentation rates decrease from ~270 mm ka^{-1} below the Kaena subchron, to ~110 mm ka^{-1} between the termination of the Kaena

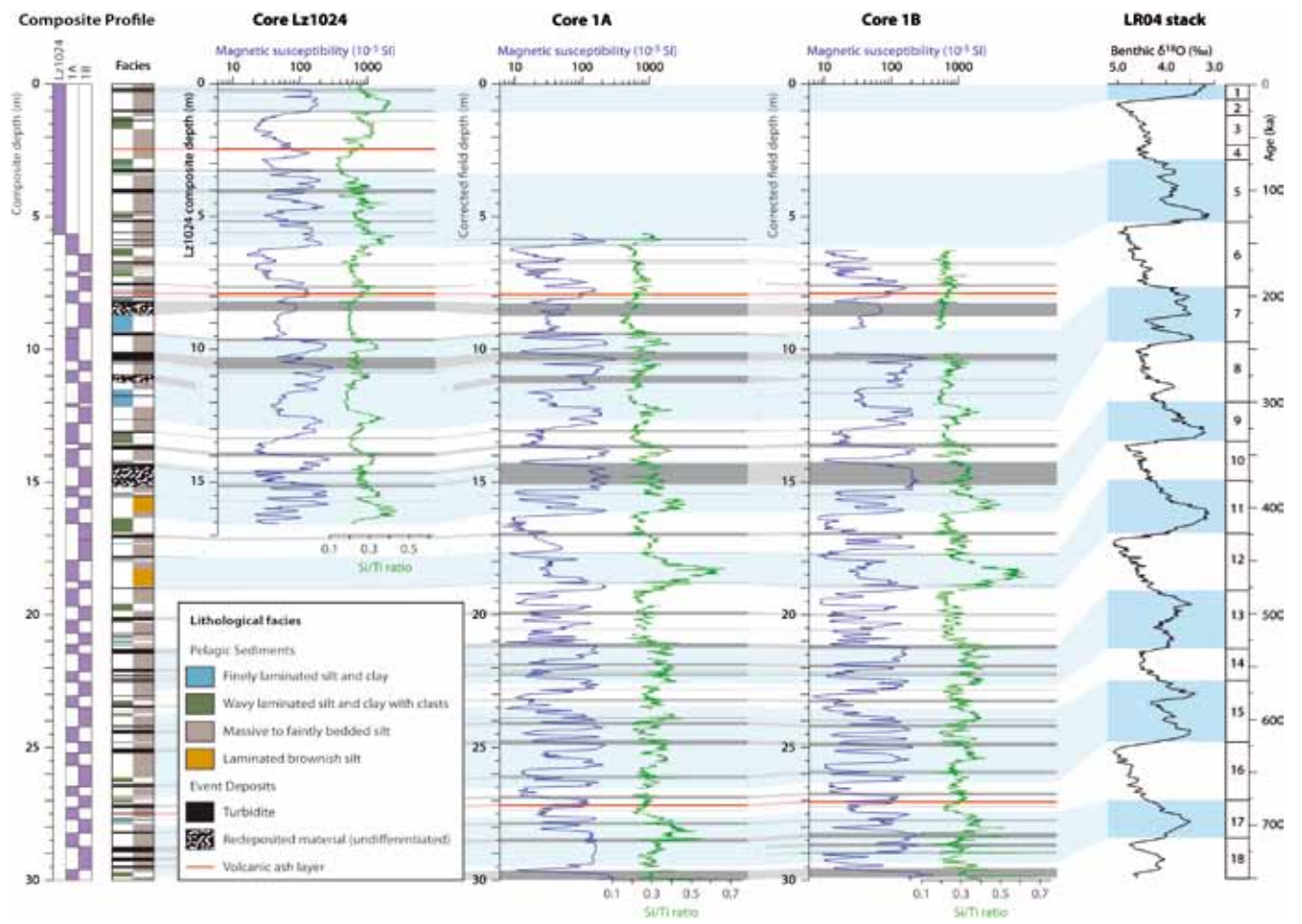

Figure 6. Initial results from the upper 30 meters of the lacustrine record from ICDP Site 5011-1 demonstrate the reasonable fidelity of the high-resolution data throughout the last ~750 ka. Note that the field depths of cores 1A and 1B were corrected by 2.7 m downward, based on the correlation with pilot core Lz1024. Left column with purple boxes shows the sections used to create the composite record. Sediment lithologic facies are shown according to the key in the legend. Columns for cores Lz1024 and ICDP 5011-1A and 1B show on-site data of whole-core magnetic susceptibility next to Si/Ti ratios from XRF scanning, used as proxies for magnetite dissolution during anoxic lake stages and bioproduction vs. clastic sedimentation, respectively. Interglacials, highlighted in light blue bars, are temporally correlated with the marine isotopic record of Lisiecki and Raymo (2005), supported by the Brunhes/Matuyama boundary (780 ka) at 31.2 corrected mblf (referring to 28.5 mblf uncorrected field depth).

subchron and the Gauss/Matuyama boundary, to ~50 mm ka^{-1} during the Quaternary. These preliminary chronological data are encouraging, because they confirm the feasibility of one of the major objectives of the El′gygytgyn Drilling Project, which is to investigate climatic developments during the Pliocene/Pleistocene transition and within the course of the Quaternary glacial/interglacial cycles. This can now be accomplished based on the core composite that was recovered from the uppermost 150 m of the lake sediment record.

Additional age control is expected to come from luminescence age estimates in the upper ~30 m and from the numerical ages of seven tephra layers identified so far in the sediment record (Fig. 5); both are still in progress. The paleomagnetic, luminescence, and tephra ages will provide chronological tie points for a more detailed age model that will be derived from the correlation of high-resolution proxy measurements with regional insolation variations. This approach was successfully employed by Nowaczyk et al. (2007) on a 13-m-long core from a different location in central Lake El′gygytgyn. Preliminary results from the uppermost 30 m of the core composite at Site 5011-1 (Fig. 6) demonstrate that this approach should also function in the deeper sediments of Lake El′gygytgyn.

The lacustrine sediment succession at Site 5011-1 is remarkably heterogeneous. Changes in lithology occur every few centimeters to decimeters throughout the entire record (Fig. 6). Based primarily on visual characteristics, qualitative grain-size information, and sedimentary structures observed in the split core halves and radiographs, the sediments are currently subdivided into four distinct facies reflecting continuous, pelagic deposition. Facies 1 is characterized by dark gray to black, finely laminated (<5 mm) silt and clay (Fig. 7A). Laminations are defined by alternating grain-size variations and are clearly observed as density variations in radiographs. Facies 2 is comprised of wavy laminations (<5 mm thick) of alternating silt and clay layers with an abundance of elongate sediment clasts made up of silt-sized particles (Fig. 7B). These clasts are typically several millimeters thick and have long axes up to ~1 cm lying parallel to the bedding plane. The most abundant unit is classified as Facies 3 and is characterized by massive to faintly banded silt of various colors (Fig. 7C). Banding typically occurs as color variations 2–5 cm thick observed in split core halves, with only slight density variations observed in radiographs. Facies 4 consists of red or brownish silt-sized sediment with distinct fine laminations (<5 mm; Fig. 7D). In contrast to other laminated sections of the core, these laminae are not associated with any obvious grain-size variations and less pronounced density variations in the radiographs, possibly reflecting a biological or chemical origin.

Facies 1 through 3 are also present in a 13-m-long pilot core (PG1351) from which additional geochemical data are available and were related to different climate modes by Melles et al. (2007). According to that study, Lake El′gygytgyn had a perennial ice cover during glacial times and some stadials of the Late Quaternary. On one hand, this restricted light penetration and thus biogenic production in the surface waters, as reflected by low biogenic silica deposition (low Si/Ti ratios, Fig. 6). On the other hand, the perennial ice cover also hampered mixing of the water column, leading to anoxic H_2S-bearing bottom waters and no bioturbation. Anoxic bottom waters dur-ing glacial/stadial times also lead to magnetite dissolution, reflected in low values of magnetic susceptibility (Nowaczyk et al., 2007). The glacial/stadial sediments in part consist of finely laminated silt and clay of Facies 1 (Fig. 7A). This facies is thought to reflect cold and relatively moist climates, when blanketing snow on the ice cover led to a reduction in biogenic primary production. In contrast, wavy laminated clast-containing sediments of Facies 2 (Fig. 7B) are pre-

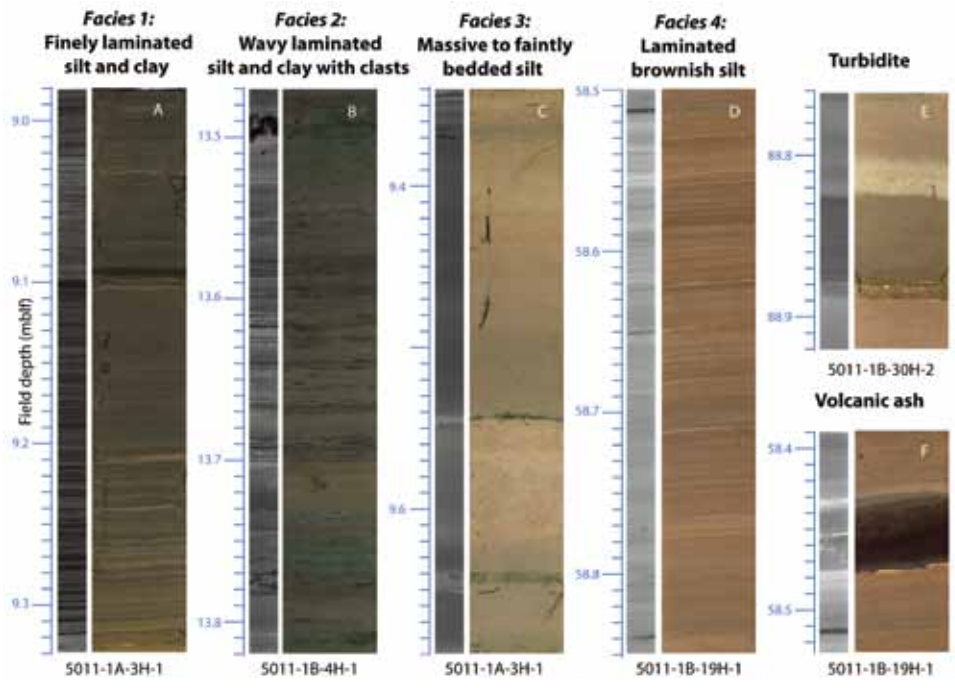

Figure 7. Examples of X-radiographs and line scan pictures from sedimentary facies occurring in the lake sediment record from ICDP Site 5011-1. The sediments shown in [A] and [B] are characteristic for glacials/stadials, which differ in aridity, whereas the sediments shown in [C] and [D] are characteristic for interglacials/interstadials of different intensity. In addition, typical examples of a turbidite and a volcanic ash layer are shown in [E] and [F], respectively.

sumed to reflect drier glacial intervals, when the absence of snow cover on the perennial ice allowed for a higher primary production. The clasts associated with Facies 2 may reflect enhanced deposition of aeolian material on the ice surface (forming cryoconites) followed by the agglomeration of these particles during their transport through the ice along vertical conduits. However, the precise origin and composition of these clasts are still being investigated.

Interglacial/interstadial sedimentation in Lake El′gygytgyn is to a degree reflected by the massive to faintly banded olive-gray to brownish sediments of Facies 3 (Fig. 7C). This facies reflects a semi-permanent ice cover that allows for a higher primary production, as evident in high Si/Ti ratios (Fig. 6). A complete mixing of the water column at the end of ice breakup leads to oxygenation of the bottom waters, as indicated by the preservation of high magnetic susceptibilities. The predominantly massive appearance of the deposits is likely due to some homogenization by bioturbation. In contrast, fine laminations in Facies 4 (Fig. 7D) are indicative of a lack or strong limitation of bioturbation. These sediments also include dark organic-rich layers and are associated with distinct maxima in Si/Ti ratios (Fig. 6). These characteristics are best attributed to deposition during an extraordinarily warm climate, with a prolonged ice-free period and enhanced nutrient supply from the catchment leading to exceptionally high rates of primary production and the exclusion of bioturbation due to depletion in oxygen content caused by enhanced decomposition of organic matter. Facies 4 last occurred at Lake El′gygytgyn during Marine Isotope Stages (MIS) 11 and 9.3 (Fig. 6). The details of this interpretation will require further study.

Pelagic sedimentation in Lake El′gygytgyn is irregularly interrupted by short-term sedimentary events (Fig. 6). These include gravitational mass movements and volcanic ash fallouts (Fig. 7E), which have formed up to 7.4-cm-thick tephra layers in the sediment record of Site 5011-1. Mass movement events are predominantly observed as turbidites, characterized by sharp basal contacts followed by a fining upwards sequence of sand to clay (Fig. 7F). Juschus et al. (2009) described the origin of the turbidites as resulting from sediment settling from suspension clouds produced by debris and density flows that originate on the lake slopes and occasionally penetrate into the center of the lake. Altogether, fifty-three graded beds have been identified in the upper 30 m of the Site 5011-1 record, and most are a few centimeters thick. Only three intervals with debrites, densites (Gani, 2004), or other re-deposited material related to mass movement events occur in this part of the core. Significant erosion by these mass movement events of the pelagic sediment record is not evident according to the age model for this part of the record, which is based on the correlation of sediment facies and proxy measurements with the global MIS stack (Fig. 6), constrained by the Brunhes/Matuyama boundary just below (Fig. 5).

The first information concerning the Pliocene history recorded in Lake El′gygytgyn relies on multi-proxy analyses of small samples taken from the core catchers (every ~3 m) and core cuttings (every meter). Based on these very preliminary data, we observe that the concentration of biogenic silica (BSi), total organic carbon (TOC), and total nitrogen (TN) is significantly lower in the Pliocene than in the Quaternary. Presumably, this is due to a much higher clastic input associated with significantly higher sedimentation rates during the Pliocene (Fig. 5). The Pliocene pollen assemblages are so far dominated mostly by tree pollen. Repeated changes in the plant assemblages through time reflect variations in forests of pine (*Pinus*), larch (*Larix*), spruce (*Picea*), fir (*Abies*), alder (*Alnus*), and hemlock (*Tsuga*). The tree pollen significantly decreases during the presumed Kaena subchron (3.116–3.032 Ma), concomitant with an increase in the relative abundance of wormwood (*Artemisia)* pollen—spores of rock spike-moss (*Selaginella rupestris)*—and coprophilous fungi. This pollen composition suggests treeless glacial environments - over some intervals - which can be described as tundra-steppe. The transition from the Pliocene to the Pleistocene still needs to be studied in detail, but it is broadly marked in the widely spaced samples studied so far by a distinct change from predominantly coniferous assemblages to pollen spectra dominated by dwarf birch, shrub alder, and herbs at ~123 mblf.

Impact Rocks

The El'gygytgyn Crater represents the only currently known impact structure on Earth formed in siliceous volcanic rocks including tuffs. The impact melt rocks and target rocks provide an excellent opportunity to study shock metamorphism of volcanic rocks. The shock-induced changes observed in porphyritic volcanic rocks from El′gygytgyn can be applied to a general classification of shock metamorphism of siliceous volcanic rocks. That El′gygytgyn is an impact crater was confirmed in the late 1970s by Gurov and co-workers (Gurov et al., 1978, 2007; Gurov and Koeberl, 2004), who found shocked minerals and impact glasses in samples at the crater. However, the impact rocks on the surface have been almost totally removed by erosion, and so the El′gygytgyn Drilling Project provides the unique opportunity to study the crater-fill impactites *in situ* and determine their relations and succession. The investigations are expected to provide information on the shock behavior of the volcanic target rocks, the nature and composition of the asteroid that formed the crater, and the amount of energy that was involved in the impact event. This will also allow us to constrain the effects this impact event had on the regional and circumarctic environment.

The impact portion of the drill core from ICDP Site 5011-1, spanning the interval ~315–517 mblf, was handled differently from the lake sediment portion to the extent that no special storage and temperature requirements were necessary for sample export from Pevek to our laboratories. The cores

were initially shipped to the Natural History Museum in Berlin, where detailed basic core characterization was done (including complete photographic documentation) during the time period November 2009 to May 2010. In May 2010 an international sampling party was held in Berlin, and samples were allocated to about half a dozen research groups around the world.

The upper part of the impact core directly underneath the lake sediments consists of a unit of so-called suevitic breccia, with a thickness of ~100 m. A suevite is a glass-bearing polymict impact breccia, which contains fragments of a variety of rocks that represent different layers in the target rocks, cemented in a fine-grained matrix (Fig. 8). The glasses, on the other hand, were formed by the melting of the target rocks at very high temperatures. Such breccias are uniquely characteristic of impact craters on Earth and not found in any other geological setting. The green color of the suevite is due to alteration and the abundance of sheet minerals in the matrix; it contains abundant black melt clasts. The suevite shows a strong anisotropic fabric with fluidal texture. Fractures crosscutting the suevite are common, as are green clay and/or white-reddish carbonate veins. The suevites continue through a highly fractured transition zone with breccia intercalated to suevite and pass into a unit of shocked and locally brecciated volcanic target rocks (which may also contain suevitic breccias), which was uplifted during the impact event. During the formation of such central peaks, which are typical for impact craters of this size (also called "complex craters"), deeper layers of target rock rebound towards the surface and then solidify; thus, a mountain several kilometers in diameter is uplifted over 1000 m vertically in less than a minute. This is truly a spectacular geological process.

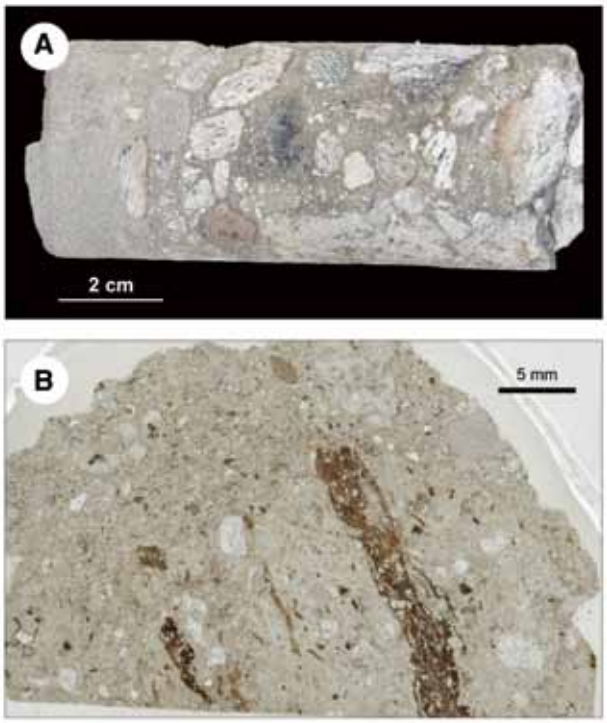

Figure 8. Typical suevitic impact breccia from the El´gygytgyn impact crater. [A] Core segment retrieved from a field depth of about 320 mblf at ICDP Site 5011-1. The rock fragments that occur in this breccia are a mixture of lithologies from the target that represent a pre-impact stratigraphic range of many hundred meters. [B] Thin-section of impact core sample 5011-107Q-4 from 343.8 mblf field depth, showing the so-called "red" suevite, which contains abundant large melt clasts, elongated and parallel to each other, comprising a general fluidal texture. The suevite is an impact breccia containing clastic components and melt clasts, and has a general light brownish color due to alteration into clay minerals. The largest melt clasts show internal fluidal texture. The groundmass of the melt clasts is glassy and brown. Clasts included are composed of fractured quartz, altered feldspar, and a minor amount of partially altered twinned amphibole. Lithic clasts include mainly fragmented quartz, fragmented and altered feldspars, finely twinned calcite, and fragments of volcanic rocks, which might be part of the target. The matrix of the suevite is microcrystalline, mainly composed of clay minerals that show a "fluidal" texture around the clasts.

Permafrost Deposits

The single deep core obtained at ICDP Site 5011-3, from the western catchment of Lake El´gygytgyn, was entirely frozen when recovered. This confirmed modeling results, which suggested that the unfrozen talik alongside the lake descends with more or less a vertical boundary until the permafrost base is reached at a depth of a few hundred meters (Fig. 4). On site, the permafrost cores were initially described and photographically documented. They were kept frozen in the field and during transport to the ice laboratory at the Alfred Wegener Institute in Bremerhaven, Germany. There, the cores were cleaned, the documentation was completed, and subsamples were taken from the sediment and ice for ongoing laboratory analyses.

The permafrost core contains ground ice throughout and largely consists of sandy gravels with volcanic clasts embedded in a sandy matrix. In the uppermost 75 m processed so far, pollen has only been found in the uppermost 10 m and within a few thin intervals below (Fig. 9). Comparison of the pollen assemblages in these cores with those in nearby permafrost and lake sediment cores retrieved during the site surveys (Lozhkin et al., 2007a, 2007b; Glushkova et al., 2009; Shilo et al., 2008; Matrosova, 2009) remains somewhat speculative, because the reworking of slope materials from the alluvial fans still needs to be assessed. However, the pollen assemblages suggest that the upper 9 m at Site 5011-3 represent a discontinuous record back to the Allerød period, with the Holocene being restricted to the upper 1.8 m and the Younger Dryas represented by the interval 1.8–2.5 m, and that the sediments at ~20 m depth were formed during MIS 5.5 or 7. While the pollen assemblages at ~36 m and ~51 m also indicate Pleistocene ages, those at about 62–65 m depth strongly indicate a Pliocene age for lower portions of the core, based on high pollen counts of pine (*Pinus* subgenus *Haploxylon*) as well as some of larch (*Larix*), fir (*Abies*), spruce (*Picea*), and hemlock (*Tsuga*; Fradkina, 1983). Hence, the Pliocene/Pleistocene boundary in core 5011-3 probably has to be placed somewhere between 51 m and 62 m depth, but additional study is required to test this conjecture.

Organic matter occurs in significant amounts (>1%) only in the Holocene sediments. The inferred climate oscillations for the transition from the Allerød via the Younger Dryas into the Holocene are also suggested in the water isotope record of the ground ice (Fig. 9). There, $\delta^{18}O$ minima and maxima support the inferred vegetation history indicated by the pollen record. Below the Allerød, the $\delta^{18}O$ values of the ground ice show less variation and tend toward more negative values, but not as negative as one would expect for full glacial values, like those seen in other regions of relict permafrost. The values observed here are currently interpreted to be due to a change in ice sources. While the ground ice in the Allerød and younger sediments likely originates from meteoric precipitation, the ice below could have been formed by freezing of lake sediment pore waters following a basinward migration of the talik boundary with lake lowering at some point in the past. Hence, it seems likely that the ground ice in these sediments is much younger than the enclosing sediments. A marginal lake environment prior to the Allerød is also indicated by the occasional occurrence of distinctly rounded pebbles, suggesting shore-line processes, and well-sorted sandy layers, possibly deposited on the upper lake slope. If this preliminary interpretation is confirmed by ongoing core analyses and modeling of the freezing front migrations, then the permafrost core 5011-3 may contribute to the reconstruction of the lake-level changes in the El´gygytgyn Crater since Pliocene times.

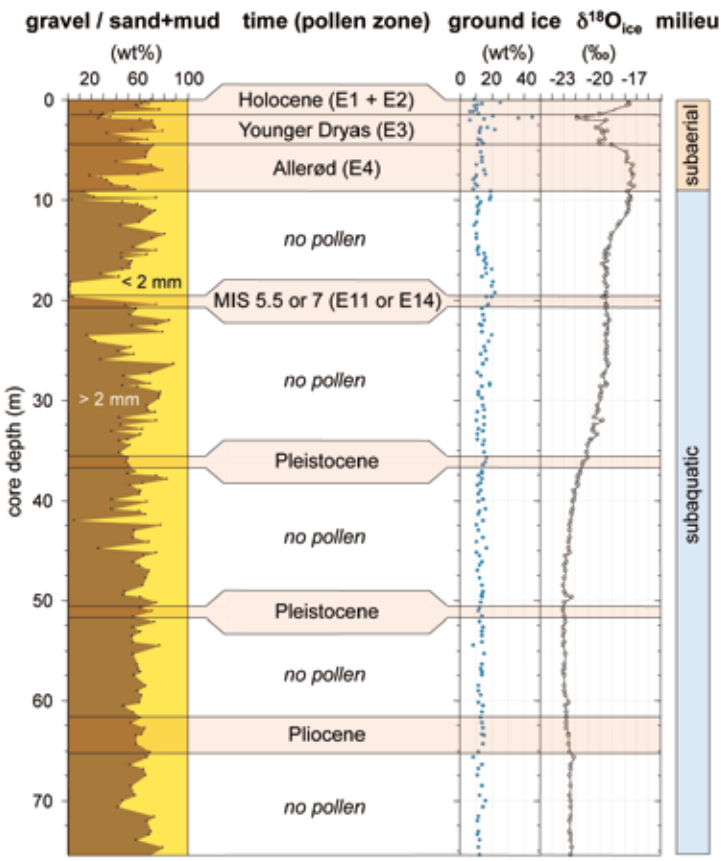

Figure 9. Initial results from the upper 75 m of the 141.5-m-long core drilled at ICDP Site 5011-3 into permafrost on the western margin of the lake basin (for location see Figs. 1 and 4). The core consists of ice-rich, coarse-grained sediments, which indicate both subaerial but mainly subaquatic, near-shore deposition, and likely has numerous unconformities. The crude chronology so far existing for this sequence is based on similarities in pollen assemblages with known records. In the lower part of the core, pollen are rarely preserved; however, the assemblages between about 62 m and 65 m depth strongly suggest a Pliocene age of the respective sediments.

Acknowledgements

Marianna Voevodskaya (RAS/CRDF) provided a smooth transition for the field parties through Moscow. In Pevek, Dmitry Koselov from Chukotrosgidromet arranged all of the necessary paperwork required by local authorities. He also managed all of the in-town shuttle services and contacts with the airport. On-site, Nikolai Vasilenko and his colleagues from the Chaun Mining Corporation provided a friendly, cooperative atmosphere for daily operations in the base camp and during drilling crew shifts. Contracts for the camp were organized by CH2MHill. We are particularly grateful to the personnel in the Pevek office of the Kinross Gold Corporation for their assistance. Ice pad preparation and safety monitoring were carried out by EBA Engineering Consultants Ltd., Canada. The Russian GLAD 800 drilling system was developed and operated by DOSECC Inc., the downhole logging was performed by the ICDP-OSG, and LacCore at the University of Minnesota handled core curation.

Funding for this research was provided by the International Continental Scientific Drilling Program (ICDP), the U.S. National Science Foundation (NSF), the German Federal Ministry of Education and Research (BMBF), Alfred Wegener Institute (AWI) and GeoForschungsZentrum Potsdam (GFZ), the Russian Academy of Sciences Far East Branch (RAS FEB), the Russian Foundation for Basic Research (RFBR), and the Austrian Federal Ministry of Science and Research (BMWF).

The El´gygytgyn Scientific Party

P. Anderson, A. Andreev, I. Bindeman, D. Bolshiyanov, V. Borkhodoev, K. Brady, J. Brigham-Grette (Principal Investigator), L. Brown, S. Burns, B. Chabligin, M. Cherepanova, T. Cook, R. Deconto, G. Fedorov, S. Forman, A. Francke, D. Froese, C. Gebhardt, O. Glushkova, V. Goette, J. Griess, A. Hilgers, A. Holland, E. Haltia-Hovi, H.-W. Hubberten, O. Juschus, J. Karls, C. Koeberl (Principal Investigator), S. Koenig, C. Kopsch, M. Kukkonen, P. Layer, A. Lozhkin, K. Mangelsdorf, T. Martin, T. Matrosova, H. Meyer, C. Meyer-Jacob, M. Melles (Principal Investigator), P. Minyuk (Principal Investigator), K. Murdock, F. Niessen, M. Nolan, A. Noren, N. Nowaczyk, N. Ostanin, S. Petsch, L.

Pittarello, V. Ponomareva, M. Portnyagin, F. Preusser, V. Pushkar, U. Raschke, J. Reed, P. Rosén, G. Schwamborn, V.S. Sakhno, T. Sapelko, N. Savva, L. Schirrmeister, V. J. Snyder, V.N. Smirnov, C. Van den Bogaard, H. Vogel, B. Wagner, D. Wagner, V. Wennrich, K. Wilkie.

References

Asikainen, C.A., Francus, P., and Brigham-Grette, J., 2007. Sedimentology, clay mineralogy and grain-size as indicators of 65 ka of climate change from El′gygytgyn Crater Lake, northeastern Siberia. *J. Paleolimnol.*, 37:105–122, doi:10.1007/s10933-006-9026-5.

Brigham-Grette, J., Melles, M., Minyuk, P., and Scientific Party, 2007. Overview and significance of a 250 ka paleoclimate record from El′gygytgyn Crater Lake, NE Russia. *J. Paleolimnol.*, 37:1–16, doi:10.1007/s10933-006-9017-6.

Cherepanova, M.V., Snyder, J.A., and Brigham-Grette, J., 2007. Diatom stratigraphy of the last 250 ka at Lake El′gygytgyn, northeast Siberia. *J. Paleolimnol.*, 37:155–162, doi:10.1007/s10933-006-9019-4.

Cremer, H., and Wagner, B., 2003. The diatom flora in the ultra-oligotrophic Lake El′gygytgyn, Chukotka. *Polar Biol.*, 26:105–114, doi:10.1007/s00300-002-0445-0.

Cremer, H., Wagner, B., Juschus, O., and Melles, M., 2005. A microscopical study of diatom phytoplankton in deep crater Lake El′gygytgyn, northeast Siberia. *Algol. Studies*, 116:147–168, doi:0342-1120/04/0157-147.

Forman, S.L., Pierson, J., Gomez, J., Brigham-Grette, J., Nowaczyk, N.R., and Melles, M., 2007. Luminescence geochronology for sediments from Lake El′gygytgyn, northwest Siberia, Russia: constraining the timing of paleoenvironmental events for the past 200 ka. *J. Paleolimnol*, 37:77–88, doi:10.1007/s10933-006-9024-7.

Fradkina, A.F., 1983. *Neogene Palynofloras of Northeast Asia*. Moscow (Nauka), [in Russian].

Gani, M.R., 2004. From turbid to lucid: a straightforward approach to sediment gravity flows and their deposits. *The Sedimentary Record*, 2:4–8.

Gebhardt, A.C., Niessen, F., and Kopsch, C., 2006. Central ring structure identified in one of the world′s best-preserved impact craters. *Geology*, 34:145–148, doi:10.1130/G22278.1.

Glushkova, O.Y., 2001. Geomorphological correlation of Late Pleistocene glacial complexes of Western and Eastern Beringia. *Quat. Sci. Rev.*, 20:405–417, doi:10.1016/S0277-3791(00)00108-6.

Glushkova, O.Y., and Smirnov, V.N., 2007. Pliocene and Holocene geomorphic evolution and paleogeography of the El′gygytgyn Lake region, NE Russia. *J. Paleolimnol.*, 37:37–47, doi:10.1007/s10933-006-9021-x.

Glushkova, O.Y., Smirnov, V.N., Matrosova, T.V., Vazhenina, L.N., and Braun, T.A., 2009. Climatic-stratigraphic characteristics and radiocarbon dates from the terrace complex in the El'gygytgyn Lake basin. *Vestnik FEB RAS*, 2:31–43 [in Russian].

Gurov, E.P., and Koeberl, C., 2004. Shocked rocks and impact glasses from the El'gygytgyn impact structure (Russia). *Meteorit. Planet. Sci.*, 39:1495–1508, doi:10.1111/j.1945-5100.2004.tb00124.x.

Gurov, E.P., Koeberl, C., and Yamnichenko, A., 2007. El'gygytgyn impact crater, Russia: structure, tectonics, and morphology. *Meteorit. Planet. Sci.*, 42:307–319, doi:10.1111/j.1945-5100.2007.tb00235.x.

Gurov, E.P., Valter, A.A., Gurova, E.P., and Serebrennikov, A.I., 1978. Meteorite impact crater El'gygytgyn in Chukotka. *Dokl. Akad. Nauk SSSR*+, 240:1407–1410 [in Russian].

Juschus, O., Melles, M., Gebhardt, A.C., and Niessen, F., 2009. Late Quaternary mass movement events in Lake El′gygytgyn, north-eastern Siberia. *Sedimentol.*, 56:2155–2174. doi:10.1111/j.1365-3091.2009.01074.x.

Juschus, O., Preusser, F., Melles, M., and Radtke, U., 2007. Applying SAR-IRSL methodology for dating fine-grained sediments from Lake El'gygytgyn, north-eastern Siberia. *Quat. Geochron.*, 2:187–194, doi:10.1016/j.quageo.2006.05.006.

Layer, P., 2000. Argon-40/argon-39 age of the El′gygytgyn impact event, Chukotka, Russia. *Meteorit. Planet. Sci.*, 35:591–599, doi:10.1111/j.1945-5100.2000.tb01439.x.

Lisiecki, L.E., and Raymo, M.E., 2005. A Pliocene-Pleistocene stack of 57 globally distributed benthic $\delta^{18}O$ records. *Paleoceanography*, 20:PA1003, doi:10.1029/2004PA001071.

Lozhkin, A.V., Anderson, P.M., Matrosova, T.V., and Minyuk, P., 2007a. The pollen record from El'gygytgyn Lake: implications for vegetation and climate histories of northern Chukotka since the late middle Pleistocene. *J. Paleolimnol.*, 37:135–153, doi:10.1007/s10933-006-9018-5.

Lozhkin, A.V., Anderson, P.M., Matrosova, T.V., Minyuk, P.S., Brigham-Grette, J., and Melles, M., 2007b. Continuous record of environmental changes in Chukotka during the last 350 thousand years. *Russ. J. Pac. Geol.*, 1:550–555, doi:10.1134/S1819714007060048.

Matrosova, T.V., 2009. Vegetation and climate change in northern Chukotka during the last 350 ka (based on lacustrine pollen records from Lake El'gygytgyn). Vestnik FEBRAS, 2:23–30 [in Russian].

Melles, M., Brigham-Grette, J., Glushkova, O.Y., Minyuk, P., Nowaczyk, N.R., and Hubberten, H.-W., 2007. Sedimentary geochemistry of a pilot core from El′gygytgyn Lake—a sensitive record of climate variability in the East Siberian Arctic during the past three climate cycles. *J. Paleolimnol.*, 37:89–104, doi:10.1007/s10933-006-9025-6.

Melles, M., Minyuk, P., Brigham-Grette, J., and Juschus, O., 2005. The Expedition El′gygytgyn Lake 2003 (Siberian Arctic). Ber. Polarforsch. Meeresforsch. 505:139 pp.

Minyuk, P., Brigham-Grette, J., Melles, M., Borkhodoev, V.Y., and Glushkova, O.Y., 2007. Inorganic geochemistry of El′gygytgyn Lake sediments, northeastern Russia, as an indicator of paleoclimatic change for the last 250 kyr. *J. Paleolimnol.*, 37:123–133. doi:10.1007/s10933-006-9027-4.

Niessen, F., Gebhardt, A.C., Kopsch, C., and Wagner, B., 2007. Seismic investigation of the El′gygytgyn impact crater lake (Central Chukotka, NE Siberia): preliminary results. *J. Paleolimnol.*, 37:17–35, doi:10.1007/s10933-006-9022-9.

Nolan, M., and Brigham-Grette, J., 2007. Basic hydrology, limnology, and meteorology of modern Lake El'gygytgyn, Siberia. *J. Paleolimnol.*, 37:17–35, doi:10.1007/s10933-006-9020-y.

Nolan, M., Liston, G., Prokein, P., Brigham-Grette, J., Sharpton, V., and Huntzinger, R., 2003. Analysis of lake ice dynamics and morphology on Lake El'gygytgyn, Siberia, using SAR and Landsat. *J. Geophys. Res.*, 108(D2):8062, doi:10.1029/2001JD000934.

Nowaczyk, N.R., Melles, M. and Minyuk, P., 2007. A revised age model for core PG1351 from Lake El′gygytgyn, Chukotka, based on magnetic susceptibility variations correlated to northern hemisphere insolation variations. *J. Paleolimnol.*, 37:65–76, doi:10.1007/s10933-006-9023-8.

Ogg, J.G., and Smith, A.G., 2004. The geomagnetic polarity scale. *In* Gradstein, F.M., Ogg, J.G., and Smith A.G. (Eds.), *A Geologic Time Scale 2004*. Cambridge (Cambridge University Press), 63–86.

Schwamborn, G., Fedorov, G., Schirrmeister, L., Meyer, H., and Hubberten, H.-W., 2008a. Periglacial sediment variations controlled by Late Quaternary climate and lake level change at Elgygytgyn Crater, Arctic Siberia. *Boreas*, 37:55–65. doi:10.1111/j.1502-3885.2007.00011.x.

Schwamborn, G., Förster, A., Diekmann, B., Schirrmeister, L., and Fedorov, G., 2008b. Mid to Late Quaternary cryogenic weathering conditions in Chukotka, northeastern Russia: inference from mineralogical and microtextural properties of the Elgygytgyn Crater Lake sediment record.In Kane, D.L., and Hinkel, D.M. (Eds.), *Ninth International Conference on Permafrost*, Fairbanks (Institute of Northern Engineering, University of Alaska), 1601–1606.

Schwamborn, G., Meyer, H., Fedorov, G., Schirrmeister, L., and Hubberten, H.-W., 2006. Ground ice and slope sediments archiving late Quaternary paleoenvironment and paleoclimate signals at the margins of El′gygytgyn Impact Crater, NE Siberia. *Quaternary Res.*, 66:259–272, doi:10.1016/j.yqres.2006.06.007.

Shilo, N.A., Lozhkin, A.V., Anderson, P.M., Vazhenina, L.N., Stetsenko, T.V., Glushkova, O.Y., and Matrosova, T.V., 2008. First data on the expansion of Larix gmelinii (Rupr.) into arctic regions of Beringia during the early Holocene. *Dokl. Akad. Nauk+*, 423:680–682.

Yershov, E.D., 1998. *General Geocryology. (Studies in Polar Research)*. Cambridge (Cambridge University Press), 580 pp, doi:10.1017/CBO9780511564505.

Authors

Martin Melles, Institute of Geology and Mineralogy, University of Cologne, Zuelpicher Str. 49a, D-50674 Cologne, Germany, e-mail: mmelles@uni-koeln.de.

Julie Brigham-Grette, Department of Geosciences, University of Massachusetts, 611 North Pleasant Street, Amherst, MA 01003, U.S.A.

Pavel Minyuk, North-East Interdisciplinary Scientific Research Institute, FEB RAS, 16 Portovaya St., 685000, Magadan, Russia.

Christian Koeberl, Department of Lithospheric Research, University of Vienna, Althanstrasse 14, A-1090 Vienna, Austria (and: Natural History Museum, A-1010 Vienna, Austria).

Andrei Andreev, Institute of Geology and Mineralogy, University of Cologne, Zuelpicher Str. 49a, D-50674 Cologne, Germany.

Timothy Cook, Department of Geosciences, University of Massachusetts, 611 North Pleasant Street, Amherst, MA 01003, U.S.A.

Grigory Fedorov, Arctic and Antarctic Research Institute, Bering Street, 199397 St. Petersburg, Russia.

Catalina Gebhardt, Alfred Wegener Institute for Polar and Marine Research, Am Alten Hafen 26, D-27568 Bremerhaven, Germany.

Eeva Haltia-Hovi, GFZ German Research Centre for Geosciences, Potsdam, Telegrafenberg C321, D-14473 Potsdam, Germany.

Maaret Kukkonen, Institute of Geology and Mineralogy, University of Cologne, Zuelpicher Str. 49a, D-50674 Cologne, Germany.

Norbert Nowaczyk, GFZ German Research Centre for Geosciences, Potsdam, Telegrafenberg C321, D-14473 Potsdam, Germany.

Georg Schwamborn, Alfred Wegener Institute for Polar and Marine Research, Telegrafenberg A43, D-14473 Potsdam, Germany.

Volker Wennrich, Institute of Geology and Mineralogy, University of Cologne, Zuelpicher Str. 49a, D-50674 Cologne, Germany.

and the El′gygytgyn Scientific Party

Related Web Links

http://elgygytgyn.icdp-online.org
http://www.elgygytgyn.uni-koeln.de
http://www.geo.umass.edu/lake_e/index.html
http://www.dfg-science-tv.de/en/projects/polar-archive
http://www.polartrec.com/geologic-climate-research-in-siberia

Figure Credits

Fig. 1: satellite images from NASA WorldWind
Fig. 3A: photo by Tim Martin, Greensboro Day School
Fig. 3B: photo by Jens Karls, University of Cologne

Twenty Years of Drilling the Deepest Hole in Ice

by Nikolay I. Vasiliev, Pavel G. Talalay, and Vostok Deep Ice Core Drilling Parties

doi:10.2204/iodp.sd.11.05.2011

Introduction

Ice sheets and glaciers contain stratified ancient ice that fell as snow years to millions of years ago. The dust particles, soluble chemicals, and gases trapped in the ice can be used to study how Earth's climate system operated in the past. However, this requires deep ice coring. The retrieved glacial ice can be utilized for an accurate measure of past greenhouse gases with climate clearly documented in the same core. Therefore, ice core data have become crucial to our understanding of past climate change and to making assessments about future climate.

The Soviet Antarctic research station Vostok was founded at the center of the East Antarctic Ice Sheet (78°28'S, 106°48'E, 3488 m.a.s.l.) in 1957 (Fig. 1). This place turned out to be the coldest on Earth; the lowest reliably measured temperature of -89.2°C was recorded on 21 July 1983. In addition, by good fortune Vostok was set above the southern end of the largest subglacial lake in Antarctica, discovered in 1996 by Russian and British scientists (Kapitsa et al., 1996) while drilling deep boreholes.

Deep ice core drilling at Vostok station began in 1970. In the 1970s a set of open uncased holes were drilled by a thermal drill system suspended on cable. The deepest dry hole in ice reached 952.4 m (Hole #1, May 1972). It was concluded that for drilling at greater depths it is necessary to prevent hole closure by filling of the borehole with a fluid. Thus, from 1980 on new thermal and electromechanical drill systems working in fluid were used. Two boreholes reached depths of more than 2000 m. Hole #3G-2 was deepened to 2201.7 m depth in 1985 (Kudryashov, 1989) and Hole #4G-2 to 2546.4 m depth in 1989 (Kudryashov et al., 1994). Drilling of both holes was aborted because of stuck tools.

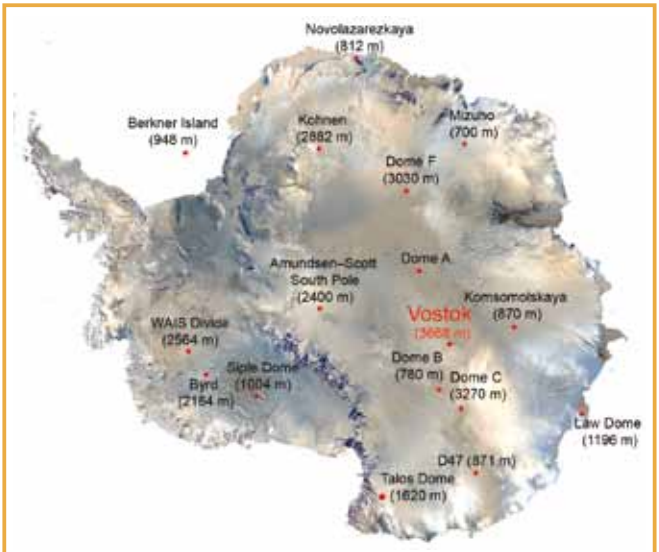

Figure 1. Vostok station and other deep ice coring sites on Antarctica.

Drilling Operations 1990–2010

Drilling a new deep Hole #5G started in February 1990, using a TELGA-14M thermal drill for dry coring to a depth of 120 m (Table 1). Thereafter, the thermal drill TBZS-152M for fluid-filled holes was used down to 2502.7 m, at which point it became stuck during tripping out due to hole closure caused by insufficient fluid pressurization. As recovery attempts failed, the cable was pulled out of the top of the drill (Tchistiakov et al., 1994).

About 35 meters of artificial core was dropped on top of the stuck drill, creating a base for a new offset hole. The TBZS-132 thermal drill was used to sidetrack and drill Hole #5G-1 (Fig. 2). The main difference between the thermal drills TBZS-132 and TBZS-152M was the outer diameter of the drill head and the tubing used for the core barrel and water tank (Kudryashov et al., 1998). In 1993 Hole #5G-1 reached 2755.3 m depth, a new record for thermal drilling in ice.

During the summer season 1993–1994, the borehole diameter was enlarged from 180 mm to 220 mm in the upper portion using an electromechanical reaming technique. The hole was cased with fiberglass tubing with a thermal shoe at the bottom, and was sealed at a depth of 120 m to prevent fluids from entering the hole through an upper permeable zone.

In November 1994, drilling operations in Hole #5G-1 were resumed with the KEMS-135 electromechanical drill (Fig. 3), reaching 3350 m depth by January 1996. An average penetration of 2.8 m was achieved per run, but at the depth greater than 2930 m, progress decreased dramatically because of frequent sticking and jamming (Kudryashov et al., 2002).

With season 1996–97 the drilling operations were reduced to the short Antarctic summer because a vehicle traverse failed to reach Vostok in the previous season. When

drilling of Hole #5G-1 was continued until January 1998 (reaching 3623 m depth), several design changes allowed an increase in the efficiency of ice destruction and drilling chips removal from the bottom of the hole.

After an eight-year hiatus, this hole was reopened in the summer 2005–06 (Vasiliev et al., 2007). A new geometry of cutters for penetration of "warm ice" improved the drilling process. As a result, Hole #5G-1 was deepened to 3658 m (January 2007), with an average core length of 0.7–0.8 m per run (Fig. 4). At this depth the drill became stuck at the bottom of the hole. A drill team that remained at Vostok station over winter filled the lower hole with eighty liters of an anti-freeze agent using a special fluid barrel with an electro-magnetic valve. The drill was captured with an overshot gripper and was lifted to surface in the first attempt before the water-glycol solution was removed from the hole. In May 2007 drilling continued, and different lengths of core barrels were applied to ensure proper functioning of an anti-torque system in cavity intervals. A total of fifty-five runs were required between 3658 m and 3668 m.

Unfortunately, during the hole enlargement in October 2007, the core barrel suddenly dropped to the bottom of the hole. All attempts to recover it failed, and operations did not resume before December 2008. A new deviated hole was drilled using thermal directional drilling to bypass the stuck tools (Vasiliev et al., 2007). The new deviated Hole #5G-2 was drilled without using any special whipstock because the drill bit is usually pushed into a vertical position.

Deviated drilling started at the depth of 3580 m using the electromechanical drill KEMS-135 with a special drill head and cutters. The hole was successfully deviated and drilled to 3600 m where the core with a normal circular cross-section was pulled out. Sidetracking of Hole #5G-2 for testing purpose showed the high efficiency of this technology.

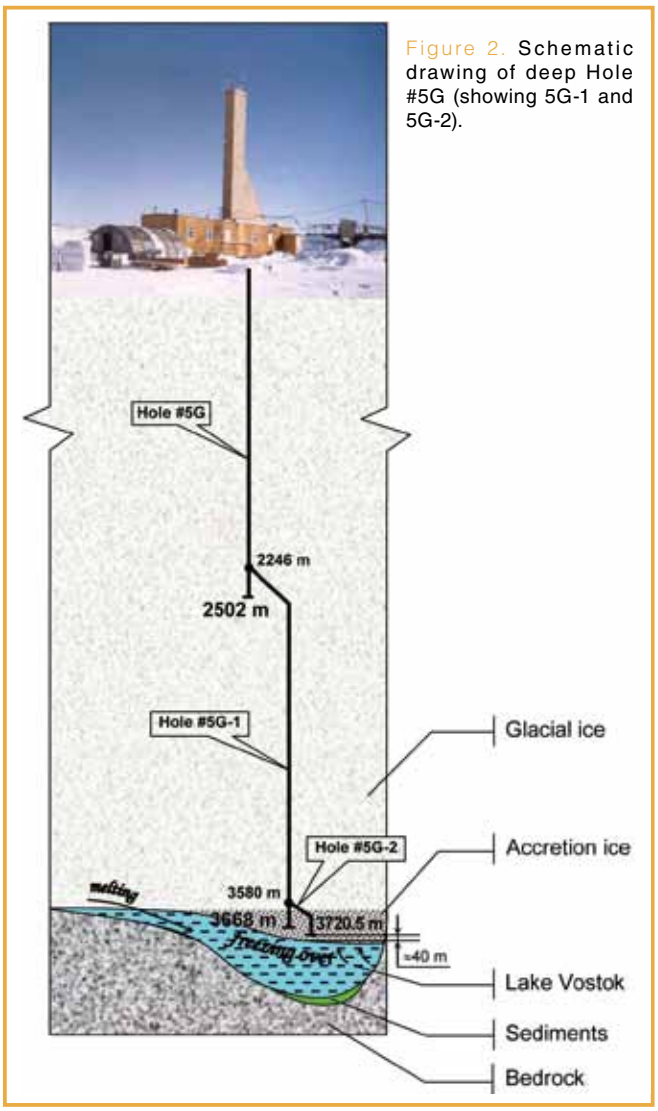

Figure 2. Schematic drawing of deep Hole #5G (showing 5G-1 and 5G-2).

In summer 2009–2010 drilling at Vostok continued, and Hole #5G-2 was deepened from 3600 m to 3650 m, nearly achieving the depth reached previously. According to our estimate the distance between the 5G-1 and 5G-2 holes at the

Table 1. Deep drilling of the Hole #5G (5G-1, 5G-2) at Vostok station.

Expedition # (Year)	Leader of the drilling team	Hole #	Interval of drilling (m)	Type of drill	Mean rate of penetration (m h^{-1})	Mean length of run (m)
35 (1990)	A.A. Zemtsov	5G	0–120	TELGA-14M	1.8	1.9
			120–1279.8	TBZS-152M	2.1	2.9
36 (1991)	A.V. Krasilev		1279.8–2502.7		2.3	3.0
37 (1992)	B.S. Moiseev	5G-1	2232–2249.5	TBZS-132	2.0	1.0
			2249.5–2270.7		2.0	2.0
38 (1993)	V.K. Chistyakov		2270.7–2755.3		1.8	2.5
40 (1993)	N.I. Vasiliev		2755.3–3109	KEMS-135	8.0	2.5
41* (1995)	N.I. Vasiliev		3109–3350		8.0	2.2
42* (1995/96)	N.I. Vasiliev		3350–3523		8.0	2.1
43* (1997/98)	N.I. Vasiliev		3523–3623		8.0	1.8
51* (2005/06)	N.I. Vasiliev		3623–3650		5.0	0.8
52 (2007)	N.I. Vasiliev		3650–3668		5.0	0.7
54* (2009/09)	N.I. Vasiliev	5G-2	3580–3600		-	-
55* (2009/10)	N.I. Vasiliev		3600–3650		5.0	0.7
56* (2010/11)	N.I. Vasiliev		3650–3720.5		5.0	0.9

*The drilling was conducted during the austral summer only.

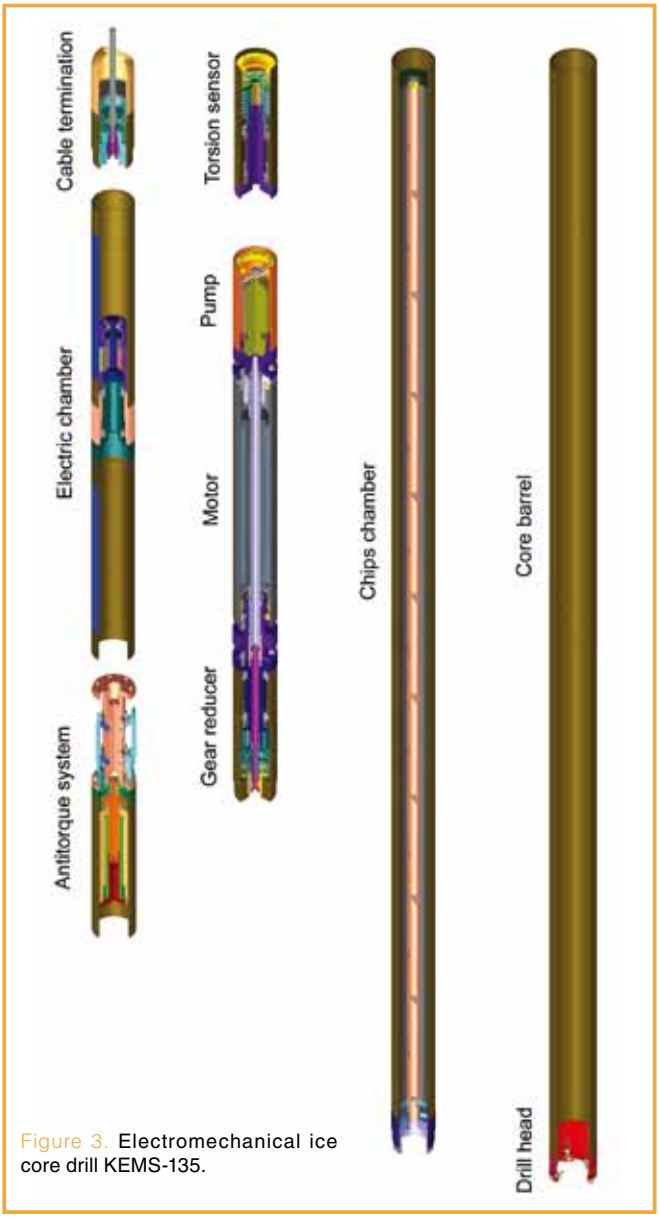

Figure 3. Electromechanical ice core drill KEMS-135.

bottom of Hole #5G-2 is nearly 1.5 m. In the summer season of 2010-11 the Hole #5G-2 reached the depth of 3720.5 m. The penetration into Lake Vostok will start in the coming years.

Summary of the Scientific Results

The upper 3310 meters of the Vostok ice core has provided a detailed paleoclimate record for the past four glacial-interglacial cycles occurring about every 100,000 years (Petit et al., 1999). The ice core record extends over the last 420,000 years (Fig. 5). The succession of changes through each climate cycle and termination was similar for the parameters shown; atmospheric and climate properties oscillated within stable limits. In contrast, interglacial periods differ in temporal evolution and duration.

Between 3310 m and 3539 m, the glacial core is disturbed by bedrock deformation (Souchez et al., 2003). Information on microparticles, crystal sizes, and chemical element distributions in that part of the core shed new light on this deformation process—the ice deformation occurred when the ice was still grounded upstream from Vostok station in a region with subfreezing temperatures.

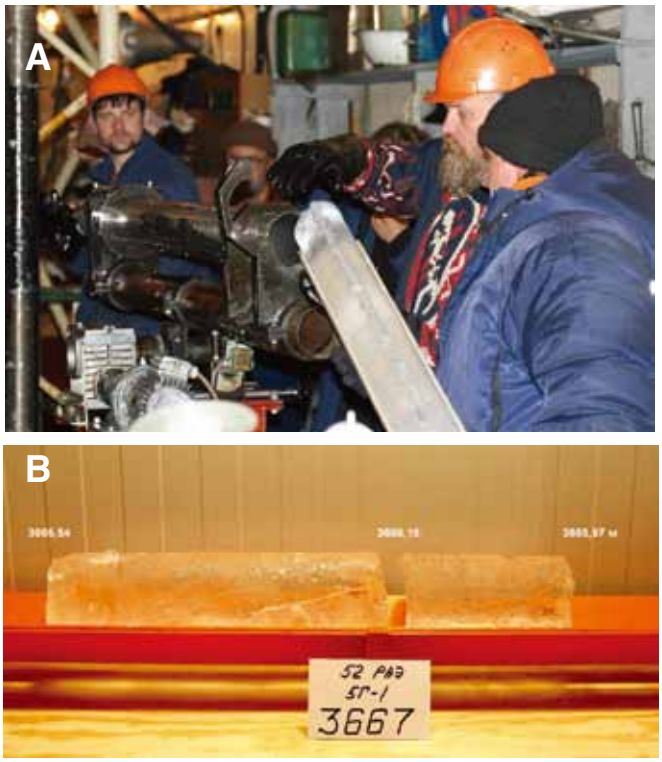

Figure 4. [A] Core recovering from the core barrel (January 2007). [B] Ice core from the deepest layers.

The deepest portion of the ice core (from 3539 m to 3668 m) has a chemistry, isotopic composition, and crystallography distinctly different from the overlying glacial ice. Geochemical and physical data indicate that it originated from the accretion of subglacial lake water to the underside of the ice sheet (Jouzel et al., 1999). Together with data on ionic chemistry, these ice core data favor an origin of the lake ice by frazil ice generation in a supercooled water plume existing in the lake, followed by accretion and consolidation from subsequent freezing of the host water.

Microbiological studies of the Vostok glacial and accreted ice have indicated that low, but detectable, concentrations of prokaryotic cells (Fig. 6) and DNA are present (Bulat et al., 2004). Many of the bacterial cells are associated with non-living organic and inorganic particulate matter. Some of the viable bacteria were deposited more than 400,000 years ago (Bobin et al., 1994).

According to petro-fabric investigation, development of shear zones in the Antarctic ice sheet is linked with global increase of the dust concentration in the atmosphere during past glacial maxima (Lipenkov et al., 2007). The ice strata forming in these periods are characterized by high impurities of microparticles, small ice-grain sizes, single-maximum c-axis orientation, and low ice viscosity.

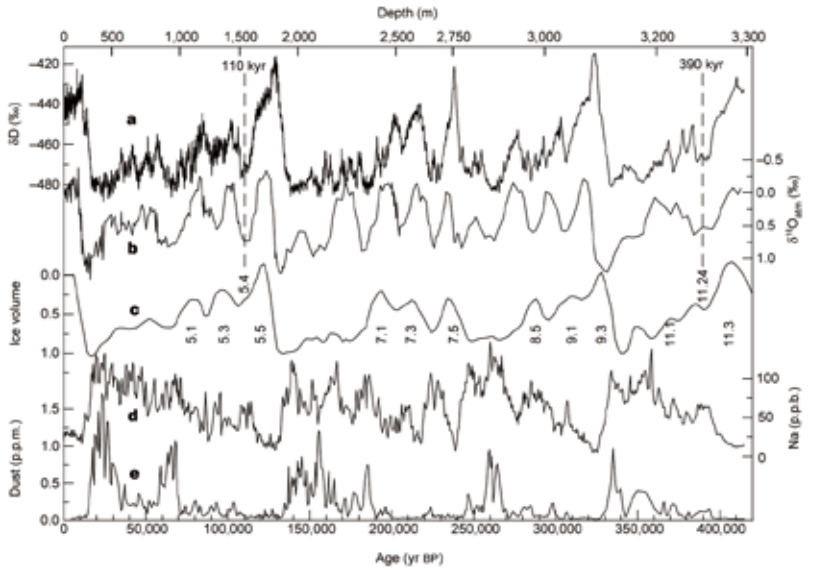

Figure 5. 420,000-year profiles of (1) deuterium, (2) $\delta^{18}O_{atm}$, (3) seawater $\delta^{18}O$ (ice volume proxy), (4) sodium, and (5) dust (Petit et al., 1999).

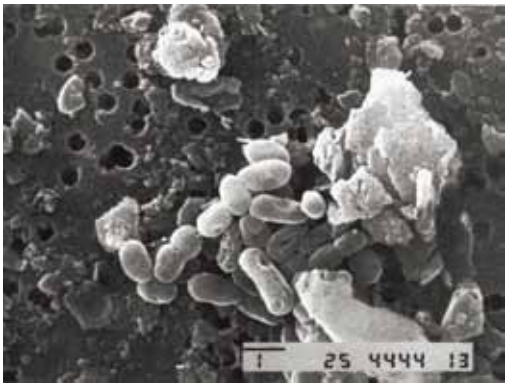

Figure 6. Microbes from Vostok ice core, depth of 2395 m, magnification x14,000 (Bobin et al., 1994).

In recent years, advances have been made in understanding and predicting the physical and chemical environment of Lake Vostok based on modeling efforts that set boundary conditions for various attributes. Future studies of the subglacial water properties and searching for ancient life are now important parts of the project at Lake Vostok.

Planning Penetration into Lake Vostok

With dimensions of 280 km x 50 km and water depth reaching 1200 m (Fig. 7) beneath an almost 4-km-thick ice sheet, Lake Vostok is the largest among more than 145 subglacial lakes identified by radar surveys in Antarctica (Siegert et al., 2005). Independent data sources indicate the ice-water interface at Vostok is at 3760±15 m depth. The remaining ice between the bottom of Hole #5G-2 and the lake is about 40 m thick. We plan to access the lake and sample its waters in three stages (Verkulich et al., 2002).

On the first stage an ecologically inert liquid (e.g., polydimethylsiloxane) will be injected to the hole bottom using a special tanker. It is anticipated that, being heavier than the drilling fluid and lighter than water, this hydrophobic liquid will create a 100-m-thick "buffer-layer" at the lower part of the hole. The hydrostatic pressure at the bottom of Hole #5G-2 should be slightly lower than the overburden ice pressure.

In a second stage, Hole #5G-2 will be deepened down to the ice-water interface. The access to the lake will be completed with the coreless thermal drill system TBPO-132 consisting of two parts: a 2-m-long pilot microdrill generating a 50-mm-diameter hole, followed by the main drill equipped with a 132-mm-diameter thermal drill bit. With this system an average penetration rate of 3–4 m hr^{-1} is expected. The drill will be cleaned by the produced melt water which creates a second clean layer separating the bottom of the hole from the drilling fluid. Once the tip of the thin pilot drill punctures the lake surface, the packer will be automatically turned on, and the drill heating and ad-vance will stop. After determination of the pressure differ-ence between hole and lake and maintaining it in a range of 3–4 bars, the thermal drill TBPO-132 will be pulled up. This will allow lake water to enter into the hole and to fill up its lower 30–40 meters.

The third stage could be conducted after checking if the water has frozen in the hole. Then, the frozen lake water will be sampled with electromechanical drill KEMS-135 to a level of about 15–20 m above the ice-water interface.

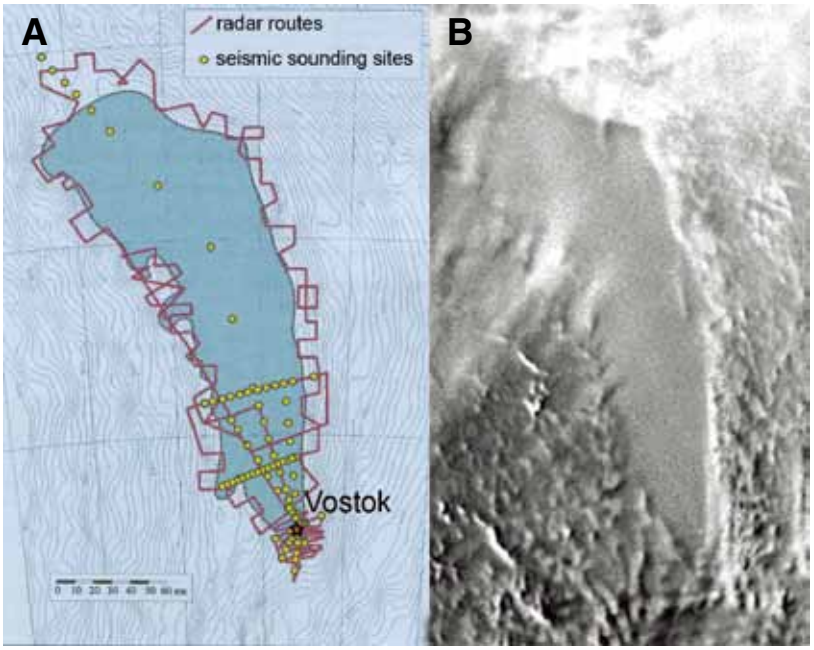

Figure 7. Lake Vostok topography according to [A] geophysical data and [B] Antarctic surface in the region of Vostok from ERS-1 radar altimeter data.

The Lake Vostok penetration approach discussed above has already been tested, though unintentionally, in the course of implementing two international glacial drilling projects in Greenland (North Greenland Ice core Project, NGRIP, 2003) and Antarctica (EPICA drilling at Kohnen station, 2006). In both cases the drilling was performed with routine electromechanical coring of ice without special precautions in the holes filled with kerosene-based drilling fluid similar to that currently used at Vostok. When the base of the ice sheet was reached, the sub-ice water flooded the hole up to several tens of meters above the bed. The water frozen in the NGRIP borehole was drilled in 2004 and later analyzed.

References

Bobin, N.E., Kudryashov, B.B., Pashkevitch, V.M., Abyzov, S.S., and Mitskevich, I.N., 1994. Equipment and methods of microbiological sampling from deep levels of ice in central Antarctica. *Mem. Natl. Inst. Polar Res. Spec. Issue*, 49:184–191.

Bulat, S.A., Alekhina, I.A., Blot, M., Petit, J.R., de Angelis, M., Wagenbach, D., Lipenkov, V.Ya., Vasilyeva, L.P., Wloch, D.M., Raynaud, D., and Lukin, V.V., 2004. DNA signature of thermophilic bacteria from the aged accretion ice of Lake Vostok, Antarctica: implications for searching life in extreme icy environments. *Int. J. Astrobiol.*, 3(1):1–12.

Jouzel, J., Petit, J.R., Souchez, R., Barkov, N.I., Lipenkov, V.Ya., Raynaud, D., Stievenard, M., Vassiliev, N.I., Verbeke, V., and Vimeux, F., 1999. More than 200 meters of lake ice above subglacial Lake Vostok, Antarctica. *Science*, 286(5447): 2138–2141, doi:10.1126/science.286.5447.2138.

Kapitsa, A.P., Ridley, J.K., de Robin, Q.G., Siegert, M.J., and Zotikov, I.A., 1996. A large deep freshwater lake beneath the ice of central East Antarctica. *Nature*, 381:684–686, doi:10.1038/381684a0.

Kudryashov, B.B., 1989. Soviet experience of deep drilling in Antarctica. *In* Bandopadhyay, S., and Skudrzyk, F.J. (Eds.), *Mining in the Arctic: Proc. 1st Int. Symp. Fairbanks*, London (Taylor & Francis), 113–122.

Kudryashov, B.B., Vasiliev, N.I., and Talalay, P.G., 1994. KEMS-112 electromechanical ice core drill. *Mem. Natl. Inst. Polar Res.*, 49:138–152.

Kudryashov, B.B., Krasilev, A.V., Talalay, P.G., Tchistyakov, V.K., Vassiliev, N.I., Zubkov, V.M., and Lukin, V.V., 1998. Drilling equipment and technology for deep ice coring in Antarctica. *In* Hall, J. (Ed.) *Proc. 7th Symp. Antarctic Logistics and Operations,* Cambridge, U.K. (British Antarctic Survey), 205–210.

Kudryashov, B.B., Vasiliev, N.I., Vostretsov, R.N., Dmitriev A.N., Zubkov, V.M., Krasilev, A.V., Talalay, P.G., Barkov, N.I., Lipenkov, V.Ya., and Petit, J.R., 2002. Deep ice coring at Vostok station (East Antarctica) by an electromechanical drill. *Mem. Natl. Inst. Polar Res. Spec. Issue*, 56:91–102.

Lipenkov, V.Ya., Polyakova, E.V., Duval, P., and Preobrazhenskaya, A.V., 2007. Osobennosti stroenia Antartkticheskogo lednikovogo pokrova v raione stantsii Vostok po rezul'tatam petrostruktnikh issledovanyi ledyanogo kerna (Structure of Antarctic Ice Sheet in the region of Vostok station according to petro-fabric investigation of ice core). *Problemi Arktiki i Antarktiki (Arctic and Antarctic Problems)*, 76:68–77. (in Russian).

Petit, J.-R., Jouzel, J., Raynaud, D., Barkov, N.I., Barnola, J.-M., Basile, I., Bender, M., Chappellaz, J., Davis, M., Delaygue, G., Delmotte, M., Kotlyakov, V.M., Legrand, M., Lipenkov, V.Y., Lorius, C., Pepin, L., Ritz, C., Saltzman, E., and Stievenard, M., 1999. Climate and atmospheric history of the past 420,000 years from the Vostok ice core, Antarctica. *Nature*, 399:429–436, doi:10.1038/20859.

Siegert, M.J., Carter, S., Tabacco, I.E., Popov, S., and Blankenship, D.D., 2005. A revised inventory of Antarctic subglacial lakes. *Antarct. Sci.*, 17(3):453–460.

Souchez, R., Jean-Baptiste, P., Petit, J.R., Lipenkov, V.Ya., and Jouzel, J., 2003. What is the deepest part of the Vostok ice core telling us? *Earth-Sci. Rev.*, 60:131–146, doi:10.1016/S0012-8252(02)00090-9.

Tchistiakov, V.K., Kracilev, A., Lipenkov, V.Ya., Balestrieri, J.Ph., Rado, C., and Petit, J.R., 1994. Behavior of a bore hole drilled in ice at Vostok station. *Mem. Natl. Inst. Polar Res. Spec. Issue*, 49:247–255.

Vasiliev, N.I., Talalay, P.G., Bobin, N.E., Chistyakov, V.K., Zubkov, V.M., Krasilev, A.V., Dmitriev, A.N., Yankilevich, S.V., and Lipenkov, V.Ya., 2007. Deep drilling at Vostok station, Antarctica: history and last events. *Annal. Glaciol.*, 47:10–23.

Verkulich, S.R., Kudryashov, B.B., Barkov, N.I., Vasiliev, N.I., Vostretsov, R.N., Dmitriev, A.N., Zubkov, V.M., Krasiliev, A.V., Talalay, P.G., Lipenkov, V.Ya., Savatyugin, L.M., and Kuz'mina, I.N., 2002. Proposal for penetration and exploration of sub-glacial Lake Vostok, Antarctica. *Mem. Natl. Inst. Polar Res. Spec. Issue*, 56:245–252.

Authors

Nikolay I. Vasiliev, Drilling Department, St. Petersburg State Mining Institute, 2, 21 Line, St. Petersburg 199106, Russia, e-mail: vasilev_n@mail.ru.

Pavel G. Talalay, Polar Research Center, Jilin University, No. 6 Ximinzhu Street, Changchun City, Jilin Province 130026, China, e-mail: ptalalay@yahoo.com.

and Vostok Deep Ice Core Drilling Parties (Vladimir M. Zubkov, Valery K. Chistyakov, Andrey N. Dmitriev, Vladimir Ya. Lipenkov, and others)

Related Web Links

NGRIP: http://www.gfy.ku.dk/~www-glac/ngrip/hovedside_eng.htm

EPICA: http://www.awi.de/en/research/research_divisions/geosciences/glaciology/projects/epica/

Figure Credits

All photos were provided by members of Vostok drilling team.

Deep Drilling at the Dead Sea

by Mordechai Stein, Zvi Ben-Avraham, Steve Goldstein, Amotz Agnon, Daniel Ariztegui, Achim Brauer, Gerald Haug, Emi Ito, and Yoshinori Yasuda

doi:doi:10.2204/iodp.sd.11.04.2011

At the lowest point on Earth, the Dead Sea, a unique scientific project, the Dead Sea Deep Drilling Project (DSDDP), is being conducted to establish a late Quaternary paleoenvironmental, tectonic, and seismological archive. Scientific groups from Germany, Israel, Japan, Jordan, Norway, Palestine, Switzerland, and the U.S.A. gathered for the first time on 21 November 2010 to perform scientific drilling at the floor of the deep basin of the Dead Sea (Fig. 1). With current lake level of 423 m below sea level and water depth of 300 m, coring started at 723 m below mean sea level. During the first three weeks of drilling ~460 meters of sediment cores were recovered. As expected from shallow piston cores and on-land deposits from the lake level highstands, the cores are composed of alternating intervals of marly units and salts (Fig. 2). The sedimentary intervals represent several glacial and interglacial cycles spanning an estimated interval of ~200,000 years. Two coarse-grained sections imply almost complete dry-out phases of the Paleo-Dead Sea, meaning that twice the lake surface was several hundred meters below present day sea level.

Drilling is being conducted with the Large Lake Drilling Facility (see front cover of this issue) of DOSECC (Drilling Observation and Sampling of the Earth´s Continental Crust, Inc.). The upper 30 meters were cored by using a hydraulic piston coring system that is capable of penetrating several salt layers with high core recovery, while the deeper section was retrieved with the extended-nose bit coring tools (Fig. 3).

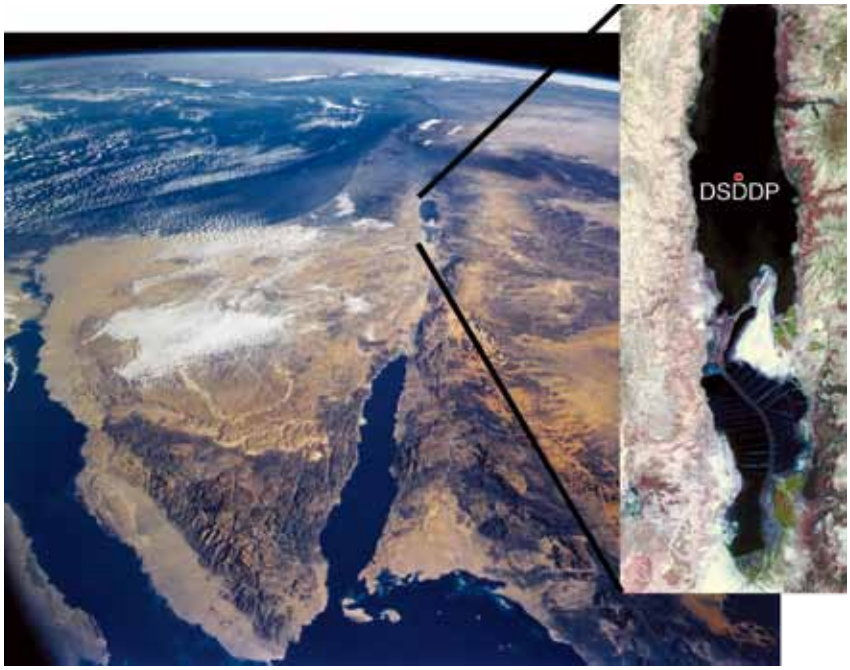

Figure 1. The Dead Sea basin and the location of the ICDP-DSDDP drilling site.

Why Drill the Dead Sea?

The Dead Sea Basin (DSB) is located between the Mediterranean and desert climate zones. In the late Neogene the basin was invaded by Mediterranean marine water that formed the Sedom lagoon. The evaporated ingressing seawater led to the deposition of thick sequences of salt and formation of the calcium chloride brine that dominated the subsequent geochemical-limnological evolution of water bodies in the basin. After disconnection of the Sedom lagoon from open sea, the basin was filled with several lakes that captured in their sedimentary filling the hydrological regime of large drainage area of the DSB, reflecting the Levant paleoclimate. The lakes expanded during ice ages and contracted during interglacials. During the last glacial (~70–14 ka ago) Lake Lisan rose up to 250 m above the Holocene Dead Sea and extended from south of the modern Dead Sea northward to the Sea of Galilee. This configuration illustrates the dramatic changes in the regional hydrology and lake configuration and reflects global climate conditions. Moreover, the formation of the DSB is associated with the tectonic activity along the Dead Sea Transform Fault (Ben-Avraham, 1997); thus, its sediments preserve the history of earthquakes (Migowski et al., 2004). The DSB is also the locus of humankind's migration out of Africa, and the home of people from Paleolithic to modern times (Goren-Inbar et al., 2000). Studies of the sedimentary sections exposed on the Dead Sea margins have been applied to issues with global and region-al implications associated with paleoclimate, tectonics, paleoseismology, paleomagnet-ism, and human history (Stein, 2001; Enzel et al., 2006; Waldmann et al., 2010).

The lacustrine sections exposed in the marginal terraces of the modern Dead Sea contain only the sedimentary archives deposited during lake highstands (e.g., the Lisan Formation). The main operational purpose of the DSDDP is to recover long, continuous, high-resolution cores that will provide a com-

Figure 2. Drill cores in liners recovered at depth around 300 m below lake floor. From top to bottom the cores show change from gravel (top core) to marls interlaced with fine-grained salt layers (middle cores). This suggests that at that time the shore was very close to the drilling site, and the wavy salt patterns were interpreted as a result of salt flow.

plementary record to the sections recovered from the marginal terraces, particularly for time interval of low lake stands when the lake retreated from the marginal terraces. The calcium chloride brine that was produced during the ingression of the Sedom lagoon is poor in bicarbonate and sulfate, and therefore, when freshwater enters the lake, primary aragonite is deposited. The aragonite provides an excellent and unique means to achieve calendar chronology down to a few hundred thousand years. This illustrates a major advantage of the sedimentary archive of the Dead Sea and allows comparison to global records such as ice cores and deep sea cores. Data from core samples will establish a pattern of abrupt hydrological events in the drainage area, and the brine-freshwater relations during the different stages will be explored to evaluate effects of long-term climatic trends versus short-term fluctuations.

Figure 3. Extended-nose coring tool with outer and inner core bit. Most of the cores were retrieved with this tool.

The project is performed under the wings and support of the International Continental Scientific Drilling Program (ICDP). The drilling operation is performed by DOSECC.

References

Ben-Avraham, Z., 1997. Geophysical framework of the Dead Sea: structure and tectonic. *In* Niemi, T.M., Ben-Avraham, Z., and Gat, J.R. (Eds.), *The Dead Sea: The Lake and Its Settings*: New York (Oxford University Press), Oxford Monographs on Geology and Geophysics, 36:22–35.

Enzel. Y., Agnon A. and Stein M. 2006. *New Frontiers in Dead Sea Paleoenvironmental Research, GSA Spec. paper 401:* Boulder, CO (The Geological Society of America).

Goren-Inbar, N., Feibel, C.S., Verosub, K.L., Melamed, Y., Kislev, M., Tchernov, E., and Saragusti, I., 2000. Pleistocene milestones on the out-of-Africa corridor at Gesher Benot Ya'aqov, Israel. *Science*, 89:944–947.

Migowski, C., Agnon, A., Bookman, R., Negendank, J.F.W., and Stein, M., 2004. Recurrence pattern of Holocene earthquakes along the Dead Sea transform revealed by varve-counting and radiocarbon dating of lacustrine sediments. *Earth Planet. Sci. Lett.*, 222:301–314.

Stein, M., 2001. The history of Neogene-Quaternary water bodies in the Dead Sea Basin. *J. of Paleolimnology* 26: 271-282.

Waldmann, N., Torfstein, A., and Stein, M., 2010. Northward migration of monsoon activity across the Saharo-Arabian desert belt during the last interglacial: evidence from the Levant. *Geology*, 38:567–570.

Authors

Mordechai Stein, Geological Survey of Israel, 30 Malkhe Israel St. Jerusalem, 95501, Israel, e-mail: motistein@gsi.gov.il.

Zvi Ben-Avraham, Department of Geological Sciences, Louis Ahrens Building, Library Road, University of Cape Town, Rondebosch, 7700, Republic of South Africa.

Steve Goldstein, Lamont-Doherty Earth Observatory, 213 Comer, 61 Route 9W - P.O. Box, 1000 Palisades, NY 10964-8000, U.S.A.

Amotz Agnon, Institute of Earth Sciences, Hebrew University of Jerusalem, Edmond J. Safra campus, Givat Ram, 91904, Jerusalem.

Daniel Ariztegui, Department of Geology and Paleontology, University of Geneva, 13, Rue des Maraîchers, CH-1205 Genève, Switzerland.

Achim Brauer, Helmholtz Centre Potsdam, GFZ German Research Centre for Geosciences, Section 5.2, Climate Dynamics and Landscape Evolution, Telegrafenberg, C 323 D-14473 Potsdam, Germany.

Gerald Haug, ETH Zürich, Geologisches Institut NO G 51.1, Sonneggstrasse 5, 8092 Zürich, Switzerland.

Emi Ito, Geology and Geophysics, Room 108, PillsH 0211, 310 Pillsbury Drive SE, Minneapolis, MN 55455, U.S.A.

Yoshinori Yasuda, International Research Center for Japanese Studies, 3-2 Oeyama-cho, Goryo, Nishikyo-ku, Kyoto 610-1192, Japan.

Related Web Links

http://deadsea.icdp-online.org
http://www.dosecc.org

Figure Credits

Fig. 1: The National Aeronautics and Space Administration, (NASA)
Fig. 2: Michael Lazar, Department of Marine Geosciences, University of Haifa, Israel
Fig. 3: Uli Harms, ICDP, GFZ Potsdam, Germany

SAFOD Phase III Core Sampling and Data Management at the Gulf Coast Repository

by Bradley Weymer, John Firth, Phil Rumford, Frederick Chester, Judith Chester, and David Lockner

doi:10.2204/iodp.sd.11.06.2011

Introduction

The San Andreas Fault Observatory at Depth (SAFOD) project is yielding new insight into the San Andreas Fault (Zoback et al., 2010; Zoback et al., this issue). SAFOD drilling started in 2002 with a pilot hole, and proceeded with three phrases of drilling and coring during the summers of 2004, 2005, and 2007 (Fig. 1). One key component of the project is curation, sampling, and documentation of SAFOD core usage at the Integrated Ocean Drilling Program's (IODP) Gulf Coast Repository (GCR) at Texas A&M University. We present here the milestones accomplished over the past two years of sampling Phase III core at the GCR.

Research Themes

Several research themes rely heavily on SAFOD core samples. These are focused on understanding the structure, composition, and a variety of physical and mechanical properties of the San Andreas Fault. Structural studies are concerned with characterizing the geometry of the fault zone, the distribution of shear displacement, the process by which rocks are deformed, and the microscopic features that record past occurrences of earthquake slip and creeping deformation. Core samples are ideal for structural study at macroscopic and microscopic scales, using non-destructive techniques such as mapping the surface of the core and X-ray computed tomography (CT scanning) to image the interior of the core, as well as destructive techniques such as cutting and polishing small sub-samples for optical and electron microscopy.

Compositional studies focus on the elemental, chemical, and mineral content of the fault zone to understand the processes and conditions which occur during faulting, such as rates of chemical reactions between minerals and pore fluids, the origin of the rock and fluids in the fault, and the pressure and temperature at depth. These studies involve a variety of subsample processing techniques and analytical instruments such as X-ray diffraction and fluorescence, electron microprobe, and mass spectrometers.

Laboratory experimentation with core samples is an important way to quantify a host of physical and mechanical properties that are important to faulting processes. Sub-samples are used to determine thermal conductivity, porosity and permeability, and seismic velocity within the fault. Mechanical testing explores the fracture, friction, and flow properties of the fault rocks in the actively deforming portions of the fault zone.

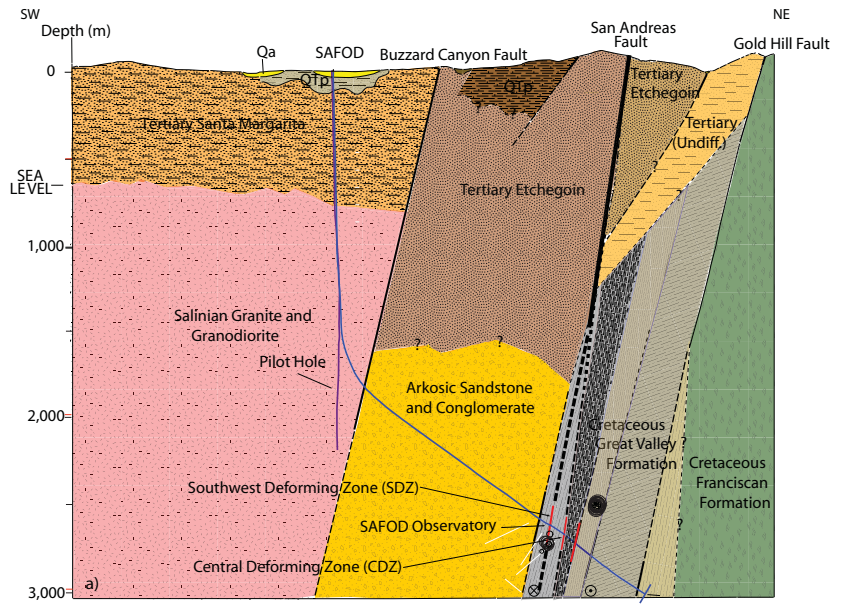

Figure 1. Diagram showing the location of both active traces of the San Andreas Fault that were spot-cored in 2007. Modified from Zoback et al., 2010.

Inter-Laboratory Comparison Project

The main objective of the Inter-Laboratory Comparison Project was to run tests on standardized sample materials to provide a baseline for the comparison of results from experiments conducted on SAFOD Phase III core samples (Lockner et al., 2009). A total of eighteen laboratories from nine countries conducted the following tests: intact rock strength, frictional strength, permeability, electrical resistivity, ultrasonic wave speed, thermal conductivity, and related properties such as porosity and density. Standardized protocols were established, and test samples were distributed to participating laboratories in the fall of 2008. Friction tests were conducted on crushed and sieved samples of

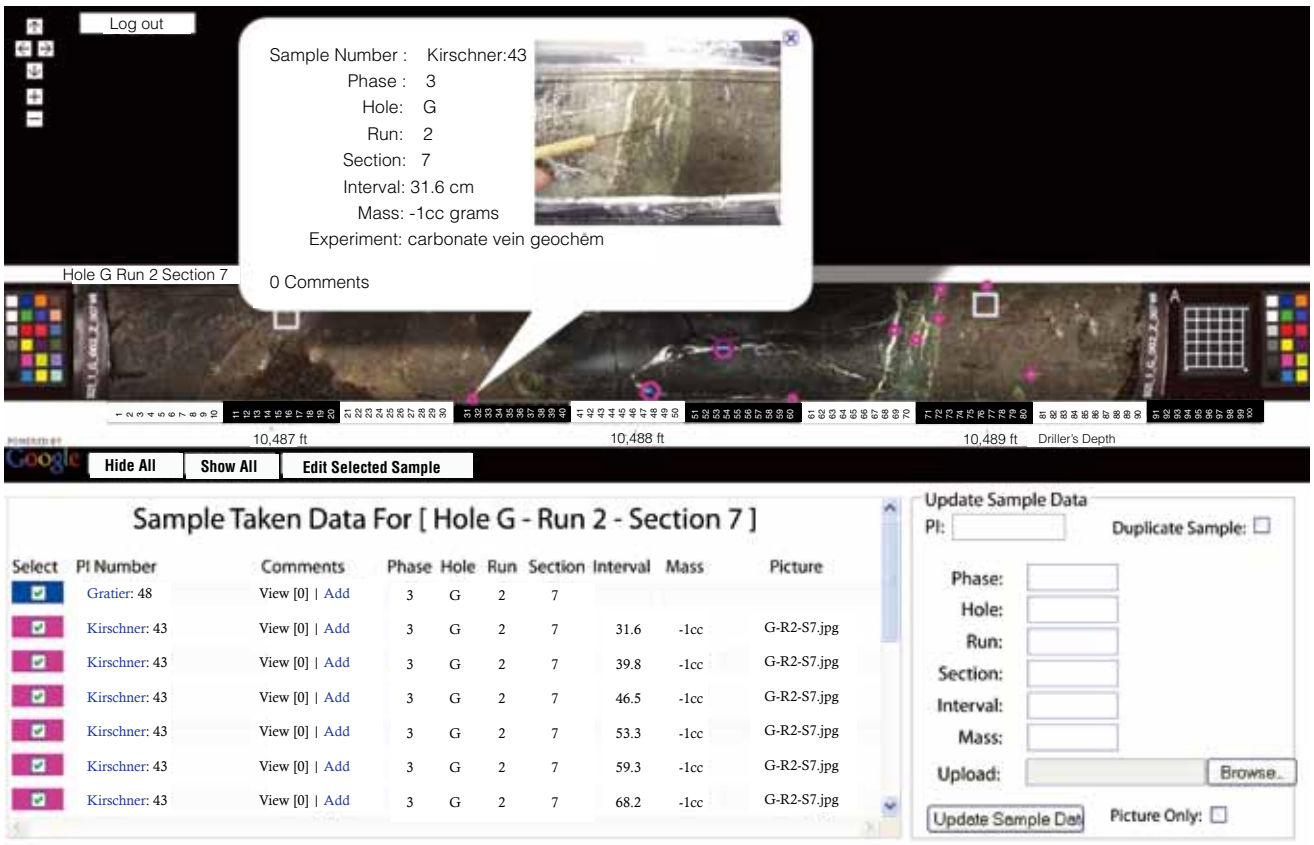

Figure 2. Example of SAFOD Core Viewer sample information taken from Round 1.

quartz, granite, talc, a quartz/smectite mixture, and SAFOD cuttings. Other physical property measurements were conducted on marble, granite, and three types of sandstones. Preliminary results of the inter-lab comparisons were discussed at the EarthScope meeting in Boise, Idaho in 2009 (Lockner et al., 2009), and further results were presented at the AGU 2010 Fall Meeting.

SAFOD Sampling at the Gulf Coast Repository

After the arrival of Phase III cores, the GCR assumed full curatorial responsibilities of all SAFOD samples (Phases 1 to 3). All SAFOD sampling follows the guidelines outlined by the SAFOD Sample Policy. This requires Principal Investigators (PIs) to submit all analytical data and metadata to the GCR for placement on the SAFOD web site in a timely manner. Currently, data are available to the public via the SAFOD Core Viewer.

The first cycle of sample requests (Round 1) were for 790 samples from twenty-eight PI groups comprising ninety-eight scientists from around the world. The approved sample distribution was 190 samples for twenty PI groups, comprising fifty-eight scientists. Round 1 sampling started on 28 June 2008 and was completed on 17 December 2008. After the completion of Round 1 sampling, the SAFOD Sample Committee (SSC) began accepting requests for Round 2.

Round 2 requests were for 344 samples from thirteen PI groups, comprising thirty-nine scientists, and all of them were approved. About 20% of the requesting PIs from Round 2 were from institutions outside the U.S. Round 2 sampling commenced on 21 July 2009 and remains a work in progress. To date, a total of 164 (as of December 2010) samples have been taken.

The SAFOD Core Viewer

A major component of the SAFOD project involved the creation and maintenance of an interactive, online core sample database and administration tool by staff at EarthScope/UNAVCO (University NAVstar COnsortium), with design input originally from Charley Weiland at Stanford University and now the IODP-GCR curatorial staff. Building upon the flexibility of Google Maps API, the SAFOD Core Viewer serves as a repository for all information related to the project from sample inventories and photo libraries to data storage. The Core Viewer has three views for each core section: (1) Samples Requested, (2) Samples Approved, and (3) Samples Taken. The Core Viewer provides the following functions (Fig. 2):

1. It allows all interested PI groups to submit their sample requests to be reviewed online by the SSC.

2. It provides the GCR curatorial staff the ability to view all approved sample requests and aids in the sampling process.
3. After samples are taken, any information pertaining to each sample, such as the type of experiment, expected results, pictures, and subsequent data, can be uploaded into the Core Viewer (Figs. 3A, 3B).
4. After review, data are also uploaded and made available on the public Core Viewer.

Acknowledgements

We thank the SAFOD Co-PI's Mark Zoback, Stephen Hickman, and William Ellsworth, as well as the support of Charley Weiland, for their guidance and support during the sampling and data management phase of the project. A special thanks to Brian Blackman, Michael Jackson, and Adrian Borsa at UNAVCO for the development and continued improvement of the Core Viewer. We also thank Kaye Shedlock and Greg Anderson at NSF, and the SAFOD Sample Committee.

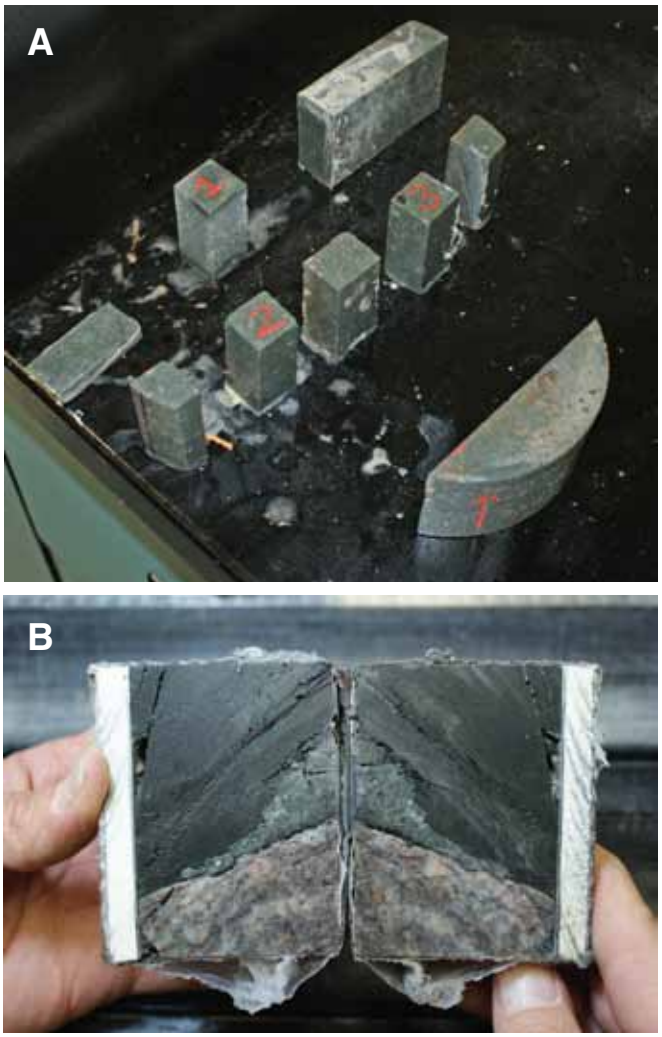

Figure 3. [A] Image of precise cuts for friction studies during Round 1 that documents the sampling process and was uploaded into the Core Viewer. [B] Example of Round 2 image within the SAFOD Core Viewer. Section E-R1-S5, showing a fault contact between dark grayish-black siltstone and grayish-red pebbly sandstone.

References

Lockner, D., Marone, C., and Saffer, D., 2009. SAFOD inter-laboratory comparisons - a progress report [poster presented at the EarthScope 2009 meeting in Boise, Idaho, 12–15 May 2009].

Zoback, M., Hickman, S., and Ellsworth, W., 2010. Scientific drilling into the San Andreas Fault zone. *Eos, Trans. AGU*, 91(22):197–204, doi:10.1029/2010EO220001.

Authors

Bradley Weymer, SAFOD Curatorial Specialist and Graduate Assistant Researcher, Integrated Ocean Drilling Program and SAFOD, Texas A&M University, 1000 Discovery Drive, College Station, TX 77845-9547, U.S.A, e-mail: weymer@iodp.tamu.edu.

John Firth, Curator, and **Phil Rumford**, GCR Superintendent, Integrated Ocean Drilling Program and SAFOD, Texas A&M University, 1000 Discovery Drive, College Station, TX 77845-9547, U.S.A.

Frederick M. Chester, Professor, and **Judith S. Chester**, Associate Professor, Department of Geology and Geophysics, TAMU, Center for Tectonophysics and Department of Geology & Geophysics, Texas A&M University, College Station, TX 77843-3115, U.S.A.

David Lockner, U.S. Geological Survey, Menlo Park, U.S. Geological Survey Earthquake Science Center, 345 Middlefield Road, MS/977Menlo Park, CA 94025, U.S.A.

Related Web Links

http://safod.icdp-online.org
http://www.earthscope.org/publications
http://www.earthscope.org/observatories/safod
http://www.earthscope.org/data/safod_core_viewer
http://www.earthscope.org/es_doc/safod/SAFOD_Core_Sample_Distribution.pdf
http://www.earthscope.org/data/safod_core_samples

Photo Credit

Fig. 3: Photos by Bradley Weymer, IODP and SAFOD, Texas A&M University

Executive Summary: "Mantle Frontier" Workshop

by Workshop Report Writing Group

doi:10.2204/iodp.sd.11.07.2011

Introduction

The workshop on "Reaching the Mantle Frontier: Moho and Beyond" was held at the Broad Branch Road Campus of the Carnegie Institution of Washington on 9–11 September 2010. The workshop attracted seventy-four scientists and engineers from academia and industry in North America, Asia, and Europe.

Reaching and sampling the mantle through penetration of the entire oceanic crust and the Mohorovičić discontinuity (Moho) has been a longstanding goal of the Earth science community. The Moho is a seismic transition, often sharp, from a region with compressional wave velocities (Vp) less than 7.5 km s^{-1} to velocities ~8 km s^{-1}. It is interpreted in many tectonic settings, and particularly in tectonic exposures of oceanic lower crust, as the transition from igneous crust to mantle rocks that are the residues of melt extraction. Revealing the *in situ* geological meaning of the Moho is the heart of the Mohole project. Documenting ocean-crust exchanges and the nature and extent of the subseafloor biosphere have also become integral components of the endeavor. The purpose of the "Mantle Frontier" workshop was to identify key scientific objectives associated with innovative technology solutions along with associated timelines and costs for developments and implementation of this grand challenge.

Background: Ocean Drilling and the Mantle Target

Scientific ocean drilling started from the first excitement of Mohole Phase I that penetrated 180 m in 3300 m water depth off Guadalupe Island (west of Baja California, Mexico) in April 1961 (Bascom, 1961; Steinbeck, 1961; Cromie, 1964), although the Mohle project was abandoned soon after (Greenberg, 1966). Fifty years after Mohole Phase I, the deepest hole into the oceanic crust is located on the Nazca Plate in the eastern equatorial Pacific (ODP Hole 504B) to 2111 m below the seafloor (mbsf) within the sheeted dikes. The second deepest hole in the Pacific, 1256D (1507 mbsf), is on the Cocos Plate northwest of 504B; it penetrates the transition zone between the upper and the lower crust, in the upper gabbroic rocks below the sheeted dike complex. Other significantly deep holes over 1000 m deep beneath the seafloor include ODP Hole 735B (1508 mbsf) in the Indian Ocean (Atlantis Bank) and IODP Hole U1309D (1415 mbsf) at the Atlantis Massif in the Atlantic Ocean. These achievements of relatively deep crustal penetration were made with the available riserless drilling technology. The deep holes outside the Pacific Ocean were drilled in uplifted fault blocks where lower crustal rocks are exhumed at shallow depths, in heterogeneous slow-spread ocean lithosphere.

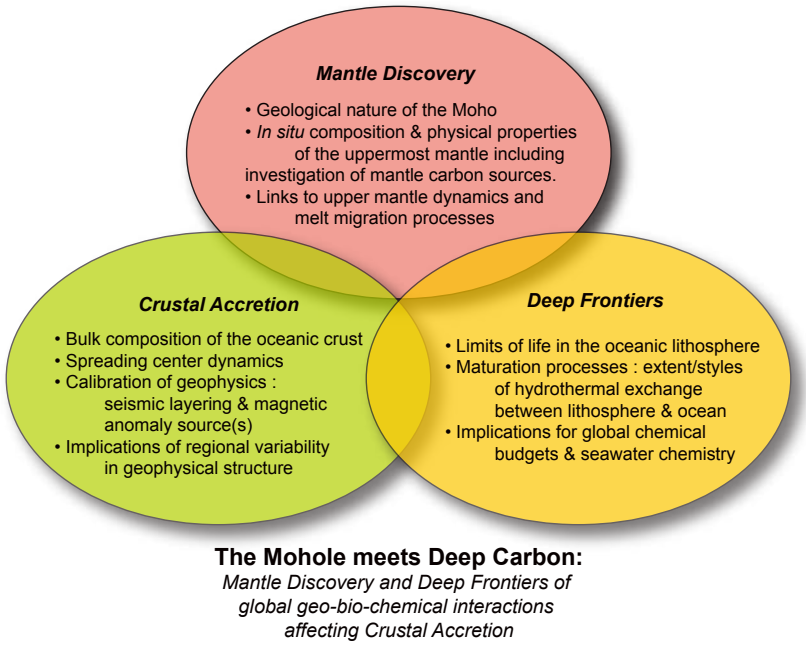

Figure 1. Scientific rationale discussed at the Workshop. After Ildefonse et al. (2010).

In 2007, a riser-equipped drilling ship was introduced to IODP (D/V *Chikyu,* owned and operated by JAMSTEC). Riser technology significantly improves the deep drilling capability as proven by oil industry experience. The science plan of IODP thus includes 21st Century Mohle as one of its initiatives (IODP, 2001). We are in an era where drilling technology is rapidly advancing to realize deep drilling (>6 km below seafloor) in deep waters (industry drilling in >3000 m water depth in the Gulf of Mexico). Scientific and industry drilling

have come a long way, and we can now seriously consider scientific drilling to the mantle.

Deep Carbon Observatory and Carbon Reservoirs

The Deep Carbon Observatory (DCO) is a multidisciplinary, international initiative dedicated to achieving a transformational understanding of Earth's deep carbon cycle. Key areas of study include the following:

- deep carbon mantle reservoirs and fluxes
- the nature and extent of the deep biosphere
- the physical and chemical behavior of carbon under extreme conditions
- the unexplored influences of the deep carbon cycle on energy, environment, and climate

The DCO's goal to advance understanding on these frontiers requires an integrated approach—incorporating field-based global sampling efforts, laboratory experiments, analytical methodology, and theoretical modeling, as well as establishing new research partnerships. Much of the DCO's work will be experimental, but much will also depend on deep Earth samples recovered using the framework of established programs like IODP and the International Continental Scientific Drilling Program (ICDP).

The present IODP and the current vision for the future International Ocean Discovery Program share numerous similar goals for understanding Earth processes and systems. Discoveries of microbial life deep in the crust beneath the oceans and continents indicate a rich subsurface biota that by some estimates may rival all surface life in total biomass. Much work also remains to understand how life adapts to deep environments, what novel biochemical pathways sustain life at high pressure and temperature, and what the extreme limits of life are. How does biological carbon link to the slower deep physical and chemical cycles? Is biologically processed carbon represented in deep Earth reservoirs? The nature and full extent of carbon reservoirs and fluxes in Earth's deep interior are not well known. The subduction of tectonic plates and volcanic outgassing are primary vehicles for carbon fluxes to and from deep in the Earth, but the processes and rates of these fluxes—as well as their variation throughout Earth's history—remain poorly understood. Likewise, there is evidence for abiogenic hydrocarbons in some deep crustal and mantle environments, but the nature and extent of deep organic synthesis is unknown. Last but not least, what are the impacts of deep carbon on energy and the surface carbon cycle?

The DCO recognizes a longstanding goal in the ocean drilling community to reach and sample *in situ* pristine mantle and—in the process—penetrate the entire ocean crust and the Moho. Samples obtained en route to and across the Moho will complement the DCO's other research efforts and may address some of the DCO questions above. Such samples and their subsequent study may also ground truth existing hypotheses and, perhaps the findings will inspire entirely new hypotheses and studies regarding the nature of Earth's upper mantle and lithosphere. Undoubtedly, the interest and participation of portions of the DCO community in such a monumental drilling project will expand the scope of the ocean drilling community with its own scientific goals related to carbon cycling deep in the Earth.

In Relation to Previous Workshops

The ocean drilling science community has met in numerous workshops over the course of Deep Sea Drilling Project (DSDP), Ocean Drilling Program (ODP), and IODP (Ildefonse et al., 2007; Teagle et al., 2009; Ildefonse et al., 2010). An international workshop on "The Mohle: a Crustal Journey and Mantle Quest" was held in Kanazawa, Japan in June 2010; it reaffirmed the scientific rationale, considered technological realities and opportunities, and identified potential drilling sites for site surveys planning (Ildefonse et al., 2010).

The "Mantle Frontier" workshop was planned to make a natural step forward in technological discussion, but the emphasis of the scientific discussion was to expand the scope irrespective of specific sites, to emphasize the mantle portion of the targeted section, and to ask the general and fundamental questions of interest to the broader scientific community, such as the DCO.

Scientific Presentations

The DCO overview was given by Robert Hazen from a program-wide perspective, by Constance Bertka from a program management perspective, and by Erik Hauri from the carbon reservoirs and fluxes viewpoint (in his presentation "REFLEX: Deep Carbon Reservoirs, Fluxes and Experiments"). We are accustomed to thinking about the carbon cycle near the Earth's surface, but we know so little about Earth's deep carbon that we lack estimates of carbon quantity or chemical structure, and the effects of carbon on mantle (or core) behavior. The nature and extent of the deep microbial biosphere also need to be investigated.

REFLEX's interests in deep carbon include 1) the pathways and fluxes of carbon exchange between the surface and deep Earth; 2) the nature and variability of carbon compounds in the deep Earth; 3) the interactions between carbon concentration and the dynamics of the Earth's interior; and 4) the ultimate origins of mantle carbon. From these perspectives, REFLEX can use the IODP database to inventory carbonate and organic carbon content in deep-sea sediment cores; analyze a complete ocean crustal section for full understanding of $CaCO_3$ addition to the mantle at subduction zones; and determine carbon flux from pore fluid release in subduction zones.

An illuminating keynote address was given by Donald Beattie, who oversaw the Apollo lunar rock sampling project (Beattie, 2001). A proper project management system to manage a project of this scope from the beginning to end is the key and challenge to success.

Benoit Ildefonse gave a summary of Mohle history and outlined the scientific rationale for the Mohle in three categories (based on the outcome of the previous recent workshops, and as summarized in the Kanazawa workshop report): mantle discovery, crustal accretion, and deep frontiers (Ildefonse et al., 2010). An anticipated timetable for the new Mohle project will enable complete preparations by 2017 and reach the mantle by 2022. Three candidate sites are being considered for reaching the mantle: Cocos Plate site (including Site 1256), off southern Baja California, and north of Hawaii. Site surveys are being planned to gather data to make the final selection.

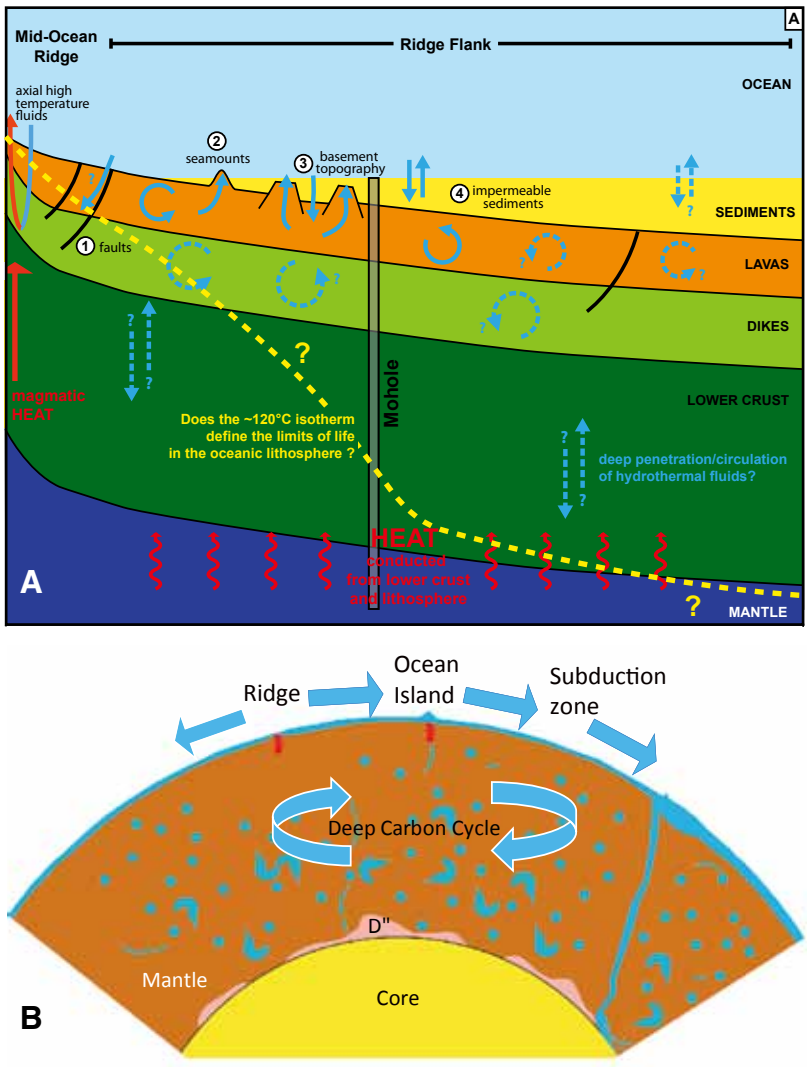

Figure 2. [A] Schematic illustration of the creation and evolution of oceanic crust near the ridge axis. After Ildefonse et al. (2010). [B] How the plate tectonics affects the physics and chemistry of mantle heterogeneities including carbon cycles are largely unknown. After Helffrich and Wood (2001).

Shuichi Kodaira presented recent high-resolution seismic profiles of oceanic Moho and mantle from active source seismic studies in the western Pacific that can help extrapolate drilling observations to mantle dynamics from ridges to trenches. Seismic images of the Moho can vary from sharp to diffuse boundaries, which may correspond to the geologic variety found at the crust/mantle transition in ophiolites. Strong seismic azimuthal anisotropy can be expected to start immediately beneath the Moho, such as measured in the NW Pacific (Oikawa et al., 2010). Lower crustal dipping reflectors matching fast Vp directions may be manifestations of basal shear near the Moho.

Donna Blackman showed how grain-scale deformation due to mantle asthenospheric flow, with melt and recrystallization overprints, may be linked to seismological observations. So far, such inferences have been made without *in situ* knowledge of crystallographic fabric. Mantle samples will document structures and ground truth petrophysical properties. Borehole experiments will provide high-resolution information to be extrapolated to kilometers beyond the hole.

Yoshiyuki Tatsumi showed how drilling could contribute to the understanding of mantle dynamics and geochemical cycles. He emphasized the important roles of water and carbon in creation-destruction cycles in the ocean lithosphere, including arc and continental crust genesis. Deep drilling at key sites along the ocean lithosphere pathway will contribute to a better constrained global geochemical model including the explanation of mantle geochemical heterogeneities.

Matt Schrenk presented how drilling can be used to discover the extent of microbial life in the deep biosphere. The subseafloor biosphere may host one-third to one-half of all prokaryotic cells on Earth, and contain biomass equivalent to that of all plant life at the Earth's surface. Furthermore, the deep biosphere is dependent upon energy in the form of chemical disequilibria and not directly coupled to photosynthesis; it is sometimes referred to as the dark energy biosphere (DEB). However, the absolute extent, the nature, and controls upon the subseafloor biosphere are not completely known. Fluid circulation (hydrology) is considered a key to nourishing the DEB; drilling and associated hydrological experiments can provide direct observations of cell density,

together with quantitative measurements of permeability and time-integrated fluid/rock ratios. Drilling through the ocean crust means penetrating from the life to the non-life regime, and it provides an opportunity to explore the connectivity and flow between deep and surface chemical reservoirs. Developing technologies to overcome contamination-by-drilling as well as distinguishing signal from "noise" introduced by drilling fluids is crucial to interpreting the results of this portion of the project.

Peter Kelemen made a presentation on deep energy, environment, and climate. Carbon is present in the mantle as a result of hydrothermal interaction followed by subduction, and perhaps as a primordial component. Shallow interaction yields fluids containing hydrogen and methane as well as more complex hydrocarbons similar to those stable at greater depth, and these could be a future fuel source. ODP data yield an average of 0.6 wt% CO_2 in altered peridotites, extrapolated to ~0.3 wt% CO_2 over a 7-km depth where mantle peridotite is exposed at the seafloor. A mass equivalent to all dissolved CO_2 in the oceans is added to altered mantle peridotite every ten million years. Optimizing this near-surface weathering holds great potential for carbon storage. Each ton of mantle peridotite can permanently store up to 600 kg of CO_2 in the form of inert, non-toxic solid carbonates. Kinetic data show that a rate of one billion tons CO_2 per km^3 of rock per year can be achieved under optimal conditions (Kelemen and Matter, 2008; Kelemen et al., 2011). There are tens of thousands of cubic kilometers of peridotite near the surface on land, and millions near the seafloor along slow spreading ridges. A Mohle would provide crucial data on the depth of natural CO_2 uptake.

Engineering Presentations

Greg Myers gave a comprehensive presentation on current technological capabilities and limitations. The uniqueness of mantle drilling is the water depth/hole depth combination and the rocks (not sediments) to be drilled. The oil and gas industry already drills deeper holes, yet in water depths less than 3300 m. An integrated approach utilizing all available IODP platforms will reduce the overall cost. Engineered mud must be circulated continuously as part of a comprehensive plan to drill and core effectively. Improved borehole pressure control for deep drilling can be achieved by utilizing dual gradient drilling, which applies mud pressure from the seafloor rather than the platform or vessel. Discussions of continuous coring vs. spot coring and downhole equipment (drilling/coring/logging) are necessary. Myers emphasized the definition of success must be clear and understood by all.

Randy Normann supplied a presentation introducing electronics, batteries, and tools that withstand very high temperatures continuously (>250°C). Michael Freeman lectured on drilling fluid and making deep holes. John Cohen introduced a riserless mud recovery (RMR) method as an application of the dual gradient drilling concept. At present, there is technology qualified for 1500 m water depth.

Michael Ojovan introduced a totally different approach to investigating Earth's interior with the use of self-sinking capsules. The capsule melts the rocks and creates acoustic signals to be detected at the surface, thus yielding information about the nature of the rocks through which the capsule and the signals pass (Ojovan et al., 2005). In their design the probe reaches the Moho in about five months (100 km depth in 35 years).

Larry Karl introduced Remotely Operated Vehicles (ROV) for deep-water applications (depth rated to 10,000 ft) used in offshore oil and gas fields. Also presented were unique and robust techniques for resupply at sea. John Kotrla made a presentation on blow-out preventers (BOP) and seafloor isolation devices. The standing water depth record well is at 3051 m in the Gulf of Mexico (Transocean "Discoverer Deep Seas"). In order to go deeper, utilizing a surface BOP and an environmental safe guard (ESG) on the seafloor was introduced.

John Thorogood presented the management aspect of mantle drilling. There are multiple technology and operational options available to achieve project goals, and yet new technologies may arrive to alter the direction of the project. Subsurface conditions may differ profoundly from the prognosis. Effective operations will involve multiple contingencies, defined rules, and protocols for changing the rules. These indicate the project is not a "normal" project, but will require skillful management from project scoping to execution.

Outcome of the Workshop

The participants agreed on the following:

1. IODP and DCO recognize the potential for synergy towards a comprehensive understanding of carbon-water cycle in the deep Earth system, including consequences of microbial activities.
2. The workshop participants endorse the following outline of the Mohle project scientific rationale (Figs. 1 and 2).
3. The participants agree that the scale of mantle drilling—which is not just drilling but requires long-term commitment before and after the drilling—needs to be recognized by the wider IODP entities from the decision making level.
4. The workshop participants propose to establish a Mohle scoping group. The group will review and refine the science goals, identify technology, and review plans to meet the science goals. Also recognized was the need to establish a management structure, estimate the total cost of the project, and seek funding

along with outreach and communication activities within a broad IODP umbrella.

Acknowledgements

The Integrated Ocean Drilling Program (IODP) and the Deep Carbon Observatory (DCO) initiative jointly supported the workshop with primary financial support from the Alfred P. Sloan Foundation.

References

Bascom, W., 1961. A Hole in the Bottom of the Sea, *The Story of the Mohle Project*: New York (Doubleday & Co.).

Beattie, D.A., 2001. *Taking Science to the Moon: Lunar Experiments and the Apollo Program*: Baltimore MD (The Johns Hopkins University Press).

Cromie, W.J., 1964. *Why the Mohle: Adventures in Inner Space*: Boston (Little, Brown and Co.).

Greenberg, D.S., 1966. News and Comment. *Science*, 152:895–896, doi:10.1126/science.152.3724.895.

Helffrich, G.R., and Wood, B.J., 2001. The Earth's mantle. *Nature*, 412:501–507.

Ildefonse, B., Christie, D.M., and Mission Moho Workshop Steering Committee, 2007. Mission Moho workshop: drilling through the oceanic crust to mantle. *Sci. Drill.*, 4:11–18, doi:10.2204/iodp.sd.4.02.2007.

Ildefonse, B., Abe, N., Blackman, D., Canales, J.P., Isozaki, Y., Kodaira, S., Myers, G., Nakamura, K., Nedimovic, M., Skinner, A.C., Seama, N., Takazawa, E., Teagle, D.A.H., Tominaga, M., Umino, S., Wilson, D.S., and Yamao, M., 2010. The MoHole: a crustal journey and mantle quest, workshop in Kanazawa, Japan, 3–5 June 2010. *Sci. Drill.*, 10:56–63.

IODP, 2001. *Earth, Oceans and Life, Initial Science Plan*, 2003-2013, IODP Planning Subcommittee, pp. 110.

Kelemen, P.B., and Matter, J., 2008. *In situ* carbonation of peridotite for CO2 storage. *Proc. Natl. Acad. Sci.*, 105:17295–17300, doi/10.1073/pnas.0805794105.

Kelemen, P.B., Matter, J., Streit, E.E., Rudge, J.F., Curry, W.B., and Blusztajn, J., 2011. Rates and mechanisms of mineral carbonation in peridotite: natural processes and recipes for enhanced, *in situ* CO2 capture and storage. *Ann. Rev. Earth Planet. Sci.*, in press.

Oikawa, M., Kaneda, K., and Nishizawa, A., 2010. Seismic structure of the 154–160 Ma oceanic crust and uppermost mantle in the Northwest Pacific Basin. *Earth Planets Space*, 62:e13–e16, doi:10.5047/eps.2010.02.011.

Ojovan, M.I., Gibb, F.G.F., Poluetkov, P.P., and Emets, E.P., 2005. Probing the interior layers of the Earth with self-sinking capsules. *Atomic Energy*, 99:556–562, doi:10.1007/s10512-005-0246-y.

Steinbeck, J., 1961. High drama of bold thrust through ocean floor. *Life*, 50(15):111–122.

Teagle, D., Ildefonse, B., Blackman, D., Edwards, K., Bach, W., Abe, N., Coggon, R., and Dick, H., 2009. Melting, magma, fluids and life: challenges for the next generation of scientific ocean drilling into the oceanic lithosphere. [Workshop Report, National Oceanographic Center, Southampton, 27–29 July 2009], http://www.interridge.org/files/interridge/MMFL_wkshp_rpt_2009_final.pdf.

Workshop Report Writing Group (in alphabetical order)

Constance Bertka, Deep Carbon Observatory, Senior Consultant, Geophysical Laboratory, 5251 Broad Branch Road NW, Washington, DC 20015, U.S.A., e-mail: cbertka@ciw.edu.

Donna K. Blackman, IGPP, Scripps Institution of Oceanography, University of California San Diego, 9500 Gilman Drive, La Jolla, CA 92093-0225, U.S.A., e-mail: dblackman@ucsd.edu.

Benoit Ildefonse, CNRS, Géosciences Montpellier, Université Montpellier 2, CC 60, 34095 Montpellier Cédex 05, France, e-mail: benoit.ildefonse@univ-montp2.fr.

Peter B. Kelemen, 211 Comer, 61 Route 9W – P.O. Box 1000, Palisades, NY 10964-8000, U.S.A., e-mail: peterk@ldeo.columbia.ed.

Andrea Johnson Mangum, Deep Carbon Observatory, Program Associate, Geophysical Laboratory, 5251 Broad Branch Road NW, Washington, DC 20015, U.S.A., e-mail: amangum@ciw.edu.

Greg Myers, Senior Technical Expert: Engineering and Technology, Department: Ocean Drilling, Consortium for Ocean Leadership, 1201 New York Avenue NW, 4th Floor, Washington, DC 20005, U.S.A., e-mail: gmyers@oceanleadership.org.

Jason Phipps-Morgan, Professor, Earth and Atmospheric Sciences, Cornell University, Snee Hall, Room 2122, Ithaca, NY 14853, U.S.A., e-mail: jp369@cornell.edu.

Matthew Schrenk, Assistant Professor, Howell Science S301B, Department of Biology, East Carolina University, Greenville, NC 27858, U.S.A., e-mail: schrenkm@ecu.edu.

Kiyoshi Suyehiro (corresponding author), President & CEO, IODP-MI, Tokyo University of Marine Science and Technology, Office of Liaison and Cooperative Research 3rd Floor, 2-1-6, Etchujma, Koto-ku, Tokyo 135-8533, Japan, e-mail: ksuyehiro@iodp.org.

Yoshiyuki Tatsumi, Institute for Research on Earth Evolution (IFREE), Japan Agency for Marine-Earth Science and Technology, 2-15 Natsushima-cho, Yokosuka-city, Kanagawa 237-0061, Japan, e-mail: tatsumi@jamstec.go.jp.

Jessica Warren, Assistant Professor, School of Earth Sciences, Department of Geological and Environmental Sciences, Stanford University, 450 Serra Mall, Stanford, CA 94305, U.S.A., e-mail: warrenj@stanford.edu.

Related Web Links

Integrated Ocean Drilling Program: http://www.iodp.org
Deep Carbon Observatory Initiative: http://dco.gl.ciw.edu/
Mission Moho Proposal: http://www.missionmoho.org
Kanazawa MoHole Workshop Report: http://www.mohole.org

Postglacial Fault Drilling in Northern Europe: Workshop in Skokloster, Sweden

by Ilmo T. Kukkonen, Maria V.S. Ask, and Odleiv Olesen

doi:10.2204/iodp.sd.11.08.2011

Introduction

The majority of Earth's earthquakes are generated along plate margins, and the theory of plate tectonics provides the explanation for the occurrence of these earthquakes. However, a minority of earthquakes occurs within continental plates, and the theoretical understanding for these earthquakes is largely lacking (Stein and Mazzotti, 2007). The general assumption is that intraplate earthquakes tend to be relatively small in size. This report summarizes a workshop devoted to a special type of intraplate earthquake-generating faults—postglacial (PG) faults—that so far have been observed only in northern Europe.

Altogether, there are fourteen well-known PG fault structures in northern Sweden, Finland, and Norway with fault scarps up to 160 km in length and up to 30 m in height (Figs. 1, 2; Olesen et al., 1992; Lagerbäck and Sundh, 2008; Kukkonen et al., 2010). Assuming that these distinct faults were formed in single events, they would represent earthquakes with magnitudes of up to 7–8 (Bungum and Lindholm, 1997; Kuivamäki et al., 1998). This estimate is supported by numerous observations of massive landslides associated with these structures and dated to have occurred at the last stages of the glaciation. PG faults represent earthquakes with considerable contrast to the present seismic activity in continental northern Europe, where earthquakes are usually smaller than magnitude 4.

All known PG faults are located in old reactivated zones of weakness in crystalline rocks and are usually SE dipping, SW-NE oriented thrusts. The last major reactivation of these faults is believed to have occurred during the last stages of the Weichselian glaciation (~9,000–15,000 years B.P.). The earthquakes are believed to have been triggered by the combined effects of tectonic background stresses and rapidly changing stresses from glacial loading by the shrinking Weichselian ice sheet (Johnston, 1989; Wu et al., 1999; Lund, 2005; Lund et al., 2009).

From what is known today, large-scale types of PG faults appear to be restricted in occurrence to northern Fennoscandia. In other previously glaciated areas, such as Canada, postglacial faults are significantly smaller in size (Adams, 1989). Seismological data reveal that the PG faults are currently seismically active, and that small earthquakes are associated with these structures over a significant depth range (down to 37 km depth; Bungum and Lindholm, 1997; Arvidsson, 1996). They are obviously structures of crustal dimensions and relevance, but not thoroughly understood at the moment (Arvidsson, 1996).

Postglacial faulting has important implications for predicting the behavior of fault zones during future glaciations. Therefore, PG fault research is expected to contribute significantly in planning the disposal of spent nuclear fuel, CO_2 and toxic waste into bedrock that currently is prepared in the Nordic countries. Other fields of applied geoscience which may benefit from PG fault research are mineral exploration and estimation of mine stability, as some of the faults are located in areas which host gold, copper, and nickel mineralizations in northern Fennoscandia. Major hydropower and tailing dam complexes may also be influenced by PG faults and their current earthquake activity. An improved understanding of the prevailing *in situ* stress, erosion, uplift, and sedimentation also has implications for the understanding of offshore petroleum reservoirs on the Lofoten-Barents margin.

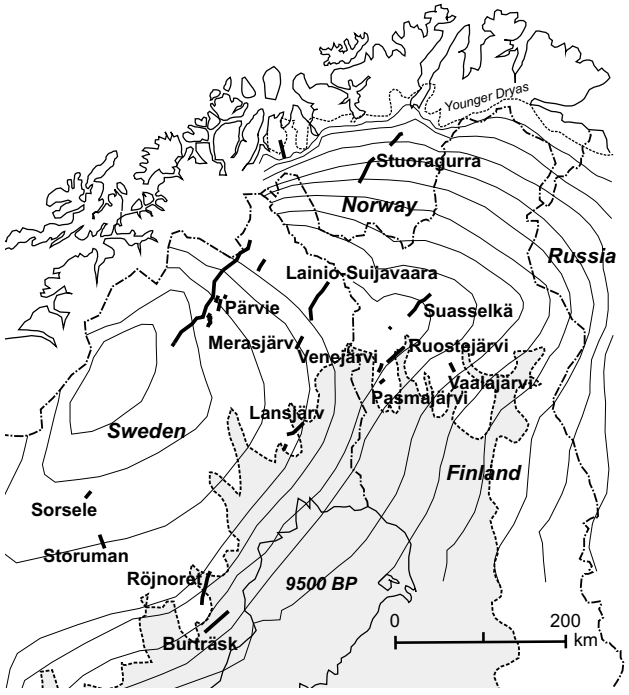

Figure 1. Location of PG faults in northern Fennoscandia (thick lines), and successive ice-marginal lines between ~10,000 years B.P. and 9,000 years B.P. (thin lines). The gray area shows the highest shoreline of the Baltic. Adopted from Kukkonen et al. (2010).

Figure 2. Helicopter view of the southwestern part of the Pärvie PG fault (see Fig. 1 for location). The red arrows show the trace of the fault scarp. The insert shows the fault scarp from the ground surface, about 85 km to the northeast of the location of the large photo, including a helicopter for scale.

Methods applied in PG fault research so far include bedrock and Quaternary field geology, trenching, seismicity, airborne and ground geophysics, and shallow drilling to about 500 m (Kukkonen et al., 2010). Revealing the mechanisms and processes related to PG faulting is highly relevant for understanding seismicity in these intraplate areas. Several disciplines and approaches can be used to improve our understanding of PG faults, for example, through earthquake seismology, stress field measurement and modeling, as well as geodetic surface monitoring of fault activity. Scientific drilling and coring is the only way to obtain direct core samples from PG faults at depth, and the resulting boreholes provide direct access to the fault structures for geophysical, hydrogeological, and biological sampling, monitoring and *in situ* experiments. We organized the ICDP-supported international workshop "Postglacial Fault Drilling in Northern Europe" in Skokloster, Sweden on 4–7 October 2010; thirty-nine participants represented basic research, applied geosciences, industry and authorities from eight countries. At the workshop, the status of PG fault research was discussed, and plans were made towards developing a realistic drilling plan.

Major Scientific Issues/Problems

The major scientific tasks of PG fault research were identified as follows:

1. What is the tectonic style, deep structure and depth extent of the PG faults?
2. Are PG faults still active?
3. What are the paleoseismic implications of postglacial faults?
4. Did PG faults reactivate more than once? Is it possible to provide quantitative ages of the tectonic systems hosting PG faults?
5. What are the present and paleostress fields and pore pressure of PG faults?
6. How has the faulting affected the rock properties, structure, and deformation in and near the fault surface?
7. What are the hydraulic properties of PG faults, and how did they control fresh glacial meltwater recharge?
8. What is the composition of groundwater (chemistry, salinity, pH, Eh, gas content) in PG faults?
9. Is there a deep biosphere in PG faults?

One of the relevant issues of PG faulting is whether their current appearances really are the result of single earthquake events. The risk and implications of PG faulting to intraplate seismicity in general, and waste disposal repositories in particular, is highly dependent on this. Previous investigations by Lagerbäck and Sundh (2008) suggest that massive landsliding and seismites in soft sediments occurred concurrently with the faulting. They based their arguments mainly on the relatively small erosion of the Weichselian glaciation, and stated that such dramatic faulting which generated the great PG faults in northern Sweden very probably did not occur in glaciations earlier than the Weichselian.

Workshop Discussions

The workshop presentations can be subdivided roughly into four sub-groups: (1) geology, tectonics, age determination studies; (2) seismic structures, seismicity and other geophysics; (3) stress field, land uplift and plate tectonic forces; and (4) hydrogeology, hydrochemistry, geothermics, and deep biosphere. The participants subsequently discussed the major scientific tasks within these four sub-groups.

The main aim for drilling is to penetrate a fault which presently is seismically active. It is also commonly agreed that it would be useful to compare an active fault with an inactive one. When defining drilling targets it will be important to locate the fault exactly at depth, but this may be difficult. Even in the shallow drilling of the Lansjärv fault in the 1980s, it was not easy to decide where the PG fault actually was because the rock was generally very fractured and broken (Bäckblom and Stanfors, 1989). One of the goals is to drill into the seismogenic zone of a PG fault. Although the macroseismic activity in Fennoscandia seems to be characterized by focal depths of 10–20 km (Ahjos and Uski, 1992; Bungum and Lindholm, 1997), the present seismic activity of PG faults seems to start from surface, at least in the case of the Pärvie fault. The need of seismic monitoring of several faults was considered relevant before the best candidate for drilling can be identified.

A major issue that may be addressed before the start of drilling is if surface studies can reveal whether the fault scarps were formed by one big earthquake or by several smaller ones. Closer inspection of the fault scarps themselves, as well as investigations of the sediment cover using traditional trenching coupled with ^{14}C-dating, would help

address this question. Bungum and Lindholm (1997) and Kuivamäki et al. (1998) did comparative studies of the relationship between fault length and fault scarp height of PG faults in Scandinavia, and compared the data with recent large earthquakes. Their approach may be pursued to investigate what the scale effect is for the fault (i.e., if there is a relationship between the size of the earthquake and the size of the fault scarp). Furthermore, drill cores would reveal whether there have been paleodynamic weakening effects (thermal pressurization, frictional melting, etc.) related to major periods of faulting in the geological history.

Site survey data that needs to be collected include 2D and 3D reflection seismic surveys to identify the geometry of PG faults, and passive seismic network data to identify earthquake activity and tomography studies. In addition, ground penetrating radar, 2D resistivity measurements, gravity data, magnetotelluric soundings, and high-resolution topographic surveys with laser scanning (LIDAR) are needed. Drilling of shallow and relatively inexpensive pilot holes may allow characterization and identification of the fault at shallow depths as well as installation of instruments monitoring microseismicity. It is important to expand the seismic surveys and seismic networks to as many of the remaining faults as possible to allow the selection of the best candidates for drilling.

In addition, use of existing data may also improve an ICDP drilling proposal (e.g., synthesizing results on existing cores and their mechanical properties, and reinterpretation of the state of *in situ* and paleo-stresses). Finally, site investigation data can be utilized to calibrate and improve viscoelastic ice sheet numerical modeling within the site survey areas.

Challenges for Drilling

Different strategies of drilling geometry were outlined in the workshop. Assuming that drilling takes place on one fault site only, the alternatives would be (1) to drill only shallow (<1 km) boreholes located on a profile perpendicular to the fault plane, (2) drill one deep borehole (2–5 km) penetrating the fault at great depth, (3) drill a deep borehole with several shorter boreholes deviating from the main borehole at 1.5–2 km depth, or (4) combine 1–3 shallow boreholes and a deep (2–5 km) one. Option no.4 would allow learning while drilling (i.e., modification of drilling plans of the main borehole would be possible from the experience gained in the shallow ones). Such a drilling geometry would also allow cross-borehole experiments and various sampling and monitoring activities *in situ* and would provide good control of fault properties with depth.

We identified a range of criteria that is helpful to determine the best site for drilling. At the site of drilling, the selected PG fault should (1) be seismically active over a depth interval that can be reached by drilling and beyond; (2) reveal contrasting geology across the fault to allow unambiguous determination of the fault location; and (3) be a site with good logistics capacity. In addition, pre-drilling investigations should suggest the site has a very good scientific capacity (i.e., the majority of research hypotheses should have a good chance to be tested with drilling).

In order to address the scientific problems, a detailed drilling and testing program needs to be developed. The program should include the collection of oriented cores, borehole logging, fluid sampling, stress measurements, and long-term monitoring of strain/tilt, microseismicity, fluid pressure, and temperature. Preferred core tests include physical properties (petrophysics), rock mechanical determinations, deformation microstructures, mineralogy and geochemistry, and dating. Good quality downhole logging data will be required to allow as complete characterization of the fault as possible, including image logs, density, resistivity/induction, magnetic, full waveforms, and spectral gamma.

After drilling, the most important measurements are stress measurements, strain/tilt and microseismic monitoring, fluid pressure and temperature monitoring, borehole image logging, and geophysical logging. Hydrogeological and microbial studies require post-drilling time for long-term pumping of fluid and gas. Important laboratory investigations include geological logging, petrophysical measurements, rock mechanic testing, and core studies of deformation and fault related microstructures. They also include the capacity to link such data to geochemical studies of the core (e.g., fluid inclusions, if they exist) and geochronology. These data would help improve the models and quality of viscoelastic ice sheet modeling within the site survey area. The possibility for induced seismicity tests should be investigated.

Potential Drilling Targets

The workshop participants could already identify several potential drilling targets. At the moment the most promising ones would be structures which have long surface scarps, thus indicating crustal scale relevance. The targets should preferably be seismically active, and they should have structures which have been sufficiently imaged with various geophysical techniques. Seismicity has been monitored already in a number of faults with arrays designed for PG faults, but many major faults lack monitoring at the moment. An interesting option would be to compare two structures, one showing seismic activity and one devoid of any activity.

Identification of the scientifically most optimal drilling targets was not possible without more site-specific studies such as seismic arrays to be run for about one to two years. In addition, geodetic monitoring should be started to observe any creep. Previous geodetic leveling and GPS measure-

ments in Finland (Kuivamäki et al., 1998, Poutanen and Ollikainen, 1995) did not show any measurable movement.

Conclusions and Road Map Forward

The workshop community considered drilling into PG faults a feasible scientific initiative which would lead to a research project with important societal implications. The present state of the art in PG fault studies is very promising for developing an ambitious new ICDP project "Postglacial Fault Drilling Project" (PFDP).

Many PG faults are seismically active, and they may represent structures which release the current plate tectonic stresses accumulating in the Fennoscandian continental plate. A concept for the project would be to define an active target fault where the preliminary results of seismic monitoring may suggest that the upper parts of the seismogenic zone could be reached with boreholes shallower than about 3 km. The fault would be investigated with both shallow boreholes (<1 km) and a deep borehole (max 2–5 km). Core drilling is essential for a representative sampling of the rocks at least in the expected depth levels of the fault. Furthermore, a combination of several boreholes would allow a variety of downhole experiments, logging, samplings, and monitoring after drilling.

Existing shallow cores (Kukkonen et al., 2010) should be re-examined with modern mineralogical and isotope methods. Pre-drilling science should also include re-analysis of stress field measurements (Bäckblom and Stanfors, 1989; Bjarnason et al., 1989). Pre-drilling science and gathering of site-specific data sets are estimated to take 2–3 years before a well-defined drilling proposal can be compiled. Meanwhile, information will be disseminated on the PFDP in international conferences, and working group meetings are planned to be organized in association with the EGU and AGU conferences. A session "Intraplate faulting and seismicity with special reference to the Fennoscandian postglacial fault province" is currently arranged at the EGU in Vienna, Austria, in April 2011.

References

Adams, J., 1989. Postglacial faulting in eastern Canada: nature, origin and seismic hazard implications. *Tectonophysics*, 163:323–331.

Ahjos, T., and Uski, M., 1992. Earthquakes in northern Europe 1375-1989. *Tectonophysics*, 203:1–23.

Arvidsson, R., 1996. Fennoscandian earthquakes: whole crustal rupturing related to postglacial rebound. *Science,* 274:744–746.

Bäckblom, G., and Stanfors, R., 1989. *Interdisciplinary Study of Post-Glacial Faulting in the Lansjärv area, northern Sweden, 1986-1988*. Swedish Nuclear Fuel and Waste Management Co., Stockholm, Technical Report 89-31.

Bjarnason, B., Zellman, O., and Wikberg, B., 1989. Drilling and borehole description. *In* Bäckblom, G., and Stanfors, R. (Eds.), *Interdisciplinary Study of Post-Glacial Faulting in the Lansjärv area, northern Sweden, 1986–1988*, 7:1–7:14. Swedish Nuclear Fuel and Waste Management Co., Stockholm, Technical Report 89–31, 7:1–7:14.

Bungum, H., and Lindholm, C., 1997. Seismo- and neotectonics in Finnmark, Kola Peninsula and the southern Barents Sea. Part 2: seismological analysis and seismotectonics. *Tectonophysics*, 270:15–28.

Johnston, A., 1989. The effect of large ice sheets on earthquake genesis. *In* Gregersen, S., and Basham, P. (Eds.), *Earthquakes at North-Atlantic Passive Margins: Neotectonics and Postglacial Rebound:* Dordrecht (Kluwer Academic Publishers), 581–599.

Kuivamäki, A., Vuorela, P., and Paananen, M., 1998. Indications of postglacial and recent bedrock movements in Finland and Russian Karelia. Geological Survey of Finland, Nuclear Waste Disposal Research, Report YST-99, 92 p.

Kukkonen, I.T., Olesen, O., Ask, M.V.S., and the PFDP Working Group, 2010. Postglacial faults in Fennoscandia: targets for scientific drilling. *GFF*, 132:71–81.

Lagerbäck, R., and Sundh, M., 2008. Early Holocene faulting and paleoseismicity in northern Sweden. *SGU Research Paper C836*, 80 pp.

Lund, B., 2005. *Effects of Deglaciation on the Crustal Stress Field and Implications for Endglacial Faulting: A Parametric Study of Simple Earth and Ice Models*. Swedish Nuclear Fuel and Waste Management Co., Stockholm. Technical Report TR-05-04, 68 pp.

Lund, B., Schmidt, P., and Hieronymus, C., 2009. *Stress evolution and fault instability during the Weichselian Glacial Cycle*. Swedish Nuclear Fuel and Waste Management Co., Stockholm. Technical Report TR-09-15, 106 pp.

Olesen, O., Henkel, H., Lile, O.B., Mauring, E., and Rønning, J.S. 1992. Geophysical investigations of the Stuoragurra postglacial fault, Finnmark, northern Norway. *J. Appl. Geophys*., 29:95–118.

Poutanen, M., and Ollikainen, M., 1995. *GPS Measurements at the Nuottavaara Postglacial Fault*. Finnish Geodetic Institute, Report 95, 6 pp.

Stein, S., and Mazzotti, S., 2007. Continental intraplate earthquakes: science, hazard, and policy issues. *GSA Special Paper 425*, Boulder, Colo., (The Geological Society of America, Inc.), 402 pp.

Wu, P., Johnston, P., and Lambeck, K., 1999. Postglacial rebound and fault instability in Fennoscandia. *Geophys. J. Int.*, 139:657–670.

Authors

Ilmo T. Kukkonen, Geological Survey of Finland, Espoo, P.O. Box 96, FI-02151 Espoo, Finland, e-mail: ilmo.kukkonen@gtk.fi.

Maria V.S. Ask, Luleå University of Technology, SE-971 87 Luleå, Sweden.

Odleiv Olesen, Geological Survey of Norway, NO-7491 Trondheim, Norway.

Figure Credits

Fig. 2: Björn Lund, Uppsala University, Sweden (large photo); and Roger Lagerbäck, Geological Survey of Sweden (insert photo).

The Scandinavian Caledonides—Scientific Drilling at Mid-Crustal Level in a Palaeozoic Major Collisional Orogen

by Henning Lorenz, David Gee, and Christopher Juhlin

doi:10.2204/iodp.sd.11.10.2011

Introduction

The Caledonides of western Scandinavia and eastern Greenland have long been recognized to have been part of a collisional orogen of Alpine-Himalayan dimensions, essentially the result of the closure of the Iapetus Ocean during the Ordovician, with development of island-arc systems, and subsequent underthrusting of continent Laurentia by Baltica in the Silurian and Early Devonian during Scandian collisional orogeny. Several hundreds of kilometers of thrust emplacement of allochthons have been demonstrated, E-directed in the Scandes and W-directed in Greenland.

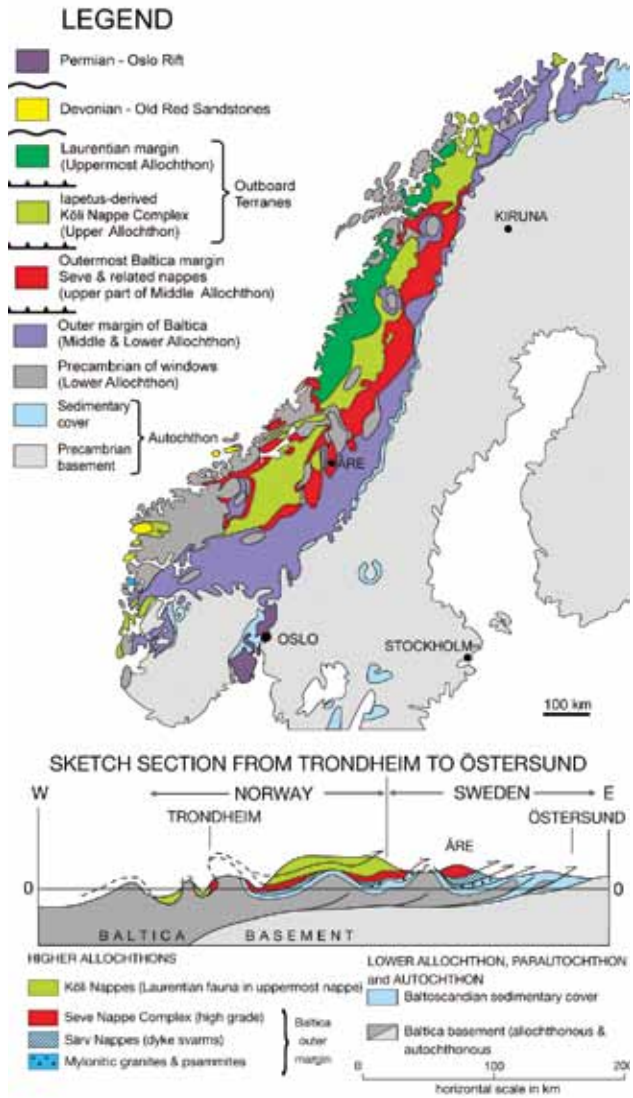

Figure 1. Tectonostratigraphic map of the Scandinavian Caledonides and sketch section along the geotraverse from Östersund to the Norwegian coast (modified from Gee et al. 2010).

In Scandinavia, major allochthons (Fig. 1) were derived from Baltica's outer shelf, dyke-intruded continent-ocean transition zone (COT), Iapetus oceanic domains and (uppermost) from the Laurentian margin. On the western side of the North Atlantic, exposed along the eastern edge of the Greenland ice cap, there are major thrust sheets, all derived from the Laurentian continental margin and transported at least two hundred kilometers westwards onto the platform. In the Scandinavian and Greenland Caledonides, the major allochthons that were derived from the outer parts of the continent margins have been subject to high-grade metamorphism and apparently were emplaced hot onto the adjacent platforms.

The International Continental Scientific Drilling Program (ICDP) workshop in Sweden provided an opportunity to examine the evidence for Caledonian collisional orogeny in Scandinavia and to discuss its relevance for understanding other orogens, particularly Himalaya-Tibet, and also the subduction systems along the margin of the western Pacific. The Scandinavian Caledonides are one of the best places on the planet to study the emplacement not only of highly ductile allochthons generated in an outer continental margin subduction complex, but also of associated hot (granulite facies paragneisses with leucogranites) extruding nappes that were the potential heat source for the metamorphism of underlying and overlying long-transported allochthons.

COSC Project Rationale

The Collisional Orogeny in the Scandinavian Caledonides (COSC) project focuses on the transport and emplacement of subduction-related high-grade COT assemblages (the Seve Nappe Complex) onto the Baltoscandian platform and their influence on the underlying allochthons and basement. Research will be performed by an international working group with experience from studying fossil and active mountain belts. Orogenic processes and their development over time will be investigated by scientific drilling in the deeply eroded (mid-crustal levels) Scandinavian Caledonides, and the results will be compared from this unique locality with a modern analogue of similar size, the Himalaya-Tibet mountain belt, and the arc collisional systems between the Eurasian and Pacific plates.

The Workshop

The workshop was attended by about sixty participants—half from outside of the Nordic countries—on 21–25 June 2010 in Åre, Sweden, close to the planned drilling sites. The workshop was divided into two parts, separated by a full day's excursion on 23 June (Fig. 2). The Scandinavian Caledonides, a modern analogue (the Himalaya-Tibet mountain belt), and the highly successful ICDP project in the Sulu ultra-high pressure belt (the Chinese Continental Scientific Drilling Program) were presented on the first day. Presentations on the emplacement of hot allochthons were made on the second day, followed by geological and geophysical workshop sessions on orogen-scale processes. The afternoon session focused on the Scandian hinterland, before taking a rapid ascent to the "hot allochthon" on cold and snowy Åreskutan mountain. Evening lectures provided introductions to ICDP and the Swedish Deep Drilling Program, in particular the purchase of a mobile drilling rig capable of coring down to depths of at least 2.5 km. The mid-workshop excursion concentrated on the rock units (excluding the unknown basement) through which we plan to drill, from the amphibolite facies Seve Nappe Complex to underlying greenschist facies metasedimentary units of the Middle Allochthon and Cambro-Silurian Lower Allochthon. On the fourth day, lectures were held about drillhole-related geophysics and western Pacific subduction systems, particularly the Izu-Bonin-Mariana Arc; workshop sessions covered details of the science related to the drillholes and drill cores; and general discussion of COSC science was conducted. The day ended with presentations on the hydrological and geothermal aspects of the Scandian mountain belt and drilling program. The last morning of the workshop was spent winding up the COSC science plan and defining a road map for the coming six months, with preparation of a comprehensive drilling proposal to ICDP and applications to funding agencies.

Figure 2. Scenes from the COSC science workshop presentations, discussions, and excursions. Participants on one of the key localities of the lower, poorly exposed tectonostratigraphic units.

COSC Drilling Program

Two drillholes, each ~2.5 km deep, are planned to core a composite profile from the "hot" Seve nappes downwards, through the underlying lower grade allochthons, into the Fennoscandian basement. They are located near the towns of Åre and Järpen (Fig. 3).

The geology of the Åre area is renowned for classical studies of vast overthrusting (Törnebohm, 1888), with high-grade metamorphic rocks (granulite facies) on the top of Åreskutan mountain emplaced over Cambro-Silurian sedimentary rocks in the valley below. Drilling will start in the lower part of the well-exposed section and continue through less exposed amphibolite and greenschist facies units in the underlying nappes. The second hole, near Järpen, will continue the section through the underlying autochthonous cover and deep into the Fennoscandian basement.

The high spatial resolution provided by continuous drillcore will allow a detailed study of the metamorphism and its changes through and across tectonic contacts, from the high-grade allochthons into the underlying less metamorphosed nappes and basement. Oriented drillcore will serve as a basis for understanding deformation and thrust emplacement, as well as heat transport and fluid migration during metamorphism, in time and space. COSC drilling will then penetrate the lower allochthonous units and the basal décollement, most likely in Cambrian alum shale, and enter Precambrian crystalline basement. Prominent basement seismic reflectors will be studied in detail. Investigation of the apparent deformation pattern in the autochthonous basement that is observed in the seismic data will be achieved by drillcore studies and in-hole measurements. *In situ* and drill core investigations are also necessary to study the amount of Caledonian and older deformation and metamorphism in the basement.

Two coreholes to ~2.5 km instead of one deep hole (~5 km) will make the COSC project economically feasible. The second drillhole will be located further towards the foreland of the Caledonides, starting in the tectonostratigraphy just above the base of the first hole (Fig. 3). These holes will be drilled with a diamond coring drill rig to maximize core recovery and minimize costs. Both boreholes will investi-

gate regional heat flow, water circulation patterns, the deep biosphere, and the mineral potential of the area. They will also allow calibration of high-quality surface geophysical data at depths which are not normally accessible to drilling in this tectonic environment.

Working Groups

Working groups have been established for tectonics, geophysics, geothermics, hydrogeology, and the deep biosphere. Technical operations and research will be performed by the drilling management and technology working group, utilizing the Swedish scientific drilling infrastructure.

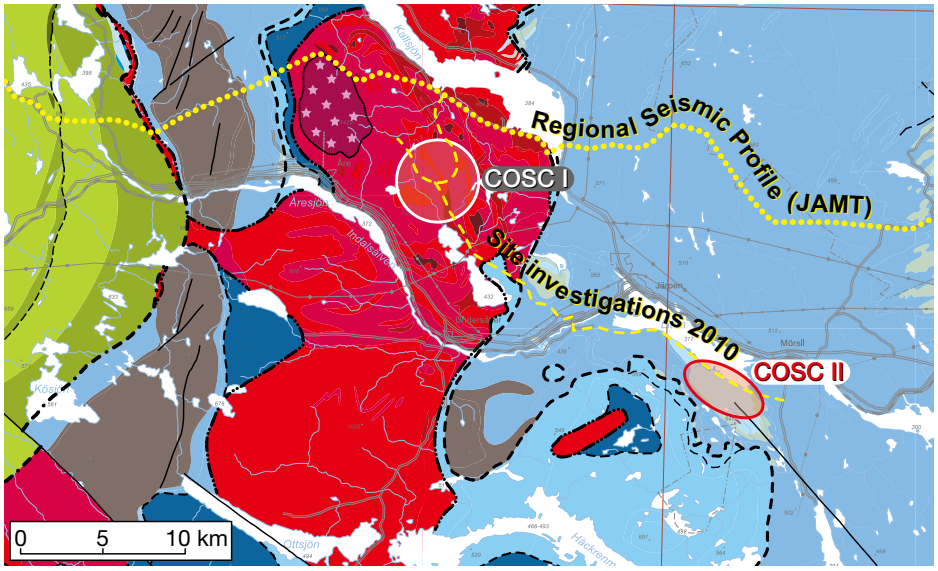

Figure 3. Geological map of the Åre-Järpen area. Marked are the areas of interest for scientific drilling (COSC I & II), the regional seismic profile from the early 1990s (yellow dotted line, see Figure 4) and the 2010 site investigations by reflection seismics (yellow dashed line). In gray: Fennoscandian basement exposed in anticlines; in light blue: the lower-grade metamorphic Lower Allochthon; in dark blue: lower part of the Middle Allochthon; in red: the high-grade upper part of the Middle Allochthon, the Seve Nappe Complex, with highest grade rocks on the top of Åreskutan mountain (stars); in green: the overlying lower metamorphic Upper Allochthon (Köli nappes).

The main objectives of the tectonics working group concern the mechanisms of emplacement of hot allochthons and the establishment a coherent model of mid-Palaeozoic (Scandian) mountain building in the North Atlantic Caledonides. Orogenic processes will be considered in ongoing and older orogens, with underthrusting of continents, doubling (even trebling) of continental thicknesses, elevation of a high plateau, partial melting of hinterland regions and ductile extrusion of allochthons many hundreds of kilometers onto adjacent platforms. In addition, new insights will be applied to the interpretation of modern analogues, in particular the Himalaya-Tibet mountain belt. The geophysics working group will map the large-scale geological structure around the boreholes and relate it to surface measurements. Cores and in-hole observations will allow determination of the origin of the observed seismic reflections during site investigations and regional seismic profiling across the mountain belt (Fig. 4). The geothermics working group focuses on assessing the heat flow and temperature in the crystalline bedrock—in the Fennoscandian Shield basement and the overlying Caledonian allochthons—and on investigating shallow boreholes (300–400 m) that have been drilled for mineral exploration purposes several decades ago. The hydrogeology working group will model the large-scale groundwater circulation patterns in the mountain belt and their influence on the hydrosphere of the Fennoscandian Shield basement beneath other parts of Sweden. For this purpose it is necessary to build a regional geological model which is as yet an unaddressed problem in shield areas, with importance beyond the borders of Scandinavia. The microbiology working group will investigate microbial life in highly metamorphosed sedimentary and crystalline bedrock; this study will introduce challenges different from those dealt with in sediments. Anticipated differences include distribution of biota within the rocks formations and nutrient sources to the deep biosphere, where microbial life must utilize inorganic, geological sources such as energy-rich gases.

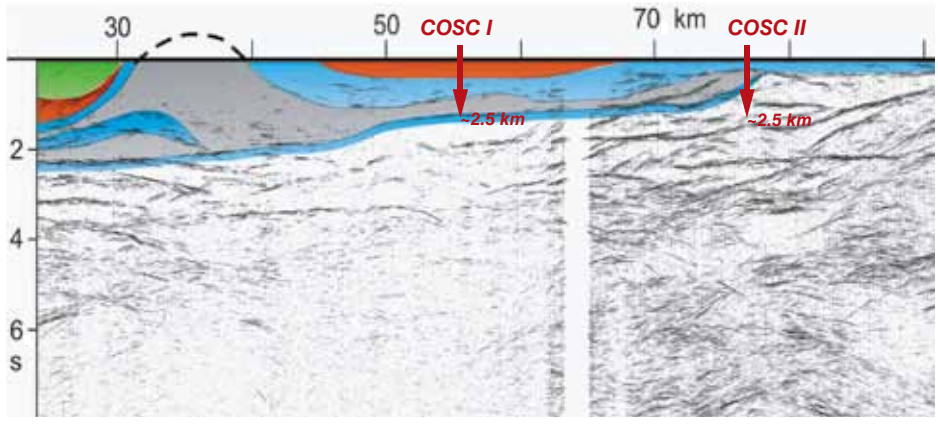

Figure 4. Detailed view from the regional seismic profile (from the early 1990s) with approximate drillhole locations. Note that the vertical scale is time, and that borehole locations are only approximate. Actual locations will be based on new seismic reflection data that is currently being processed (from Gee et al. 2010).

The availability of a diamond core drill rig, recently funded by the Swedish Research Council primarily for the Swedish Deep Drilling Program, will allow the drilling management and technology working group to develop and test new drilling technologies and tools. The emphasis will be on

enhanced sampling methods in fractured formations, data transmission while drilling, measurement while drilling, integration of true-gyro measurements while drilling, core orientation tools, and hydraulic conductivity tools.

Relevance of COSC Science

Comparison of the North Atlantic Caledonides and the Himalaya-Tibet orogen is stimulating much new research. Very different interpretations of both orogens (Soper et al., 1992; Gee et al., 2010; Streule et al., 2010) are being tested. The Caledonides in Scandinavia provide special opportunities for understanding Himalayan-type orogeny and the Himalayan Orogen itself. The last two distances comparable to those in the Scandes have seen a growing appreciation of the importance of ductile emplacement of long-transported allochthons in the Scandes and elsewhere. In particular, in the Himalayas vast lateral transport of ductile allochthons over distances exceeding those in the Scandes has been demonstrated. The Izu-Bonin-Mariana arc system, target of the ODP leg 125 (Fryer et al., 1990), takes the comparison of collisional systems a step further—to a fore-arc system where subduction, collision, thrusting, and related igneous activity and exhumation have been studied in a currently existing smaller framework.

Geological processes along active continental margins, followed by collisional tectonics and mountain building, have a profound influence on human society. Massive mountain belts like the Himalayas influence climate and weather; natural disasters are common for settlements on its steep slopes and narrow valleys. Active collisional systems are known for inflicting earthquakes on inhabitants. COSC takes a comprehensive approach to mountain building processes and their development through geological time by integrating the drilling project in the fossil orogen of the Scandinavian Caledonides with research on the Himalayas and the Izu-Bonin-Mariana arc collisional systems. The project will contribute to the ICDP themes "Collision Zones and Convergent Margins", "Active Faulting and Earthquake Processes" and "Climate Dynamics and Global Environments".

After the COSC drilling project, the Jämtland transect across the Scandinavian Caledonides will be one of the best investigated profiles across a Palaeozoic mountain belt. Calibrated geophysical investigations will give insight into the structure of the shield basement and the overlying allochthons. Detailed geological studies will cover the section from the upper allochthons into the Precambrian basement (Fig. 1), including ore-bearing horizons. Intraterrestrial life, its activity, nature and origin are much less studied in crystalline bedrock than in sedimentary environments. This is also true for the hydrogeological conditions. An integrated geological-geophysical-hydrogeological model is envisaged based on new knowledge concerning the structure of the thrust sheets and the underlying basement. Results will be of importance for all kinds of underground infrastructure projects, in particular when very long-term resistance to the underground environment is central, like for waste storage. Heat flow studies will increase our knowledge about the thermal regime in the allochthons and the crystalline basement of the Fennoscandian Shield and, together with the hydrogeological results, will assess the potential for energy extraction in the Åre-Järpen region. For a more far-reaching approach, the evaluation and development of methodology to more reliably predict the geothermal gradient from shallow drill holes is important. Inversion of heat flow data will also provide valuable information about palaeotemperature. Hence, COSC will also contribute to the ICDP themes "Geobiosphere and Early Life", "Natural Resources", and "Volcanic Systems and Thermal Regimes".

References

Fryer, P., Pearce, J.A., Stokking, L.B., et al., 1990. *Proc. ODP, Init. Repts.*, 125: College Station, TX (Ocean Drilling Program).

Gee, D.G., Juhlin, C., Pascal, C., and Robinson, P., 2010. Collisional Orogeny in the Scandinavian Caledonides (COSC). *GFF*, 132:29–44.

Soper, N.J., Strachan, R.A., Holdsworth, R.E., Gayer, R.A., and Greiling, R.O., 1992. Sinistral transpression and the Silurian closure of Iapetus. *J. Geol. Soc.*, 149:871–880.

Streule, M.J., Strachan, R.A., Searle, M.P., and Law, R.D., 2010.. Comparing Tibet-Himalayan and Caledonian crustal architecture, evolution and mountain building processes. *Geol. Soc. London Spec. Pub.*, 335:207–232.

Törnebohm, A.E., 1888. Om fjällproblemet. *GFF*, 10(5):328–336. (in Swedish)

Authors

Henning Lorenz, David Gee, and Christopher Juhlin, Uppsala University, Department of Earth Sciences, Villavägen 16, 752 36 Uppsala, Sweden, e-mail: henning.lorenz@geo.uu.se.

Related Web Links

http://www.sddp.se/COSC
http://are-jarpen.icdp-online.org/

Figure Credits

Fig. 3: Geological map, copyright Geological Survey of Sweden (SGU).

U.S. Continental Scientific Drilling Community Looks to the Future

by Anthony W. Walton

doi:10.2204/iodp.sd.11.11.2011

Continental scientific drilling in the U.S.A. may be poised to take a significant step forward as a result of two recent workshops that laid out the possibilities for the future. The meetings, in June 2009 in Denver, Colorado and in June 2010 in Arlington, Virginia, brought together about 100 members of the community. The first meeting stressed the themes and topics of important science for which drilling is a necessary means of collecting samples and data. The second workshop developed recommendations for implementation of a strong U.S. program including its position as a necessary component of the International Continental Scientific Drilling Program (ICDP).

The June 2009 workshop reviewed the range of scientific interests that continental drilling alone enables and specified possible interactions between continental and ocean drilling. Four overarching themes emerged: (i) global environmental and ecological change (emphasizing Earth history), (ii) geodynamics (broadly defined), (iii) the geobiosphere, and (iv) natural resources and environmental concerns (Table 1). Within each theme are a number of topics. Each topic has enough intellectual coherence for a consensus to be developed that reviews the field, identifies subjects for future growth, and suggests the means to reach goals. Most of these topics are familiar ones that have been expounded previously. Progress constantly brings new topics to the drilling community; for example, it has recently emerged that lake sediments preserve records of rates, processes, and triggers of evolutionary events, so that a whole community of evolutionary biologists will have interests in drilling projects.

The two main problems identified were (i) the thematic breadth of scientific drilling allowing no single focus and (ii) the path to funding being hindered by obstacles and delays (Fig. 1). To strengthen the U.S. community an enlarged Science Planning Committee of DOSECC has been charged with overseeing overall and topical scientific planning, considering advances in equipment or facilities that are necessary for the drilling community, and communicating internally, to the broader scientific community as well as to key funding agencies and to the ICDP.

Both workshops concluded that scientific planning should be a bottom-up effort, with communities gathering to reflect, assess, propose, consider, and develop consensus. Three special considerations emerged. First, planning efforts should be inclusive and international, including participants who address the same questions through different means. Where appropriate, they should include ocean drillers. Second, these efforts should be broadly announced and their results communicated so that members of other communities who might profitably participate in projects are fully informed of the opportunities. For example, study of the deep biosphere can be a part of many investigations. Third, any plan should be a guide, not a limit. The seemingly infinite creativity of investigators should not be discounted simply because their proposal is not in line with a pre-existing document.

Currently, the DOSECC office acts to bind the U.S. community together and inform the broader Earth science profession through annual workshops, newsletters, and booths at large professional meetings. It also has a very successful but poorly known program of internships for students and schoolteachers. Workshop participants recommended that these efforts should be expanded and supplemented by the wealth of modern communication modes.

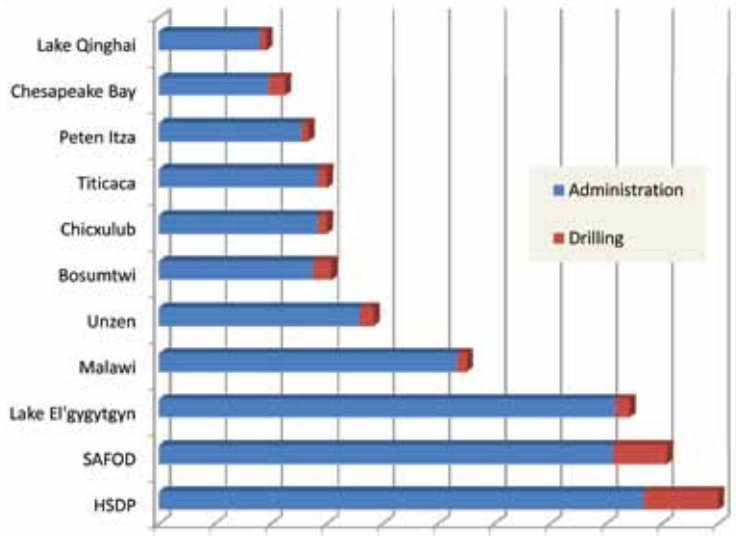

Figure 1. Comparison of drilling time to preparation time for representative projects. Administrative time includes the time from first workshop or first contact with DOSECC office until drilling actually begins. Projects undergo a year or more of planning and refinement before that occurs. The spectacle of 4–10 years of delay before operations begin effectively precludes young U.S. investigators from undertaking continental scientific drilling efforts (courtesy of Dennis Nielson).

Broadening the community is an important goal. An open planning process will do much to involve more investigators in drilling activities. The internship program should inform younger professionals of the potential rewards of drilling to gather necessary samples for their investigations and should enlist new members of the community. An important task will be to explore other ways to encourage investigators to undertake projects where drilling promises substantial rewards, despite the costs in money and time. Furthermore, the community will be looking at ways to mentor neophyte drilling scientists and to provide timely guidance to strengthen their proposals and projects.

Table 1. Themes and topics in continental scientific drilling.

Themes	Topics	
Global environmental and ecological change	High-resolution time-series records	Plio-Pleistocene climate records Evolution in isolated lake systems Climate and evolution of hominins and associated faunas (History of the magnetosphere)
	Deep-time records	Climate history Sea-level history Paleoceanography Atmospheric history and early life Cryospheric history from near-field sub-ice records (Stratigraphic architecture and crustal deformation) Evoluton and extinction Dynamics of the solar system (History of the magnetosphere) Antarctic deep-time records
Geodynamics	Crustal evolution (Stratigraphic architecture and crustal deformation) Hotspots, mantle plumes, and large igneous provinces Processes and hazards at volcanoes Fault mechanics (History of the magnetosphere) Ice-sheet history and dynamics	
Geobiosphere	Microbiology, including ichnofossils Biogeochemistry	
Natural resource systems and related environmental concerns	Hydrothermal resources and core deposits Groundwater Hydrocarbons CO_2 sequestration	

For international projects, the ICDP remains a key source of funding. Currently the principal source of funds in the U.S.A. is the National Science Foundation (NSF). However drilling activities are supported by other federal agencies and private sources. The 2010 workshop recommended several steps to deal with funding issues.

1. The 2010 workshop encouraged the NSF to identify a central internal point of contact and to secure funding arrangements for the costs of continental drilling, much as it supports telescopes for astronomers and ships for oceanographers. Ideally the central point of contact would be a formal program at NSF with a director and budget. NSF should also coordinate with scientific drilling efforts in other agencies.
2. Workshop participants strongly favored maintaining an appropriately funded facility, the current DOSECC office or a similar agency, to serve the community and provide drilling services coupled with a formal program at NSF with a director and budget.
3. The workshop recommended that the allocation of funding for drilling operations be based upon a set amount each year or a set number of drilling days, with some flexibility to deal with significant opportunities in a timely fashion. Funds from other agencies would extend the level of activity. This arrangement would remove the severe obstacle of including drilling costs in proposals.
4. One of the most pressing perceived obstacles to developing drilling projects is the need for funds to do preliminary site and feasibility studies. Consequently, the workshops recommended development of a system of funding necessary preliminary studies.

To implement the recommendations of the workshops, the continental scientific drilling community must work together, justify its science, plan its future, and work with funding agencies to develop mutually satisfactory arrangements. An enhanced continental scientific drilling effort in the U.S. A. requires an active community, thoughtful planning, and a clear pattern of funding to synergistically interact with related organizations and overlapping communities, and it will strengthen the international drilling communities and the Earth science effort as a whole.

Acknowledgements

The workshops were funded by the National Science Foundation through grants EAR 1039441 and EAR 0923056 to the University of Kansas with additional contributions from DOSECC, Inc. Comments by Walter Snyder, Wilfred Elders, and Ulrich Harms improved the manuscript.

Author

Anthony W. Walton, Chair, Board of Directors, DOSECC Inc., Department of Geology, The University of Kansas, Lawrence, KS 66045, U.S.A., e-mail: twalton@ku.edu.

Ultra-Deep Drilling through 3.5-Billion-Year-Old Crust in South Africa

by Maarten de Wit

doi:10.2204/iodp.sd.11.09.2011

Introduction

The Makhonjwa Mountains of South Africa and Swaziland comprise some of the most sought-after geo-real estate in the world. It is priceless—that is, for geoscientists—because the rocks of this approximately 120 km by 60 km corner of southern Africa, also known as the Barberton Greenstone Belt, date back to 3.2–3.6 billion years (Ga), representative of Earth in early Archean times when it was still ~1 Ga years young. They are not the very oldest rocks on Earth (those occur in Greenland and Canada), but they are the oldest best-preserved ones; thus, this stretch of land is without equal for research into the early history of our Earth. It is home to some of the earliest fragments of island arc, oceanic crust, and vestigial tracts of continent covered with sedimentary and volcanic rocks. So well-preserved are these rocks that unless one radiometrically dates them, it is near impossible to distinguish them from many modern rocks. This exceptional preservation has ensured that the Makhonjwa rocks yield the oldest directly dated and undisputed signs of life on Earth, and compared to our present biosphere they also provide detailed clues about the hostile nature of the paleoenvironments under which this life struggled to persist. One severe challenge entailed coping with more potent solar radiation to which life is particularly sensitive, when Earth's magnetic field was too weak to efficiently shield the surface from the relentless solar wind of lethal charged particles. Another is to explore for paleo-suture zones that can help establish when plate tectonics first emerged as the dominant solid earth recycling process to nurture the only sustainable habitable zone in our solar system. These then represent some of the targets of a new deep drilling project, on which an ICDP workshop was focused and held on 13–19 April 2010.

Table 1. Workshop participants.

Name	Affiliation
L Ameglio	Exige, Geophysical Services, RSA
R Armstrong	Australian National University, Australia
N Arndt	University of Grenoble, France
N Banerjee	University of Western Ontario, Canada
A Biggin	University of Liverpool, UK
M de Wit	AEON, University of Cape Town, RSA
T Dhansay	student, AEON and Council of Geoscience, RSA
M Doucouré	AEON, University of Cape Town, RSA
J Ebbing	Geological Survey of Norway, Norway
J Erzinger	GFZ German Research Centre for Geosciences, Potsdam, Germany
C Fourie	TUT, Tshwane University of Techology, RSA
D Frei	Geol Survey of Denmark, Denmark
C Jaupart	IPGP, Institute de Physique du Globe, Paris, France
C Langereis	University of Utrecht, Holland
S MacLennan	student, AEON, University of Cape Town, RSA
M Mesli	Geological Survey of Norway, Norway
C Rice	Drilling Technology SA, RSA
O Ritter	GFZ German Research Centre for Geosciences, Potsdam, Germany
P Robinson	Dept Earth Sciences, Dalhousie University, Canada
G Stevens	Stellenbosch University, Dept Earth Science, RSA
A van Wyk	Drillers in Training CC, RSA
U Weckman	GFZ German Research Centre for Geosciences, Potsdam, Germany
A Wilson	University of Witwatersrand, RSA

The workshop was attended by two students and twenty-one international scientists from four continents (Table 1), each with a different expertise and perspective with which to contemplate an 8–10 km drillhole through this unique terrain, as part of building an Early Earth Conservatory. The workshop was held at Travelport, the 'Cradle of Life' Conference-Conservation center, some 15 km from the town of Emanzana (formerly Badplaas), South Africa. The site is within walking distance from the world's oldest identified suture zone, the prime drilling target for this project (Fig. 1).

The project is both scientific and applied in scope. It is meant to characterize Earth's oldest subduction/suture zone and its paleoenvironments, to study the deep ancient and modern biosphere in pristine Archean crust, to establish a permanent 'on-site' early Earth laboratory-museum-educatorium in rural Africa, and to link these facilities to an African college of drilling technology.

Scientific Background

Tectonics

The existence and especially the onset of early Archean (>3.0 Ga) present-day style plate tectonics remains controversial, despite many studies having addressed this topic. Alternative models include plume dominated processes and crustal delamination during which vertical motions controlled Archean tectonics (Van Kranendonk, 2007; Hamilton,

Figure 1. Workshop participants in the field at a potential drill area.

2007). This controversy on the nature of Archean tectonics has been extensively debated over the last two decades without reaching consensus. Recent field-based research has provided some evidence for plate tectonics as early as 3.1 Ga and possibly as early as 3.8 Ga, but this is not generally accepted as conclusive (Schoene and Bowring, 2010; de Wit et al., 2011; Furnes et al., 2009). Geochemical analysis of Archean rocks shows that between 3.5 Ga and 3.8 Ga, Archean crust formation can, with apparent equal validity, be interpreted to have been generated during mantle plume magmatism or through subduction processes similar to that associated with plate tectonics (Bédard, 2006). Numerical modeling based on high mantle temperatures and geotherms, as is generally assumed for the Archean, is consistent with whole mantle plume tectonics (Davies, 2007). Similar modeling, particularly with a hydrous mantle, shows that plate tectonics is also capable of removing the required excess heat produced in the Archean at a rate of operation comparable to, and possibly even lower than, its current rate (Grove and Parman, 2004). In any case, recent thermochronology and petrology have questioned the existence of ubiquitous higher geothermal gradients everywhere during the Archean (Moyen et al., 2006; Diener et al., 2005).

A fundamental difference between plate tectonics and other scenarios is the occurrence of large horizontal lithosphere motion. Geological observations have revealed early Archean horizontal crustal motion. Extension and formation of sedimentary basins as early as 3.49 Ga and 3.45 Ga, as well as significant horizontal shortening episodes between 3.4 Ga and 3.2 Ga, suggest significant horizontal tectonic processes that possibly, but not definitively, reflect plate tectonic motions. The shortening episodes include associated high-pressure, low-temperature metamorphism in the Barberton Greenstone Belt at 3.2 Ga. Attempts at establishing extents and rates of horizontal motions of Archean terrains using paleomagnetism, have been suc-cessful only in terranes younger than 3.0 Ga (Strik et al., 2003; de Kock et al., 2009). Thus, a unified tectonic model for the early Archean Earth remains elusive. The interpretations and models remain controversial largely because of lack of geophysical data and robust structural/paleomagnetic analyses of tectonic events without precise thermochronology and pristine borehole samples.

Early life and ancient life-support systems

It has long been argued that understanding Archean tectonic processes provides fundamental keys to unraveling the origin and formation of Earth's earliest continents (cratons), its paleoenvironments, early ecosystems, and life.

Several decades have passed since the first description of recognizable early Archean microfossils (de Wit, 2010), yet morphology-focused imaging techniques of fossil-like objects and stable isotope (C, N, S) compositions of putative organisms have repeatedly failed to pose limits on the interpretation of the biogenic origin of the microstructures. Additionally, several abiologic metamorphic and hydrothermal reactions have been identified that can produce kerogen and graphite, and specific abiologic processes have been described that can generate complex structures that resemble microfossils (McLoughlin et al., 2007). In view of these uncertainties and controversies, it is clear that elucidating how and when life may have originated on Earth requires first to understand the conditions that prevailed early in Earth's history and the environments in which life may have appeared and later evolved. The recent discovery (Furnes et al., 2004) and *in situ* dating of ichnofossils in the rims of the world's oldest pillow lavas in Barberton (Fliegel et al., 2010) has dramatically shown that rocks previously ignored in studies of early life (e.g., basaltic igneous rocks) now offer a new paleoenvironment as habitats for early life. This holds great potential to track life back even further in time and must be considered a promising focus for such early life studies in places like the Barberton Greenstone Belt.

What the Makhonjwa Mountains can offer Archean science

The lower rock sequences of the Barberton Greenstone Belt and its surrounding granitoid terranes comprise the best well-preserved Paleo-Archean section of continental crust in the world (Fig. 2). The area contains rocks that have never been deeply buried, except within a limited zone in the southwest part of the belt where high-pressure, low-temperature metamorphism at 3.2 Ga has been recorded. This zone—part of the Inyoka fault system—has recently been suggested to represent a 3.2-Ga suture zone, separating two low-grade continental arc/back-arc/oceanic terranes of slightly different ages and geological history (Moyen et al., 2006). A similar second zone has been identified on the basis of thermochronology and structural mapping (Schoene et al., 2008, 2009) flanking the southeast margin of the belt, separating the central Barberton belt from a continental arc terrane, the Ancient Gneiss Complex. This implies that the two oldest sutures of the world are present in this area. Recent paleomagnetic studies on these older

sequences of the Barberton terranes provide intriguing preliminary evidence that a stable and reversing geomagnetic field was up and running at ~3.5 Ga, and that horizontal motions were on the order of ~12 cm yr^{-1}—fast by today's standards, but well within the range of plate velocities observed in the Phanerozoic (Biggin et al., 2011).

Key scientific questions analyzed during the workshop

- Did plate tectonics operate 3.5 billion years ago?
- What is the geophysical character/image of the world's oldest suture zones?
- Do the proposed suture zones of the Barberton Greenstone Belt, which separate at least three different terranes, penetrate the entire crust, and how do they affect the old underlying lithospheric mantle?
- Are paleomagnetic reconstruction of plate motions fast or slow, and are we dealing with large or small plates?
- What was the intensity of earliest geomagnetic field in relation to inner core growth?
- What is the nature/age of the crust beneath the oldest preserved terranes?
- How did the earliest continental fragments of the Kaapvaal craton form and amalgamate to create Earth's first stable continent? What was its geothermal gradient?
- Are we dealing with a 'hot/dry' mantle or a 'wet/cool' Archean mantle? What were the geothermal gradients within different Archean terranes?
- How did early suture zone tectonics and related thermo-chemical fluid processes, including serpentinization, influence early life and ecosystems and gold metallogenesis?
- What is the depth distribution and biochemistry of extremophiles in the deep biosphere of the Archean compared to that of today in the same rock sequences?
- What was the optimum temperature window for preservation of microfossils in different Archean terranes?
- Can we define chemical fingerprints of interactions between fluids, rocks and microbes?
- Were Archean ocean/atmosphere temperature and composition hot or cold?
- Is the atmosphere redox state reduced or oxidized, or episodically both?
- Can microbial contamination be defined and quantified?

What the Makhonjwa Mountains can offer rural development in Africa

The Barberton Greenstone Belt is a geological hotspot that is presently being considered as a UNESCO world heritage site. The region has been a 'mecca' for countless generations of Earth and life scientists and has been a key location where significant new scientific ideas have emerged. This remains so to this very day, with new research programs and at least three shallow scientific drilling projects having been completed recently and/or planned for completion soon. The Barberton Greenstone Belt is a well-known region for teaching of field geology and studies in early Earth processes to undergraduates and research students from South Africa and other countries. Tourist routes are now also starting to include the region, but few local people benefit from its rich history. The area under investigation is rural and poor, without adequate schooling and health facilities in crowded townships. Education opportunities for young people are scarce and uninspiring. Field schools and excursions (national and international) are frequent, but few if any engage with local youth. The plans for a deep drill site will be dovetailed with outreach and education requirements of the local, rural communities. Several scientists at the workshop cooperate closely with local nature reserves (Songimvelo and Nkomazi), the Mpumalanga Parks Board, and local tourist agencies. In addition, in-depth discussions have been held with local farmers and entrepreneurs, traditional leaders, and regional and national government representatives about the vision of linking a deep drilling site to a local center for early Earth studies attractive to schoolteachers, schoollearners, undergraduate students, and research scientists alike. These discussions have been welcomed by all these stakeholders.

Key socioeconomic & education questions addressed during the workshop

- How can we develop a long-lasting scientific interest in the early Earth that will also benefit the local rural communities, and in particular develop science and engineering skills related to geo-technology in rural Africa?
- How can we best dovetail scientific research with science and environmental outreach programs for general public awareness and youth education?
- Can we develop a local training center for drilling and related mining technology?
- Can we develop a rural center for early Earth studies, with open access for all researchers and learners to relevant materials and literature?

Workshop summary

Talks were presented on the regional geology and geophysics of the Barberton Greenstone Belt and surrounding regions, together with detailed overviews about the petrology and thermodynamics of the rocks found within and flanking the Inyoka Shear Zone (ISZ). These data form the backbone for models that represent the ISZ as a 3.2–3.3 Ga paleo-suture zone, within which evidence is preserved for a low Archean geothermal gradient of 10°C–20°C km^{-1} that was subsequently overprinted by higher temperatures at lower pressures, indicative of collision and exhumation tec-

tonics. This is contrary to conventional theories that all Archean environments had high geotherms (Hamilton, 2007). The drilling through the ISZ is thus a prime target for the study of a range of early Earth processes in an environment similar to those in modern subduction and suture zones. Geologically, the ISZ coincides with a number of highly deformed serpentinized peridotites and tectono-sedimentary melange rocks similar to those found along Phanerozoic suture zones and active plate boundary faults such as the Alpine Fault in New Zealand. Midway through the workshop, participants visited a potential drill site near the surface exposure of the ISZ (Fig. 1) flanked on one side by serpentinites and on the other by a sequence of sandstones and conglomerates, not unlike that found at the San Andreas Fault Observatory at Depth across the San Andreas Fault.

Overviews of the geophysics and a preliminary 3-D model of the greenstone belt indicates that a 10-km-deep drillhole also has the potential to pierce the base of the belt and thus allow a detailed examination of the contact with the underlying rocks of the middle Archean crust. These contacts are invariably interpreted as deep tectonic boundaries that have been explicitly implicated (de Wit and Ashwal, 1997) as incubators for epi-mesothermal gold deposits, hallmarks of greenstone belts throughout the world. In view of the relatively poor surface outcrop, a complete section (assuming high core recovery) will allow systematic changes to be recorded through the com-

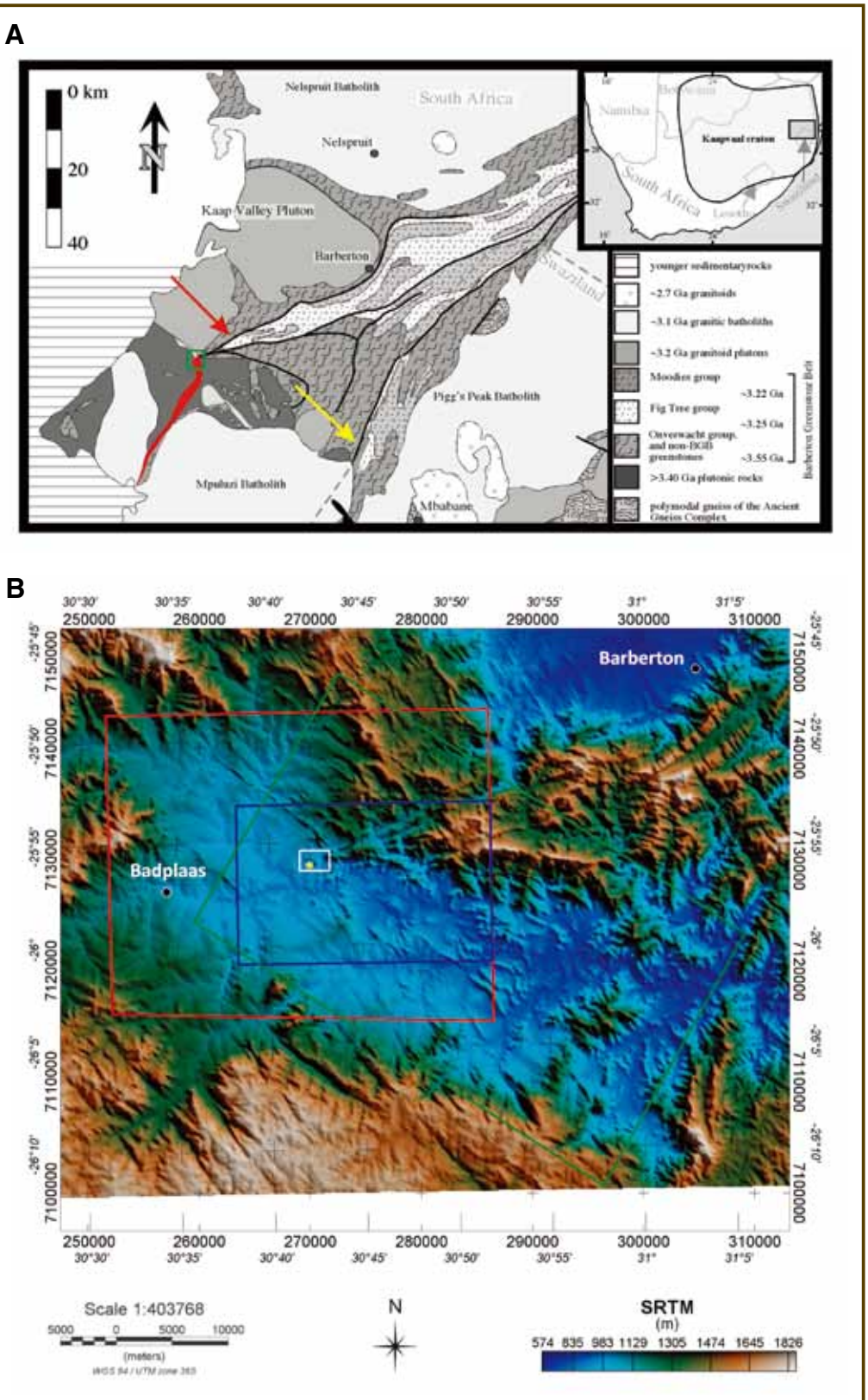

Figure 2. [A] Archean tectono-stratigraphic map of the Barberton Greenstone Belt as part of the Archean Kaapvaal craton (inset upper right). Three major tectonic terranes that comprise the Barberton region are separated by major tectonic boundaries (black solid lines), two of which (the Inyoka and Manhaar shear systems, indicated by red and yellow arrows, respectively) may represent ~3.2-Ga suture zones. Also shown in thick red is the inferred continuation of the Inyoka shear system within the granitoid terrain to the southwest of the greenstone belt, and the potential area for a deep drill site (green box). [B] SRTM image of the southern part of the greenstone belt, showing the area of ongoing high-resolution aeromagnetic surveying (dark blue box), and the potential deep drill site area (pale blue box). Also shown are the locations of Badplaas and Barberton. Note the undeformed NW-SE dykes swarm (positive topography) that cut the area that have been dated at 2990 Ma.

plex rock sequences with tectonic zones, and small features that are likely to be hidden in even the best outcrops will be much easier to interpret. Measurements on detailed chemical and physical parameters of the core are needed to ground truth geophysical profiles. Misapplication of seismic models developed for sedimentary sequences to metamorphic basement in the German Continental Deep Drilling Project, for example, resulted in erroneous interpretations (Emmermann and Lauterjung, 1997).

Workshop talks were presented also on how to collect fluids and gases, past and present, at all levels through a drilled sequence of this nature, and to measure changes in these over time and depth. The most abundant volatiles in common crustal rocks are water and carbon dioxide. However, little is known about the distribution and behavior of hydrocarbons, hydrogen, nitrogen, and noble gases in ancient continental crust. Generally these elements are minor components in crystalline rocks and, hence, do not significantly influence the physical or thermodynamic properties of a rock, but they have a large potential in tracing mass and heat transport processes. Moreover, noble gases (^{4}He, ^{40}Ar) and N in natural gases, crustal fluids, and fluid inclusions can be used as indicators of the fluid sources, and they are thus helpful in trying to solve questions of fluid generation, flow, and evolution in the deep crust.

These talks were complemented by biogeochemical views of how such a deep laboratory can further probe the present and past deep biosphere (microbiota) in rocks that may have harbored life as long ago as 3.4 Ga. The paleomagnetists also emphasized the need for careful magnetic measurements to constrain magnetic field strength variability, and the heat-flow modelers recommended *in situ* measurements of heat flow, conductivities, heat-producing elements, and high-resolution thermochronology to constrain variations in paleogeotherms.

The value and pitfalls of different types of geophysical surveys prior and during deep drilling projects, including the German KTB borehole, were presented and deliberated extensively during the workshop. In addition, an overview of the technical drilling capacity and training in South Africa was given by professional drilling consultants to the African mining industry. In 2009 the Mining Qualifications Authority estimated that there was a shortage of some 1200 drillers in South Africa, and the requirement for a steady stream of trained drillers into the broader African drilling industry will always be large. South African mining houses have for many years drilled some of the deepest cored boreholes in the world. In 2010 approximately fourteen boreholes were being drilled to depths in excess of 3500 m, but all of this drilling is still done using drilling systems that were developed many years ago. The need for an innovative approach to deep level core drilling is very great indeed.

The workshop also included an open 'town hall' meeting for the public, land owners, local school teachers and learners, non-governmental organization (NGO) representatives, and the media. Clearly, the workshop was a success judging not only by the interest in this project from a curiosity driven perspective, but also from the perspective of developing new drilling technology and the dire need for a sustainable education/training facility to ensure drilling expertise from Africa. It was perhaps surprising to learn that despite a severe shortage of drilling expertise and the great number of ongoing drilling projects in the exploration and extraction industries throughout onshore and off-shore Africa, there is nowhere in Africa for young people to pursue a career in drilling other than on-site learning on the job. The establishment of a training college focused on improving drilling (and possibly mining) skills would advance the goals of developing educational opportunities and drilling capabilities.

Recommendations

There was strong consensus at the workshop that we need to firmly establish whether more can be learned from two 5-km holes or several shallower holes, instead of one 10-km hole. Before further deliberations on this, and before honing in on a potential area, let alone a precise drill-site, there was unanimous agreement that a number of detailed surveys need to be completed. For example, more detailed surface mapping of the ISZ is required, in particular through higher resolution structural mapping and analyses. However, because of limited exposure a number of geophysical surveys are also prerequisites before the project can move into a drill-planning stage.

While preliminary 3-D gravity and magnetic models of the Makhonjwa Mountains were presented, their present utility is severely hampered by the lack of sufficiently high-resolution gravity, magnetic, and borehole data. Moreover, no crustal seismic reflection data are available. Although a teleseismic experiment has yielded a crustal thickness in this region of ~43 km from converted P-S wave receiver-function analyses, this experiment failed to provide any significant insights into the internal crustal structures (Nguuri et al., 2001). Current aeromagnetic data is too coarse to resolve the geology of the area. Additional geophysical methods (magnetotelluric magnetic, seismic) are therefore required, and only high-resolution data will improve the reliability of 3-D models required to understand surface structures with depth.

Developing plans for on-site, real-time mud-gas analysis during drilling—similar to those developed during drilling of the German KTB borehole, and in numerous scientific drilling projects since then—was proposed as essential at an early stage. Hydrocarbons, helium, radon, and (with limitations) carbon dioxide and hydrogen are the most suitable gases for the detection of fluid-bearing horizons, shear zones, open fractures, and sections of enhanced permeabil-

ity. These will provide critical samples and analyses of ephemeral gas/fluid pockets penetrated during drilling that might otherwise escape unnoticed, and will provide essential guidance for decisions related to later fluid sampling and *in situ* hydrologic testing. Subsequent off-site isotope studies on mud gas samples help reveal the origin and evolution of deep-seated crustal fluids. Studies of crustal scale fluid transport over large distances and times indicate that fluid transport rates are significantly in excess of predictions based on simple theory (Erzinger and Stober, 2005). This implies that fluid flow in the deep crust is mechanically enhanced and/or episodic. The specific rare gas components will indicate the relative proportions of fluids arising from meteoric, magmatic, metamorphic, and mantle sources. Information about the evolution of fluids in space and time should result from investigations of the chemical and isotopic fingerprints of rocks and minerals, which were influenced by fluid/rock interaction and fluid inclusions trapped as remnants of past fluids but also from the chemical-isotopic composition of fresh fluids present in open cavities and fractures. Therefore, such studies are fundamental to the success of a deep drilling project. Thus, while drilling campaigns provide unique opportunities to sample indigenous fluids/gases continuously from a section of the upper crust, site survery work needs to be completed prior to actual drilling.

As drill sites are selected, it is necessary to evaluate existing information on the local hydrology, hydrochemistry, and the occurrence of aquifers. A science team will plan to measure hydrologic properties at several levels by packing off favorable sections and to collect water samples (e.g., for tritium and noble gas isotope analyses [He, Ne, Ar, Kr, and Xe], stable isotope analyses [H, C, O, and S]), and for complete chemistry of dissolved constituents.

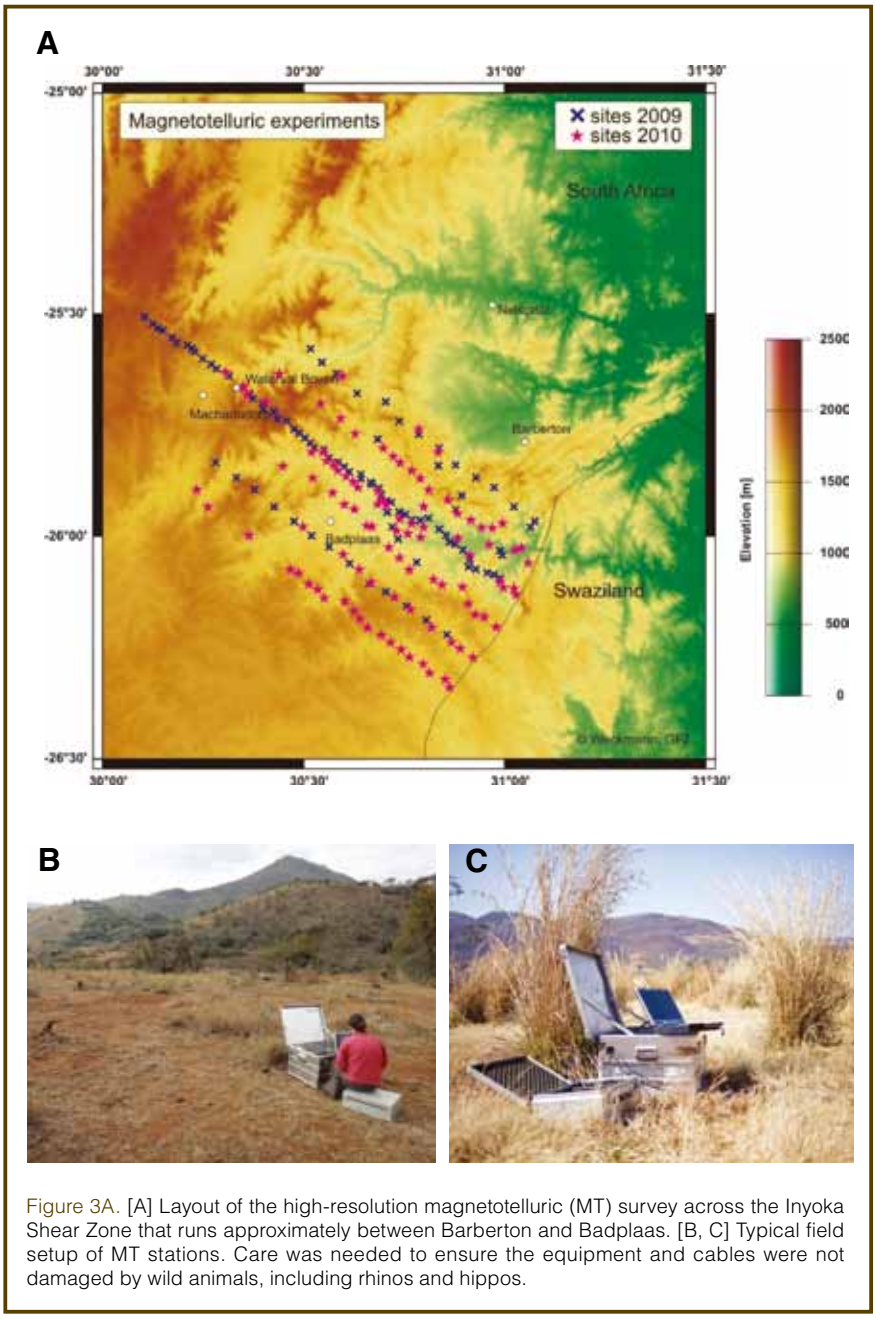

Figure 3A. [A] Layout of the high-resolution magnetotelluric (MT) survey across the Inyoka Shear Zone that runs approximately between Barberton and Badplaas. [B, C] Typical field setup of MT stations. Care was needed to ensure the equipment and cables were not damaged by wild animals, including rhinos and hippos.

Ensuring successful drilling deep into the oldest suture zone will require the early cooperative efforts of many nations and experts, and good coordination is essential. Prior to drilling, a long lead time is required to establish a precise location where the suture will occur at depth and how its local dip might vary. Besides detailed geophysics, it will be important to obtain additional information through a number of shallow reconnaissance pilot holes at relatively low cost. Both partial core recovery and downhole geophysical logging will provide crucial information to improve 3-D modeling.

Ongoing Work

As part of laying further foundations for this project, ongoing work has focused on a detailed magnetotelluric (MT) survey (Weckmann et al., 2009) across the Inyoka paleo-suture zone and surrounding rocks to obtain high-resolution images of the shear zones. Over two consecutive years (2009–2010), two large MT experiments were carried out. To gain good 3-D coverage, 5-component MT data were recorded in a frequency range from 0.001 s to 1000 s at almost 200 sites (at an average spacing of ~2 km) arranged along a 110-km-long transect and five shorter transects covering an area of ~300 km^2 (Fig. 3). This setup provides good areal coverage of the ISZ and also a vertical resolution on lithospheric scale. The main difficulties for electromagnetic experiments in the Barberton area are the various man-made noise sources (e.g., electric fences, power lines, mining

activities and a major DC railway line). Hence, the natural electromagnetic field variations are overprinted by these strong electromagnetic signals. Nevertheless, the first 2-D inversion tests along the 110-km transect with a reduced data set already show strong correlation with subsurface geology, and zones of high electrical conductivities appear to correlate well with the surface location of known faults. The results of the MT work is being further integrated with ongoing laboratory conductivity measurements on representative rock samples collected across the suture zone during detailed structural mapping of a well exposed part of the ISZ.

A high-resolution aeromagnetic and radiometric survey is planned for March 2011, using the low flying Gyrocopter Kreik IIB from GyroLAG (Gyrocopter Light Airborne Geophysics), to complement the MT work. A special feature of this light airborne geophysics platform, which requires no formal landing strip, is its capability of performing safely at survey heights as low as 5 m above ground level at relatively slow speeds (75–100 km hr^{-1}), resulting in a significant improvement in quality of data (equivalent of 2–3 m ground equivalent sampling intervals).

Plans to establish an Africa college for drilling technology are in progress with the Tswana University of Technology (TUT) and relevant government agencies. Local property owners have identified several suitable sites where such a rural extension of TUT might be built. As part of a new drilling technology development initiative, an early start on developing a new type of high-speed coring turbine drill bit has begun at TUT. Although the design has not been finalized, the proto-drill includes a fluid-powered and cooled rotating drill head with a stationary drillstring, and a mechanism for core to be brought up via a core-mouse inside the drilling stem. Also part of this initiative is design of new drill bits (based on recent developments in synthetic diamond manufacturing techniques), face discharge designs, and hybrid bit designs.

Conclusion

We are confident that the proposed geophysics transects in the Barberton area will yield high quality depth profiles down to Moho and possibly deeper. This will allow imaging of the proposed suture zones, the bottom of the greenstone belt, and possibly other features not yet identified. The proposed suture zones are also principle zones of structurally controlled gold mineralization, allowing for significant spin-off for understanding links between these sutures and Archean metallogenesis. The suture zones are also the focus of significant serpentinization that must have been the source of large-scale fluid flow and hydrogen production, both important ingredients for the emergence of primitive life and thereafter to sustain it to the present day.

The Makhonjwa Mountain treasure chest continues to yield unique observations with which to model how our planet transformed from a near molten ball to a plate tectonic driven recycling plant. There is always a ripple of excitement at scientific meetings whenever the lid of the Makhonjwa Mountain chest is pierced further open, ever so slightly. It is hoped that a deep geoscientific drillhole with associated science and technology related infrastructure will provide new scientific opportunities and also add significant value to the local communities.

Acknowledgements

Funding for the workshop was provided through the ICDP, the SA National Research Foundation (NRF), the Africa Earth Observatory Network (AEON), the bilateral South Africa-German program Inkaba yeAfrica project, and Travelport through Mr. Fred Daniel. These support structures are gratefully acknowledged. The MT work is financed through the GFZ, the DFG, and Inkaba yeAfrica program, and is led by Ute Weckmann and Oliver Ritter and their MT Group at Potsdam. The high-resolution aeromagnetic survey was conducted by Laurent Ameglio of GyroLAG and EXIGE (EXpertise In GEophysics), South Africa.

Nazla Hassen and UCT students are thanked for logistic support, and the staff at Travelport for their efficient and friendly hospitality, and for arranging transport to the potential drill site. I would in particular like to thank all participating scientists. This is AEON contribution number 94.

References

Bédard, J.H., 2006. A catalytic delamination-driven model for coupled genesis of Archaean crust and sub-continental lithospheric mantle. *Geochimica et Cosmochimica Acta*, 70:1188–1214, doi:10.1016/j.gca.2005.11.008.

Biggin, A.J., de Wit, M.J., Langereis, C.G., Zegers, T.E., Voute, S., Dekkers, M.J., and Drost, K. 2011. Palaeomagnetism of Archaean rocks of the Onverwacht Group, Barberton Greenstone Belt (southern Africa): Evidence for a stable and potentially reversing geomagnetic field at ca. 3.5 Ga. *Earth Planet. Sci. Lett.*, (2011), doi:10.1016/j.epsl.2010.12.024.

de Kock, M.O., Evans, D.A.D., and Beukes, N.J., 2009. Validating the existence of Vaalbara in the Neoarchean. *Precambrian Res.*, 174(1–2):145–154.

de Wit, M.J and Ashwal, L.D., 1997. *Greenstone belts*: Oxford, U.K. (Oxford University Press).

de Wit, M.J., 2010. The deep-time treasure chest of the Makhonjwa Mountains. *S. Afr. J. Sci.*, 106(5/6), Art. #277, 2 pages, doi:10.4102/sajs.v106i5/6.277.

de Wit, M.J., Furnes, H., and Robins, B., 2011. Geology and tectonostratigraphy of the Onverwacht Suite, Barberton Greenstone Belt, South Africa. *Precambrian Res.*, in press, doi:10.1016/j.precamres.2010.12.007.

Davies, G. F. (2007), Controls on density stratification in the early mantle, *Geochem. Geophys. Geosyst.*, 8, Q04006, doi:10.1029/2006GC001414.

Diener, J.F.A., Stevens, G., Kisters, A.F.M., and Poujol, M., 2005. Metamorphism and exhumation of the basal parts of the Barberton greenstone belt, South Africa: constraining the rates of Mesoarchaean tectonism. *Precambrian Res.*, 143:87–112, doi:10.1016/j.precamres.2005.10.001.

Emmermann, R., and Lauterjung, J., 1997. The German Continental Deep Drilling Program KTB: overview and major results. *J. Geophys. Res.*, 102:18179–18201.

Erzinger, J., and Stober, I., 2005. Long-term fluid production in the KTB pilot hole, Germany. *Geofluids, Special Issue*, 5:1–7, doi:10.1111/j.1468-8123.2004.00107.x.

Fliegel, D., Kosler, J., McLoughlin, N., Simonetti, A., de Wit, M.J., Wirth, R., and Furnes, H., 2010. *In situ* dating of the Earth's oldest trace fossil at 3.34 Ga. *Earth Planet Sci. Lett.*, 299:290–298, doi:10.1016/j.epsl.2010.09.008.

Furnes, H., Banerjee, N.R., Muehlenbachs, K., Staudigel, H., and de Wit, M., 2004 Early life recorded in Archean pillow lavas. *Science*, 304:578–581, doi:10.1126/science.1095858.

Furnes, H., Rossing, M., Dillik, Y., and de Wit., M.J., 2009. Isua supracrustal belt (Greenland) — a vestige of a 3.8 Ga suprasubduction zone ophiolite, and the implications for Archean geology. *Lithos*, 113:115–132, doi:10.1016/j.lithos.2009.03.043.

Grove, T.L., and Parman, S.W., 2004. Thermal evolution of the Earth as recorded by komatiites. *Earth Planet. Sci. Lett.*, 219:173–187.

Hamilton, W.B., 2007. Earth's first two billion years —the era of internally mobile crust. *GSA Memoir*, 200:233–296.

McLoughlin, N., Brasier, M.D., Wacey, D., Green, O.R., and Perry, R.S., 2007. On biogenicity criteria for endolithic microborings on early Earth and beyond. *Astrobiology*, 7(1):10–26, doi:10.1089/ast.2006.0122.

Moyen, J-F., Stevens, G., and Kirsters, A., 2006. Record of mid-Archean subduction from metamorphism in the Barberton terrain, South Africa. *Nature*, 422:559–562, doi:10.1038/nature04972.

Nguuri, T.K., Gore, J., James, D.E., Webb, S.J. and the Kaapvaal Seismic Group, 2001. Crustal structure beneath southern Africa and its implications for the formation and evolution of the Kaapvaal and Zimbabwe cratons. *Geophys. Res. Lett.*, 28:2501–2504, doi:10.1029/2000GL012587.

Schoene, B., and Bowring, S.A., 2010. Rates and mechanisms of Mesoarchean magmatic arc construction, eastern Kaapvaal craton, Swaziland. *Geol. Soc. Am. Bull.*, 122(3/4):408–429, doi:10.1130/B26501.1.

Schoene, B., de Wit, M.J., and Bowring, S.A., 2008. Mesoarchean assembly and stabilization of the eastern Kaapvaal craton: a structural-thermochronological perspective. *Tectonics*, 27:TC5010, doi: 10.1029/2008TC002267.

Schoene, B., Dudas, F.O.L., Bowring, S.A., and de Wit, M.J., 2009. Sm-Nd isotopic mapping of lithospheric growth and stabilization in the eastern Kaapvaal craton. *Terra Nova*, 21:219–228.doi:10.1111/j.1365-3121.2009.00877.x.

Strik, G.H.M.A., Blake, T.S., Zegers, T.E., White, S.H., and Langereis, C.G., 2003. Palaeomagnetism of flood basalts in the Pilbara Craton, Western Australia: late Archaean continental drift and the oldest known reversal of the geomagnetic field. *J. Geophys. Res.*, 108:(B12), EPM 2–1–EPM 2–21.

Weckmann, U., Nube, A., Chen, X., Ritter, O., and de Wit, M. 2009. Overview and preliminary results of a magnetotelluric experiment across the southern Barberton greenstone belt. [11th SAGA Biennial Technical Meeting and Exhibition, Swaziland, 16–18 September], 583–586.

Van Kranendonk, M.J., 2007. Tectonics of early Earth. In Van Kranendonk, M.J., Smithies, R.H., and Bennet, V. (Eds.), *Earth's Oldest Rocks. Developments in Precambrian Geology, 15*: Amsterdam (Elsevier), 1105–1116.

Author

Maarten de Wit, Africa Earth Observatory Network, University of Cape Town, Rondebosch 7701, South Africa. e-mail: maarten.dewit@uct.ac.za.

Figure Credits

Fig. 1: Moctar Doucouré, AEON, University of Cape Town
Fig. 3b, 3c: Dr. Ute Weckmann, GFZ-Potsdam, Germany

IODP-Canada to Exhibit at GAC-MAC 2011

25–27 May 2011, Ottawa, Canada

IODP-Canada will have an exhibition booth at the upcoming joint annual meeting of the Geological Association of Canada, the Mineralogical Association of Canada, the Society of Economic Geologists and the Society for Geology Applied to Mineral Deposits (GAC-MAC-SEG-SGA) to be held at the University of Ottawa on 25–27 May 2011. Over a thousand Earth sciences specialists from Canada, Europe, and the U.S. will be present. Ottawa 2011's motto—*Navigating Past & Future Change*—highlights this meeting's commitment to exploring both the scientific and the societal aspects of Earth sciences.

For more details on IODP-Canada's activities please visit www.iodpcanada.ca or contact the IODP-Canada Coordinator, Diane Hanano at coordinator@mail.iodpcanada.ca.

ECORD Summer School Topic: Subseafloor Fluid Flow and Gas Hydrates

12–13 September 2011, Bremen, Germany

The 5th ECORD Summer School in Bremen, to be held on 12–23 September 2011 at the MARUM—Center for Marine Environmental Sciences—at the University of Bremen, Germany aims to bring PhD students and young postdocs in touch with IODP at an early stage of their careers, inform them about the actual research within this international scientific program, and to prepare them for future participation in IODP expeditions. Such training will be achieved by taking the summer school participants on a "virtual ship" utilizing the unique facilities linked to the IODP Bremen Core Repository where they get familiarized with a wide spectrum of state-of-the-art analytical technologies and core description methods including core logging/scanning according to the high standards on IODP expeditions. In addition, the topic "Subseafloor Fluid Flow and Gas Hydrates" will be covered by lectures and discussions with leading researchers in the field. A one-day field trip on a research vessel will round out the program.

This comprehensive approach—combining scientific lectures with practicums on IODP-style "shipboard" measurements—is the blueprint for the Bremen ECORD summer school covering the three major topics of the IODP Initial Science Plan. The Summer School will be organised by Dierk Hebbeln, Director of the Bremen International Graduate School for Marine Sciences (GLOMAR), Gerhard Bohrmann, Head of Department of Marine Geology, Heiner Villinger, Head of Department of Marine Sensors, and Ursula Röhl, Head of the IODP Core Repository, all at the University of Bremen, Germany. For detailed information visit www.glomar.uni-bremen.de/ECORD_Summer_School.html.

ECORD Invites You to Host a Lecture

Since 2007, the European Consortium for Ocean Research Drilling has sponsored the ECORD Distinguished Lecturer Programme, an initiative for a lecture series to be given by leading scientists involved in the Integrated Ocean Drilling Program. The program is designed to bring the exciting scientific discoveries of the IODP to the geosciences community in ECORD and non-ECORD countries.

2010–2012 Lectures:

Kai-Uwe Hinrichs, MARUM, University of Bremen, Germany

Title: "Benthic archaea – the unseen majority with importance to the global carbon cycle revealed by IODP drilling."

Dominique Weis, Pacific Center for Isotopic and Geochemical Research, University of British Columbia, Canada

Title: "What do we know about mantle plumes and what more can we learn by IODP drilling?"

Helmut Weissert, ETH Zürich, Switzerland

Title: "Carbon cycle, oceans and climate in the Cretaceous: lessons from ocean drilling (DSDP to IODP) and from records on continents."

Applications to host a Distinguished Lecturer are accepted from any college, university or non-profit organization in all European countries and Canada. Applications from non-traditional IODP and ECORD audiences within the European Community are especially welcome. Apply via e-mail to essac.office@awi.de. Further information at http://www.essac.ecord.org/index.php?mod=education&page=dlp.

The ESF Magellan Workshop Series Program

The ESF Magellan Workshop Series Program, launched in 2006 with the aim of nurturing and coordinating innovative marine scientific drilling proposals for European scientists, is in its last phase of operation. The program will run until 31 July 2011. A decision was made in Burkheim, Germany in August 2010 to propose a successor program, The Magellan Plus Program. Currently, a committee lead by Lucas Lourens, (The Netherlands), Marit-

Solveig Seidenkrantz (Denmark), Ales Spicak (Czech Republic), and representatives from seven other European countries are developing a program proposal which, if funded, will support both marine and continental scientific drilling and coring.

To date the ESF Magellan Workshop Series Program has provided opportunities for senior level researchers and young scientists as well as students to contribute to ocean drilling research goals in Europe. More than eighteen workshops, fifteen short visit grants and one educational activity have been supported. Three workshops were held in 2010: Volcanic Basins: Scientific, economic and environmental aspects in Vienna (AU) by N. Arndt; RAMBO (Real-time Amphibic Monitoring & Borehole Observations) held in Bremen (GE) by A. Kopf; and The GOLD project, drilling in the Western Mediterranean Sea held in Banyuls (FR) by M. Rabineau. The most recent supported workshop, CCS (Carbon Capture & Storage) Oman 2011 convened by M. Godard, was held in the Sultanate of Oman in January 2011.

The final Magellan workshop, Arctic Ocean drilling and the site survey challenge, will be held in early November 2011 in Copenhagen (DK) and is being organized by N. Mikkelsen, Denmark.

Although no more workshops will be supported, there is currently a call open for short visit travel grants to support both young scientists and keynote speakers to attend meetings. This call will remain open until the end of the program. All scientists and students who are interested are encouraged to submit a proposal for a short visit grant. Priority will be given to proponents from ESF Magellan member countries and/or workshops to be held in member countries. ESF Magellan member countries are: Austria, Belgium, Denmark, Finland, France, Germany, Ireland, The Netherlands, Norway, Portugal, Sweden, and Switzerland.

For more information and to apply to the ESF Magellan Workshop Program, please see www.esf.org/magellan, or contact the ESF program administrator at edegott@esf.org, or the Chair of the Program Jochen Erbacher Jochen.Erbacher@bgr.de.

The First IODP Meeting at AOGS in India

India is an associate member of IODP and has been regularly participating in various IODP expeditions around the world aimed at addressing geo-scientific issues. In order to showcase various IODP-related activities in India, a parallel poster session was organized in conjunction with the IODP-MI at Asia Oceania Geosciences Conference in Hyderabad, India, 5–9 July 2010. The objective of this stall was to promote overall awareness about the benefits of deep-sea scientific drilling and its role in researching various scientific questions.

A dedicated session was also organized to discuss thrust areas of research in the Indian Ocean that could be potentially addressed through ocean drilling. The meeting was chaired by the Secretary, Ministry of Earth Sciences, Government of India and attended by delegates from numerous institutes/organizations across the country, such as Physical Research Laboratory, National Institute of Oceanography, National Geophysical Research Institute, and National Centre for Antarctic and Ocean Research. The meeting was open to all the participants of the AOGS meeting to receive feedback for developing a comprehensive drilling proposal for the northern Indian Ocean. The meeting was highly significant in terms of collecting valuable suggestions related to the IODP and scientific ocean drilling interests in India.

Report of the 4th ECORD Summer School 2010

The ECORD Summer School 2010 on "Dynamics of Past Climate Changes" was held at the MARUM (Center for Marine Environmental Sciences) Bremen University, Germany, on 13–24 September 2010. It was organized by Prof. Dierk Hebbeln, Director of the Bremen International Graduate School for Marine Sciences "Global Change in the Marine Realm" (GLOMAR), by Prof. Dr. Michael Schulz, Head of the Geosystem Modelling Group at the University of Bremen, and by Dr. Ursula Röhl, IODP Curator at the Bremen Core Repository (BCR). Twenty-eight PhD students and postdoctoral fellows from several European countries and Canada participated in the two-week course which combined lectures, interactive discussions, practical exercises on a "virtual ship" (i.e. in the lab and in the facilities of the IODP core repository), and a field trip to the Late Quaternary Landscapes in the vicinity of B9.25

Successful Port Call of *JR* at Victoria, B.C., Canada

Taking advantage of the *JOIDES Resolution* port call in the Victoria harbor between the Juan de Fuca Hydrogeology Expedition 327 and the Cascadia CORK Expedition 328 on 5–9 September 2010, lectures and guided tours on the ship were organized for the public by Ocean Leadership in collaboration with IODP-Canada and Ocean Networks Canada.

Kiyoshi Suyehiro, President of IODP-MI, Catherine Mével, Chair of the ECORD Managing Agency and Anne de Vernal, Chair of IODP-Canada, participated in the event, which was covered by the local press.

During the port call, about 150 people had the opportunity to get acquainted with IODP by visiting the

JOIDES Resolution, and more than seventy people attended the public lectures.

The lecture by Earl Davis focused on deep-ocean boreholes for long-term observation of crustal temperature and pressure along active seismogenic margins. The other lecture by Michael Riedel addressed the question of gas hydrates in marine sediments as a potential energy resource and cause of geohazards.

Workshop about MELAGUS at Burgos, Spain

Intramontane basins have the potential for providing unique, continuous sedimentary records of paleoclimate and paleoenvironmental changes. The Guadix-Baza Basin in southern Spain—the largest, southernmost paleolake in Europe—is a particularly important example of such valuable sedimentary archives. Its rich and extensive depositional sequence are key to understanding the Neogene Mediterranean-Atlantic seaway and provides an unprecedented paleoclimatic, paleogeographic, and fossiliferous record of the region throughout the Neogene and Pleistocene. A program of drilling, which is about the Mediterranean-Atlantic seaway and Lacustrine strata Guadix-Baza Basin, Spain (MELAGUS), is seen as the key for obtaining continuous sedimentary records from this intramontane basin, since its deposits are otherwise inaccessible or only partially exposed along degraded outcrops. On 21 October 2010, a group of twenty-five scientists met at the Centro Nacional de Investigación sobre la Evolución Humana (CENIEH), Burgos, Spain, to discuss an initial blueprint for drilling and obtaining sediment cores from the Guadix-Baza Basin. The attendees included researchers from Spain, the United Kingdom and Italy: they specialize in a wide variety of disciplines, including geophysics, paleontology, sedimentology, geochemistry, geochronology, paleopedology, mineralogy, and palynology. At present, there are no precedents of lacustrine drilling programs in any of the major mid-latitude paleolakes of Europe. The proposed drilling project would furnish an unparalleled southernmost reference framework for understanding past environmental changes during the Pliocene and Pleistocene, and their implications for human evolution. Contacts: Josep M. Parés (Josep.pares@cenieh.es) and César Viseras (viseras@ugr.es).

Sub-Seafloor Microbes and Wandering Hotspots Meet in Auckland, New Zealand

Perhaps it is more accurate to say that two deep-sea drilling expeditions with *JOIDES Resolution* (*JR*) "crossed over" in Auckland last mid December.

The scientific ocean drilling ship *JR* undertook two expeditions in the southwest Pacific, northeast of New Zealand: one to learn more about the limits to life deep beneath the seafloor (Expedition 329), and the other to test if and how much the Louisville hotspot has moved over the past eighty million years (Expedition 330).

In the intervening time, as *JR* was moored in Auckland, several activities had been organized by the New Zealand IODP Office (GNS Science), the Auckland Museum Institute, and the University of Auckland, with the support of the Integrated Ocean Drilling Program and the Consortium for Ocean Leadership.

These included eight ship tours, a lunch reception, talks by expedition co-chief scientists Steven d'Hondt (329: University of Rhode Island) and Anthony Koppers (330: Oregon State University), and evening public lectures. Thus, many Aucklanders learned about IODP and the importance and relevance of its programs.

Port call activities and the two cross-over expeditions generated interest in the local media, including TV3NZ, RadioNZ, the New Zealand Press Agency, Australia ABC Science and the Australian Science Media Centre.

The *JR* visited Auckland again in mid February, and visitors to the Auckland Museum followed the Louisville expedition through an interactive exhibit.

DFDP, Alpine Fault, New Zealand

The Deep Fault Drilling Project (DFDP) completed its first two boreholes through the Alpine Fault in early February. DFDP-1A penetrated fault gouge at 91 m and reached a total depth of 101 m in gravel. DFDP-1B penetrated fault gouge at 128 m, reached a total depth of 152 m, and collected the first continuous record of cataclasites on both sides of the fault. Initial results include the discovery of a large fluid pressure difference across the fault. Fluid pressures are hydrostatic above the fault, with a water level at 7 m below ground surface. In contrast, the water level in the sampling tube from beneath the fault is 40 m below ground surface. This pressure difference decreased borehole stability in the highly fractured fault rocks,

but the fault has now been resealed in both boreholes with a bentonite-cement grout. All aspects of the project were successful. High-quality cores and a comprehensive suite of wireline logs were collected from both boreholes. DFDP-1A has a seismometer installed at a depth of 83 m, just below steelcasing. DFDP-1B has a seismometer, 4 piezometers, and 24 temperature sensors installed within it, and a 25-mm fluid sampling tube to a depth of 133 m. An additional seismometer and piezometer will be installed later. Additional information can be found at wiki.gns.cri.nz/DFDP. DFDP-1 drilling was managed by Dr. Rupert Sutherland, GNS Science, Lower Hutt, NZ (r.sutherland@gns.cri.nz). It was funded by Germany (DFG, University of Bremen), New Zealand (Marsden Fund; GNS Science; and Victoria, Otago, Auckland, and Canterbury Universities), and the United Kingdom (NERC, University of Liverpool). Reference: Townend, J., Sutherland, R., and Toy, V., 2009. Deep Fault Drilling Project—Alpine Fault, New Zealand. *Sci. Drill.*, 8:75–82, doi: 10.2204/iodp.sd.8.12.2009.

Towards an Integrated Biochronology for the Cenozoic

One of the magnificent legacies of ocean drilling is the recovery of abundant marine microfossils. These microfossils provide an excellent evolutionary record that can be readily utilized in biostratigraphy. From the earliest days of the Deep Sea Drilling Project it became clear that marine microfossils in deep ocean basins were the same morphospecies as those recognized in marine sediments studied from outcrop, allowing global recognition of biostratigraphic schemes. Applying an age to an evolutionary or extinction events of marine microfossils relies upon sediments with continuous sedimentation and a clearly defined magnetostratigraphy or cyclostratigraphy—ocean cores do just that. In a recent paper published in *Earth Science Reviews*, Wade et al., (2011) bring together 187 tropical and subtropical planktonic foraminiferal biostratigraphic events for the Cenozoic. Such a compilation has not been attempted since 1995, however, the *JOIDES Resolution* began renewed ocean drilling operations in 2009, following a major refit, which acted as a catalyst to reassess the existing bioevents. Major advances by ODP and IODP in improved drilling recovery, multiple coring and high-resolution sampling, has allowed many biostratigraphic events to be refined. For example, detailed biostratigraphic investigations from Ocean Drilling Program Leg 154 (Ceara Rise; Chaisson and Pearson, 1997; Pearson and Chaisson, 1997; Turco et al., 2002), Leg 199 (Equatorial Pacific; Wade et al., 2007), as well as outcrop sections (Payros et al., 2007, 2009) have resulted in revision of the calibrations of numerous bioevents. The compilation by Wade et al., (2011) includes a series of convenient "look-up" tables against multiple geomagnetic time scales. The revised and recalibrated data provide a major advance in biochronologic resolution and a template for future progress to the Cenozoic time scale. This is one step towards the development of an integrated bio-magneto-astrochronology for the Cenozoic. The new cores drilled during IODP on cruises such as Expedition 320/321 in the equatorial Pacific Ocean (Pälike et al., 2010) will allow further refinements.

References

Chaisson, W. P, and Pearson, P. N. 1997. Planktonic foraminifer biostratigraphy at Site 925: Middle Miocene – Pleistocene. *In* Shackleton, N. J., Curry, W. B., Richter, C., Bralower, T. J. (Eds.), *Proc. ODP, Sci. Results* 154: College Station, TX (Ocean Drilling Program), 3–31.

Pälike, H., Nishi, H., Lyle, M., Raffi, I., Gamage, K., Klaus, A., and the Expedition 320/321 Scientists, 2010. Pacific Equatorial Age Transect. *Proc. IODP*, 320/321: Tokyo (Integrated Ocean Drilling Program Management International, Inc.). doi:10.2204/iodp.proc.320321.2010.

Payros, A., Bernaola, G., Orue-Etxebarria, X., Dinares-Turell, J., Tosquella, J., and Apellaniz, E., 2007. Reassessment of the Early-Middle Eocene biomagnetochronology based on evidence from the Gorrondatxe section (Basque Country, western Pyrenees). *Lethaia* 40:183–195.

Payros, A., Orue-Etxebarria, X., Bernaola, G., Apellaniz, E., Dinarès-Turell, J., Tosquella, J., and Caballero, F., 2009. Characterization and astronomically calibrated age of the first occurrence of Turborotalia frontosa in the Gorrondatxe section, a prospective Lutetian GSSP: implications for the Eocene time scale. *Lethaia* 42:255–264.

Pearson, P. N., and Chaisson, W. P. 1997. Late Paleocene to middle Miocene planktonic foraminifer biostratigraphy of the Ceara Rise. *In* Shackleton, N. J., Curry, W. B., Richter, C., Bralower, T. J. (Eds.), *Proc. ODP, Sci. Results* 154: College Station, TX (Ocean Drilling Program), 33–68.

Turco, E., Bambini, A.M., Foresi, L.M., Iaccarino, S., Lirer, F., Mazzei, R., and Salvatorini, G., 2002. Middle Miocene high-resolution calcareous plankton biostratigraphy at Site 926 (Leg 154, equatorial Atlantic Ocean): paleoecological and paleobiogeographical implications. *Geobios* 35:257–276.

Wade, B.S., Berggren, W.A., and Olsson, R.K., 2007. The biostratigraphy and paleobiology of Oligocene planktonic foraminifera from the equatorial Pacific Ocean (ODP Site 1218). *Mar. Micropaleontology,* 62:167–179.

Wade, B.S., Pearson, P.N., Berggren, W.A., and Pälike, H., 2011. Review and revision of Cenozoic tropical planktonic foraminiferal biostratigraphy and calibration to the geomagnetic polarity and astronomical time scale. *Earth Science Rev.* 104:111–142.

Bridget Wade, School of Earth and Environment, University of Leeds, Woodhouse Lane, Leeds, LS2 9JT, U.K., e-mail: B.Wade@leeds.ac.uk

Schedules

IODP – Expedition Schedule http://www.iodp.org/expeditions/

	ESO Operations	Platform	Dates	Port of Origin
	No expedition is currently scheduled.			
	USIO Operations *	**Platform**	**Dates**	**Port of Origin**
1	334 - Costa Rica Seismogenesis Project (CRISP)	*JOIDES Resolution*	15 Mar.–13 Apr. 2011	Balboa, Panama
2	335 - Superfast Spreading Rate Crust 4	*JOIDES Resolution*	13 Apr.–3 Jun. 2011	Puntarenas, Costa Rica
3	336 - Mid-Atlantic Ridge Microbiology	*JOIDES Resolution*	16 Sep.–17 Nov. 2011	Bridgetown, Barbados
4	339 - Mediterranean Outflow	*JOIDES Resolution*	17 Nov.–17 Jan. 2012	Ponta Delgada, Azores to Lisbon, Portugal
5	340 - Lesser Antilles Volcanism and Landslides	*JOIDES Resolution*	17 Jan.–18 Mar. 2012	Lisbon, Portugal to Curaçai
6	341 - Alaska Tectonics Climate and Sedimentation Experiment	*JOIDES Resolution*	15 Jul.–14 Sep. 2012	Victoria, British Columbia
	CDEX Operations **	**Platform**	**Dates**	**Port of Origin**
7	337 - Deep Coalbed Biosphere off Shimokita	*Chikyu*	15 Mar.–21 May 2011	Hachinohe, Japan
8	338 - NanTroSEIZE Plate Boundary Deep Riser - 2	*Chikyu*	Jun.2012–Dec. 2012	Shingu, Japan

* Sailing dates may change slightly. Staffing updates for all expeditions to be issued soon.

** CDEX schedule subject to OTF and SAS approval.

ICDP – Project Schedule http://www.icdp-online.org/projects/

	ICDP Projects	Drilling Dates	Location
1	Snake River Plain	Aug. 2010–Jun.2011	Idaho, U.S.A.
2	Barberton	Apr.–Jun. 2011	South Africa
3	Colorado Plateau	Sep. 2011	Arizona, U.S.A.
4	Campi Flegrei	Sep. 2011–Sep. 2012	Naples, Italy
5	Lake Ohrid	Jun. 2011–Jul. 2012	Macedonia, Albania
6	COREF	Jun. 2011–Jul. 2012	Ryukyu Islands, Japan
7	Songliao Basin	Jun. 2011–Sep. 2012	Daqing, China